NASA Contractor Report 182162
NEAR-TR-381

Investigation of the Validity of Reynolds Averaged Turbulence Models at the Frequencies That Occur in Turbomachinery

Gary D. Kuhn
Nielsen Engineering and Research, Inc.
Mountain View, California

July 1988

Prepared for
Lewis Research Center
Under Contract NAS3-24618

National Aeronautics and
Space Administration

TABLE OF CONTENTS

	Page
1. INTRODUCTION	1
2. BACKGROUND	2
3. DESCRIPTION OF THE TURBINE ROTOR-STATOR ENVIRONMENT	5
4. FLOW MODELS TO SIMULATE THE EFFECTS OF THE INTERACTION	7
4.1 Flow Model 1: Traveling Wave Periodic Disturbance	8
4.2 Flow Model 2: Wake-Like Disturbances	10
4.3 Flow Model 3: Oscillating Flow in a Channel	11
5. COMPUTER CODES	12
5.1 Laminar Channel Flow	12
5.2 Turbulent Channel Flow	12
5.3 Calculation of Statistics for Time-Varying Channel Flow	14
6. CHARACTERISTICS OF A TURBULENT FLOW FIELD	16
7. RESULTS FOR MODEL 1: TRAVELING WAVE DISTURBANCE	22
7.1 Statistics	24
7.2 Least Squares Analysis	26
7.3 Comparison of Laminar and Turbulent Flows	27
8. RESULTS FOR MODEL 2: SIMULATED WAKE DISTURBANCES	30
9. RESULTS FOR MODEL 3: OSCILLATING FLOW IN A CHANNEL	34
10. TURBULENCE MODELS FOR PERIODICALLY PERTURBED FLOWS	43
11. CONCLUDING REMARKS	45
REFERENCES	48
TABLES	50
FIGURES	52

1. INTRODUCTION

The concept of modeling the viscous effects in fluid flow by means of the boundary layer approximation and turbulence models has been used for many years and is an important factor in reducing the amount of computation required to predict viscous flows. Most of the derivation of boundary layer theory and current turbulence models are based on a steady flow assumption which, when used in an unsteady context, places some restrictions on the magnitude of the external unsteady effects. However, in certain cases it is possible that this order of magnitude restriction on the unsteady flow is not satisfied. One possible case occurs in turbomachinery flows where the flow unsteadiness in the turbine can have a frequency of the same order as the characteristic frequencies of the turbulence. It is not clear whether boundary layer theory is valid in such circumstances and in particular whether existing turbulence models can adequately represent the turbulence of such flows.

The starting point for predictions of turbulent flow is the Navier-Stokes equations, including mass conservation. For a generally turbulent flow these equations are "Reynolds" averaged such that the unsteady terms of high frequency are averaged over some time that is long compared to times typical of the turbulence. This averaging assumes that the time scales of the mean motion are much larger than those of the turbulence, or that the flow is "quasi-steady." However, it has been shown recently (Ref. 1) that even for simple pulsating pipe flow, quasi-steady turbulence models are not valid for high frequencies. The flow field in a turbine is much more complex, having large fluctuations of both normal and tangential velocity components arising from rotor/stator interaction causing a general unsteadiness with the wakes of the blades of upstream rows producing significant flow disturbances. It is not clear whether either the complete Reynolds averaged Navier-Stokes equations or the turbulent boundary layer equations are valid under such circumstances.

The objective of the work described in this report was to investigate the validity of Reynolds averaged turbulence models in flows subjected to high frequency periodic disturbances of the nature of those encountered in turbomachinery, especially the rotor-stator combination. A large-eddy simulation (LES) computer

code and a Navier-Stokes code employing time and spatially varying boundary conditions were used to simulate turbulent and laminar flows respectively subject to periodic disturbances in order to provide better understanding of the effects of such disturbances and of the underlying physical phenomena regarding the basic interaction between the turbulence and a wake-like external flow.

This report is organized in terms of the theoretical study of turbulent flow phenomena subjected to periodic disturbances. The environment of a turbomachine rotor-stator interaction serves as a basis to which the kind of disturbances studied can be related, but the primary emphasis is on the understanding of the underlying turbulent physics, rather than on the specific development of calculative methods or models for turbomachinery design. The first section of the report will present some background information about previous studies of unsteady turbulent flows, including experimental studies and numerical studies. Next, a description of the turbomachine rotor-stator environment will be presented, including a description of the major aspects of the turbulence modeling problem for the turbomachine. The next section will discuss three flow models for the simulation of the major aspects of the turbulence modeling problem using the simple geometry of a plane channel. Next, the Large Eddy Simulation code and the Navier-Stokes code and the application of time-varying boundary conditions will be described, followed by a discussion of characteristics of the calculated turbulent flow field with emphasis on the characteristic frequencies of significant turbulence production events. The results of calculations for the three flow models will then be described including oscillating flow in a channel and flows with blowing and suction conditions imposed on the channel walls to simulate the effects of stator wakes passing through the rotor channels. Finally, the results of the calculations will be summarized.

2. BACKGROUND

Until very recently, there was little information available on the structure of turbulence in unsteady flows. Even now, the details of the turbulence structure in unsteady flows, particularly flows of the nature of those found in turbomachinery, are not completely understood. Most studies of unsteady turbulent flows have employed either boundary layer or pipe flows with a periodic oscillation of the free

stream velocity or the driving pressure drop (Ref. 1-9). A comprehensive review of the state of the art in this field before 1981 was made by Carr (Ref. 10). Such conditions result in a perturbation on the streamwise velocity component which may in turn produce a perturbation on the normal and transverse components if nonlinear interaction occurs. While these studies have provided a significant amount of information on the effect of imposed periodicity on the behavior of turbulent shear flows, there are a large number of areas in which information is either not available or is still controversial. This is particularly true for flows in which the imposed periodicity is at a frequency in the same range as a dominant frequency of the turbulent motions, such as the "bursting" frequency. The question of whether the imposed periodicity interacts with such characteristic frequencies of the turbulence has not been definitively answered by these studies. Indeed, for a long time, there was a general feeling that imposed periodicity had no effect on the time-mean properties of the flow. However, the most recent studies by Ramaprian and Tu (Ref. 1) and the present work indicate that in certain ranges of frequency the time-mean velocity distribution in pipes and channels shows a small but measurable effect of imposed periodicity. One of the goals of the present work was to determine to what extent the effect could be attributed to interaction between the turbulence and the imposed periodicity and, therefore, what adjustments might be required in turbulence models to account for the effects in numerical analyses.

Because of the difficulty of obtaining fundamental data on the structure of turbulence in flows of practical significance, many investigators have found it useful to perform fundamental studies on unsteady turbulent shear flows which can be easily set up in a laboratory or simulated numerically. The fully developed periodic pipe flow in which the flow rate is forced to vary sinusoidally with time around a mean value represents one of the simplest of unsteady turbulent shear flows upon which fundamental studies have been performed.

For turbomachinery flows, most studies of the interaction between the flow through rotor and stator stages have been concerned with inviscid flow or with measurements of heat transfer on the blades. Recent advances in measurement techniques have given a new impetus to studying the details of turbulence in such interactions. However, the turbulence in the high frequency environment of a turbine running at operational speed still is inaccessible to detailed measurement.

Some studies have been conducted to investigate the effect of stator stage blade wakes on the blades of a passing rotor stage. Such studies have used a simplified experimental model of a cascade of blades with a sometimes even more simplified model to simulate the wake from a preceding stage. For example, Doorly et al (Ref. 11) used a rotating wire mechanism to generate wakes ahead of a fixed cascade of turbine blades. Measurements of the heat transfer to the turbine blades and spark Schlieren photographs provided information about the effect of the wake-passing on the transition of the boundary layer on the blades. In a similar experiment, Wittig et al (Ref. 12) used a plane airfoil which was traversed in front of a fixed cascade. This apparatus was used to test nonobtrusive optical measuring techniques to obtain flow velocities and turbulence structures in the cascade inlet flow and along the test blade's surface. The tests were conducted in a steady environment in which the wake generating airfoil was moved in discrete steps relative to the cascade.

Numerical studies of unsteady flow phenomena related to the turbomachinery environment are even sparser than the experimental data. Until the advent of very large computers, the solution of Navier-Stokes equations was limited to steady flows and Reynolds averaged turbulent flows. In recent years, computer codes have been developed which can provide important insights into the nature of turbulence in an unsteady environment. While the codes are not yet ready to be used for production design purposes, they are useful tools for studying generic problems which attempt to identify the important features of a flow.

Simulation of unsteady viscous flows at low Reynolds numbers has been done by a number of researchers (Hanratty et al (Ref. 13), Chapman & Kuhn (Ref. 14), Kim & Moin (Ref. 15), Kuhn et al (Ref. 16)). Generally, because of the computer storage requirements, these calculations have been limited to laminar, or at best transitional, Reynolds numbers. For slightly higher Reynolds numbers, the technique of Large Eddy Simulation has been useful. A comprehensive review of numerical methods for simulating turbulent flows was presented by Rogallo and Moin (Ref. 17).

3. DESCRIPTION OF THE TURBINE ROTOR-STATOR ENVIRONMENT

The flow in turbomachinery is a very complex three-dimensional unsteady flow. As a first approximation, the mean flow can be viewed as a two-dimensional flow. This removes from consideration the blade tip flows and other secondary flows. The essential features of the flow for the present investigation can then be identified.

According to Giles (Ref. 18) there are three dominant causes of unsteadiness in a rotor-stator interaction. The first is wake/rotor interaction in which the wakes produced by a stator row are swept downstream into the next rotor row. The second is vortex shedding at trailing edges. The third is the potential stator/rotor interaction in which the pressure field associated with the leading edge of a rotor sweeps past the trailing edge of an upstream stator, causing additional unsteadiness at the trailing edge and possibly affecting the vortex shedding mechanisms. A fourth unsteady phenomenon which can be identified is the oscillating pressure gradient imposed on the rotor blade boundary layers by the blade-passing interaction (Ref. 19). The present work is most concerned with the interaction between the wakes and the boundary layer on the blades as the wakes are swept through the rotor blade row and with the effect of an oscillating pressure gradient on the turbulence of a boundary layer. The flow field of a rotor-stator combination will now be described more specifically to identify the essential features that must be modeled.

Hodson (Ref. 20) observed that many of the phenomena associated with rotor-stator wake interactions could be explained by inviscid analysis. A sketch of the unsteady velocity vectors representing the stator wakes in a rotor cascade is shown in Figure 1. Experimental verification of such a flow pattern was provided by Binder et al (Ref. 21). Once separated from its generating blade, a wake retains its defect characteristics but is convected through the rotor cascade at the local velocity. The wake is distorted by this convection, but nevertheless retains its essential features. Since the boundary layers on the blades are thin, most of the distortion is due to the main flow field which can be considered inviscid. However, in order to predict the boundary layers on the blades, the turbulence of the

boundary layers and the turbulence in the wakes must be considered. While inviscid analysis can describe the convection of the wake flow through the blade channel, it cannot provide other information for modeling the interaction such as the convection rate of turbulent eddies in the boundary layer. Other researchers, such as Willmarth (Ref. 22), have observed that the turbulent fluctuations in a boundary layer travel at a speed which is slightly less than that of the mean flow in the boundary layer. Other important phenomena such as the effect of the wake on the dissipation of the boundary layer turbulence and on heat transfer to the blade also can not be explained by purely inviscid analysis.

From these observations, it can be seen that the interaction between the stator blade wakes and the turbulence of the boundary layer on the rotor blades is more than the periodic application of a perturbation to a steady boundary layer. If the wake moves along the boundary layer at nearly the same speed as the natural turbulence of the boundary layer, then, to an observer moving with the wake, the interaction between the wake flow and the boundary layer turbulence is a stationary process of mixing between the wake and the boundary layer. The question of whether the boundary layer turbulence "locks-in" to the wake-passing frequency, which was one of the original impetuses for this work, becomes a question of whether the turbulence is forced to match the convection speed of the wake and whether in addition the characteristics of the boundary layer turbulence are significantly changed. For example, the primary production of Reynolds stresses in the boundary layer comes from intermittent ejections of fluid from the near wall region of the layer. The effect of the wake on these ejections could have important implications for turbulence models. The importance of the wake-passing frequency concerns the spacing between adjacent wakes, the relaxation time of the boundary layer turbulence, the relative convection speeds of the wake and the boundary layer turbulence, and the oscillating pressure field produced by the interaction.

In order for a computational method to provide better understanding of the turbulence phenomena involved in the wake/boundary-layer interaction, it must be able to simulate the conditions described above. In Figure 2 is shown a sketch of a boundary layer intersected by a segment of a wake. The wake is shown at a right angle to the boundary layer although the intersection would generally be oblique. For the rotor-wake interaction, the wake appears as a negative jet

(velocity defect) on the pressure surface of the rotor and as a positive jet on the suction surface (Fig. 1). In both cases, the impingement of the wake flow on the surface is similar to a stagnation point flow, the streamlines spreading upstream and downstream in the boundary layer relative to the undisturbed boundary layer flow.

Thus, the essential features of the interaction that should be included in a simulation designed to determine the effects on the turbulence are: (1) a wake-like velocity defect region near the outer edge of the boundary layer which draws fluid away from the wall or conversely a jet-like region which feeds fluid from outside the boundary layer into the layer; (2) mixing of the turbulence of the wake with that of the boundary layer; (3) convection of the wake region along with the boundary layer flow; and, (4) oscillatory conditions which superimpose a periodic pressure pulse on the steady turbulent flow. Statistical sampling methods must be selected which will yield meaningful information on the nature of the simulated interaction and its relation to the physical problem.

4. FLOW MODELS TO SIMULATE THE EFFECTS OF THE INTERACTION

The fundamental question of interest in this study is the effect of a periodic disturbance on the turbulent fluctuations of the flow field. In order to study this phenomenon, a numerical simulation of the flow in a simple channel was used. In the channel a steady flow was established on which an unsteady disturbance could be imposed. A sketch of the geometry of the computational region considered is shown in Figure 3. Included in the sketch are the boundary conditions applied to the equations of motion. The flow is two-dimensional in the mean, with fully three-dimensional turbulent fluctuations. Thus, the geometry of the computational region is a small segment of a two-dimensional channel. Flow enters the segment at $x = 0$, and leaves at $x = 2\pi\delta$, where δ is the half-width of the channel.[1] In the

---

1 Nondimensional units are used throughout this report. Except where specifically contradicted in the text, the non-dimensionalization is by the friction velocity, U_τ of the steady mean flow which is the base for all simulations, the combination U_τ/ν for lengths, or the combination U_τ/δ for time and frequency. Thus, all quantitative velocity and length data are given in "wall units". The standard "+" notation for variables in wall units is used only where necessary for clarification.

streamwise direction, as well as in the lateral directions, the flow conditions are assumed to be periodic. In applying time dependent boundary conditions to the channel walls, it is essential that periodicity be maintained and that mass conservation be enforced. The computer codes used to calculate the flow will be described in later sections.

In examining the results of turbulent flow simulations in the channel with reference to the rotor-stator environment, it must be clearly understood that the channel in which computations of turbulent flow were performed is not a simplified model of a turbine cascade, but rather is a model of two segments of the turbulent boundary layers on the blades of such a cascade. The channel half-width is analogous to the boundary layer thickness, and the computational region is a finite rectangular segment cut from a region of infinite extent in the lateral and streamwise directions. The segment comprises approximately three boundary layer thicknesses laterally and six boundary layer thicknesses in the mean flow direction. In applying unsteady boundary conditions to the computational channel, an attempt was made to model the essential elements of the wake of a stator stage impinging upon the boundary layer of a blade of the rotor stage. Because of the unique juxtaposition of two boundary layers on the opposite walls, the channel configuration provided the opportunity to study the effects of two similar but not necessarily identical boundary layer perturbations simultaneously.

4.1 Flow Model 1: Traveling Wave Periodic Disturbance.

Several types of unsteady boundary conditions were used to produce flow models to study the response of the flow turbulence. Since the periodic passage of the remnants of stator wakes through the rotor stage can be characterized by a wavelength and a wave speed, the first flow model employed a disturbance consisting of unsteady boundary conditions imposed on one wall of the channel in the following form:

$$V = V_o \sin[2\pi/\lambda(x - ct)] \tag{1}$$

$$U = - V \tan(\theta) \tag{2}$$

where U,V are the horizontal and vertical components of the velocity at the boundary, λ is the wavelength of the disturbance, c is the propagation speed of the disturbance, and θ is the inclination of the disturbance with respect to the wall. The negative sign on U is required since the boundary condition is imposed on the upper wall of the channel. These conditions attempt to model a series of jets directed from the upper wall toward the lower wall at an angle θ and moving along the wall at the speed c (Fig. 4), alternately blowing fluid into the channel and sucking fluid out of the channel.

According to Hodson (Ref. 20), the velocity disturbances of the stator wakes travel through the rotor channel at a speed that is slightly less than the speed of the mean flow. Experimental measurements on turbulent boundary layer flows have shown that the "bursts" which are the major source of turbulence kinetic energy are convected at a speed approximately 0.8 times the local mean velocity. Thus, the value of the propagation speed used in the first flow model was

$$c = 0.8U_m \tag{3}$$

where U_m is the mean velocity of the channel flow.

The wavelength of the disturbance was also chosen to interact with the turbulence. While many experimental results have been published regarding the characteristics of turbulence, it was considered more appropriate for this study to determine a value of a characteristic wavelength by examining the turbulence from the numerical simulation of a steady turbulent flow. The calculations were based on a case that has been studied extensively by Moin and Kim (Ref. 23). The calculations were performed at Reynolds number, Re = 13800, based on the centerline velocity and channel half-width, delta. The corresponding Reynolds number based on shear velocity, U_τ, is 640.25, and the mean flow velocity in wall velocity units is U_m = 18.92. The physical realism of the data has been verified by detailed comparisons of the statistical correlations and the instantaneous and conditionally averaged flow patterns with available experimental data. Of interest here are the dimensions of the computational region and of the flow structures which are produced. In particular, the streamwise lengths of major structures and the occurrence of "bursts" of turbulence production from sweep-like and ejection-like

events were examined as a guide to choosing the wavelength of the disturbances to be imposed on the flow.

The actual determination of characteristic wavelengths of the turbulence and the results of the preliminary study will be described in more detail in subsequent sections. For the present discussion, it is sufficient to note that the preliminary results were somewhat disappointing in that effects of the imposed disturbance were observed to occur only in a thin region adjacent to the upper wall. However, the results were useful in providing insight into the affect of a disturbance on the production of turbulence in the sublayer of the turbulent boundary layer and better understanding of the nature of the turbulent flow field. Subsequent calculations for an oscillating mean flow (Flow Model 3) indicated that a longer wavelength for Flow Model 1 might be expected to produce more profound effects on the turbulence.

4.2 Flow Model 2: Wake-Like Disturbances.

In the second flow model, an improved scheme for modeling the passage of the wakes of the previous stage through the blade channel was attempted by imposing a series of two-dimensional jets on the opposite walls of the channel (Fig. 5). On one side, the jets were directed into the flow towards the opposite wall (blowing). On the other wall, the jets were directed outward (suction). Furthermore, the jets were staggered in location so that each was opposite a section of solid wall. The width of each boundary jet was one half the channel length. The entire configuration of jets moved along the wall at a prescribed speed. The region of interest for the study of wake effects upon the turbulence was confined to a narrow region centered on the solid segments and extending approximately to the channel centerline.

The actual variation of the boundary velocities was as follows:

For $0 < x\text{-}ct < \pi\delta$, on the upper wall,

$$V = V_o \{\cos[2(x\text{-}ct)/\delta] - 1\} \qquad (4)$$

and on the lower wall,

$$V = 0$$

For $\pi\delta < x\text{-}ct < 2\pi\delta$, on the lower wall

$$V = V_o \{\cos[2(x-ct)/\delta] - 1\}$$

and on the upper wall,

$$V = 0.$$

where

$$V_o = 2.0$$

and

$$c = 19.6.$$

The scheme shown in Figure 5 approximates simultaneously the interaction of the stator wakes with the boundary layers of both the suction side and pressure side of the rotor blades. The suction side of the rotor blade corresponds to the channel wall opposite the blowing condition, the pressure side to the wall opposite the suction. The velocity conditions applied at the walls have high maximum values in order to produce a significant effect at the channel centerline and on the opposite wall. As shown in Figure 6, for a laminar flow calculation the velocity variation from the center of one wall segment to the opposite wall has a high magnitude near the source of the normal flow; then the velocity decreases rapidly, finally developing the linear variation of a stagnation point flow from the channel centerline to the solid wall. The variation of the normal velocity along the channel at several levels is shown in Figure 7. For the two-dimensional laminar flow of these simulations, the spreading of the source or sink flows is small so that the regions associated with the solid segments of the walls are mostly isolated from the effects of the adjacent high velocity flow.

4.3 Flow Model 3: Oscillating Flow in a Channel.

The third flow model was designed to examine the interaction between the turbulence and a periodic disturbance which would affect the entire viscous/turbulent layer and would also simulate the effect of a pressure pulse periodically sweeping over the boundary layer. These conditions were examined using an oscillating mean flow rate. Such a condition allowed comparison with recent experimental data for oscillating flow in pipes. Such comparisons were very useful in establishing the validity of the numerical simulations and enabled the examination of aspects of the flow field which have heretofore been unavailable.

The imposition of an oscillating mean flow rate on the channel flow was used to approximate the effects of a pressure pulse moving along the boundary layer on a turbine blade. According to the time history plots shown by Dring et al (Ref. 19), the rotor blade can experience pressure fluctuations of as much as ±36 percent, with the largest fluctuations occurring at the leading edge for the rotor. Low pressure is attributable to the stator wakes, high pressure to the flow between the stator wakes. The time variation of the effects is smooth and appears to be reasonably well represented by a sinusoidal function.

The boundary conditions and parameters of the three flow models are summarized in Table 1.

5. COMPUTER CODES

5.1 Laminar Channel Flow.

In order to provide fast solutions for testing various boundary conditions to be used in this study, it was expedient to make some calculations for a laminar channel flow. Such a flow is two-dimensional and therefore requires much less computer time and memory size than the turbulent flow. The code used for this purpose was a modified version of the code described by Kim and Moin (Ref. 15). The method is based on a fractional-step, or time-splitting, scheme in conjunction with the approximate-factorization technique. The boundary conditions were the same as those used in the turbulent flow case.

5.2 Turbulent Channel Flow.

The computer code used to simulate turbulent channel flow is the large-eddy simulation code described by Moin and Kim (Ref. 23). The equations for the large-scale flow field are obtained by integration of the filtered three-dimensional time-dependent Navier-Stokes equations. The small-scale field motions are simulated through an eddy-viscosity model. The time integration is accomplished using a semi-implicit method employing the Adams-Bashforth and Crank-Nicolson methods for discretization in time. Partial derivatives in the spatial directions parallel to the walls of the channel are evaluated pseudospectrally. Partial derivatives in the

normal direction are approximated by central difference formulas. The flow variables are defined on a staggered mesh so that only velocity boundary conditions are required to determine the three velocity components and the pressure fluctuations from the three momentum equations and the equation of continuity. The program permits simulation of a turbulent channel flow at moderate Reynolds number. For the calculations of the present investigation, the computational mesh was a grid of 64 x 63 x 128 points in the x,y,z, coordinates; a total of 516,096 points.

The large eddy simulation code was shown by Moin and Kim to capture most of the important features of the turbulent channel. Calculated results were demonstrated to be in good agreement with experimental data for statistical quantities, such as turbulence intensities, and various other correlation quantities. Good qualitative agreement was shown for low and high-speed streaks alternating in the spanwise direction. The calculated production of turbulence was found to be intermittent in a manner that strongly resembles that seen in the laboratory.

The impetus for the present work was the capability of the three-dimensional time-dependent numerical simulation to provide detailed instantaneous information about the flow at many spatial locations. This information can be used effectively to study the structure and statistical properties of the flow.

In turbulence simulations, the major difficulty with specification of boundary conditions occurs at open boundaries where the flow is turbulent. The flow variables at these boundaries depend on the unknown flow outside the domain. Periodic boundary conditions are generally used for directions in which the flow is statistically homogeneous, but this implies that quantities at opposite faces of the computational box are perfectly correlated. The general approach taken in simulations such as the Moin-Kim code is to replace the physical problem, which, for a simple channel flow, is homogeneous in time, but not in the mean-flow direction, with a computational problem which is homogeneous in the flow direction but not in time. Thus, the inflow condition is replaced by an initial condition, and periodic boundary conditions are applied in the mean-flow direction.

In order to apply the Moin-Kim code to the modeling of rotor-stator-like flow fields, it was necessary to employ time-dependent boundary conditions which may include a component of flow which is normal to the solid walls. Special care must be taken to ensure mass conservation when a normal velocity component is imposed. At the same time, the length of the computational channel should be sufficiently greater than the width of the disturbance that periodicity of the normal component in the streamwise direction will be a realistic representation of the physical flow being modeled. Alternatively, the length of the computational region could be much less than the width of the disturbance so that the disturbance could be modeled as a uniform flow varying with time.

The initial condition for all calculations was a steady state flow field developed by Moin and Kim (Ref. 23). It was the result of starting the solution from an approximate flow field and integrating in time until a statistically steady state was reached. While the achievement of the original steady state required many thousands of time integration steps, useful information for the analyses of the present investigation was derived from relatively short calculations by comparing the subsequently evolving steady flow with a perturbed flow on a time-step-by-time-step basis.

5.3 Calculation of Statistics for Time-Varying Channel Flow.

Understanding a turbulent flow requires examination of several kinds of data. Instantaneous as well as statistical information can provide useful insights. Statistical quantities can include a wide variety of data, from simple averages of quantities measured (or calculated) at a single point in space or time to correlations of quantities measured at several points and combinations of space and time. In this investigation, the statistical analysis of the flow dealt primarily with instantaneous velocity distributions and statistical averages of velocity fluctuations and products of velocity fluctuations (Reynolds stresses) defined at a point. Some two-point correlations and energy spectra were also calculated.

Some statistical quantities were calculated as a normal part of the calculation process. In addition, some of the calculated flow field data were collected in disk or tape files and post-processed to determine other statistics of the flow. Two

output files were written for this purpose. One file contained the entire flow field at the final time step of a calculation. (Long calculations were always performed as a series of subsets so that flow fields were saved at various times). The other was a file containing u, v, w, and p in 11 planes symmetrically placed across the channel at specified time intervals. These data could be accumulated, stored on tape, and recalled as convenient.

Basic statistical quantities were calculated by averaging over a predefined ensemble of grid points and time steps. For steady and oscillating mean flow the basic statistical ensemble consisted of data at the grid points in planes parallel to the channel walls. Data were thus averaged over these planes to yield values of the mean velocity in the channel, the turbulence intensities, the Reynolds stress, spectra, two-point correlation functions, and several other important statistical quantities. These same data could also be accumulated to include the planar data at more than one time step, thus increasing the size of the statistical ensemble.

A modification of the standard approach to the accumulation of data for calculation of statistical quantities was necessary for Flow Model 2 which used blowing/suction jets moving along the channel. Since the wall conditions move along the wall at or near the mean flow velocity, the turbulence in the regions of interest was expected to be influenced mostly by the appropriate jet or wake flow. Statistical information on the turbulence was calculated not from integration over planes parallel to the walls as in the basic code, but from integration along lines parallel to the walls at specific streamwise stations. The most appropriate locations for these stations are the centerlines of the boundary velocity distributions as they move along the boundary. The statistical ensemble for a given time step thus consisted of the data from the spanwise distribution of the finite difference mesh at a streamwise location which moved with the boundary conditions. This is analogous to recording data at a point on the rotor blade at time intervals equal to the rotor-stator blade passing interval for a number of blades equal to the number of grid points (128) in the spanwise direction of the numerical solution. It was not considered appropriate to include results from different time steps in an expanded statistical ensemble since the flow field is in a transient state for both the real flow and the numerical simulation. Such an accumulation would be analogous to including data at different streamwise stations in the rotor boundary layer.

In the case of time varying mean flow (Flow Model 3), the time averages were computed as phase averages instead of as simple long-time averages. That is, only data at specific time steps were included in the observed statistics. Long-time averages will tend to eliminate periodic effects, while phase averages will emphasize certain effects. In a turbine, the appropriate averages would normally be phase averages since the data would most likely be obtained at a single point on the blade. The data could be averaged on a cycle corresponding to the blade passing frequency.

The primary reasons for saving data as a function of time are to provide a means of determining how the turbulence is affected by the disturbances being imposed, to give an indication of whether the disturbance is moving at the speed of the turbulence, and to calculate statistics of the flow field. Examination of the instantaneous velocity distributions at several time steps revealed that the turbulence seems to be composed of events which last for 30 to 40 time steps. Therefore, an appropriate interval for saving flow field data so that any significant turbulent eddies would be included in the statistics was estimated to be every 10 or 20 steps.

For the steady and unsteady flow rate calculations, the spectra can be computed at each output step and also at the end of each run as the average over the number of output steps at which data were output for that run. For the blowing/suction version it is not appropriate to use the data in the same way. Also, it is not appropriate to average the data over the entire plane since the data are inhomogeneous in the streamwise direction due to the distribution of blowing which has regions of no blowing and regions of high blowing.

6. CHARACTERISTICS OF A TURBULENT FLOW FIELD

In order to study the effects of periodic disturbances on turbulence, the characteristics of an undisturbed turbulent flow must be known. Much experimental data has been obtained and many reports have been published describing the turbulence in boundary layers, pipes, and channels. As discussed previously, the large-eddy-simulation code used in the present work was demonstrated by its authors to present a reasonably accurate simulation of a turbulent channel flow. However, because of certain numerical limitations, exact quantitative agreement with

experimental results for detailed turbulent structures was not obtainable. It was therefore necessary to examine certain aspects of the calculated flow field in order to select parameters such as oscillation frequency or disturbance wavelengths which might be expected to interact with the simulated turbulence.

The primary characteristic of interest in a study of turbulence subjected to periodic disturbances is the frequency of significant turbulence producing events, or "bursts." Experimental data on bursting frequency refer to a statistical sample taken from a measuring probe at a fixed point in the flow. However, the bursts occur at random intervals and not at a clearly defined periodic frequency. Also, the bursts are not distributed in a clearly periodic spatial arrangement but are scattered randomly about the surface. Thus, it was not clear at the beginning of this investigation that a single frequency could be defined to represent turbulence. Such a frequency was only one of a range of values to be tested to determine the influence of periodic disturbances on turbulence and the validity of turbulence models.

One method used to determine the characteristics of the simulated turbulence in the channel flow field was the technique of conditional sampling. The technique consists of monitoring some flow quantity, such as a velocity component, for a characteristic behavior, such as a localized gradient, or maximum value, and then computing an ensemble average of the same or other quantities for locations (or times) in the vicinity of the location (or time) of the characteristic event. Kim (Ref. 24) applied the conditional sampling technique developed by Blackwelder and Kaplan (Ref. 25) to the results obtained by large eddy simulation of the turbulent flow in a channel. He equated the time-dependence of the experimental flow situation to spatial dependence of the simulation. The results were strikingly similar to experimental measurements for conditional averages of the flow velocities, pressure fluctuations, and vorticity.

In Kim's study, no attempt was made to identify a characteristic frequency or mean distance between bursts. The criterion used by Kim to identify the characteristic of the flow which served as the trigger for conditional samples was a combination of a decreasing streamwise velocity component and a value of a localized variance which exceeded a prescribed limit value. It can be shown very simply that the variance

$$\text{var} = \langle u^2 \rangle - \langle u \rangle^2 \qquad (5)$$

where the <> denotes averaging over a short interval will reach a local maximum in either a decreasing or an increasing gradient in the vicinity of a point where the value of u crosses zero.

Characteristic of a "burst" is a decreasing streamwise velocity accompanied by an upward, or positive, normal velocity component. Such a condition would yield a local maximum of the variance as described above. However, a decreasing streamwise velocity component can also be associated with a negative normal component. In fact, experimental evidence indicates that such interactions account for a Reynolds stress which has a magnitude of about 25 percent of the total average Reynolds stress in a turbulent flow.

An example of a typical velocity distribution along a streamwise line at a distance y of 21 wall units from the wall is shown in Figure 8. The u and v components of the velocity fluctuations are presented in Figure 8a and b, respectively, while the uv Reynolds stress is presented in Figure 8c. It is noted that the uv distribution exhibits several large positive spikes. These are bursts of Reynolds stress production, the positive sign resulting from the data being obtained in close proximity to the upper wall of the channel.

The localized variance of the streamwise velocity is shown in Figure 8d. For this quantity, the length of the local averaging region was 8 mesh units, or 503 wall units (the total length of the computational region is 64 mesh units or 4021 wall units).

The subjective nature of the interpretation of significant events is illustrated by these figures. Figure 8c clearly indicates two instances of Reynolds stress production nearly 20 mesh units apart, while the u-variance in Figure 8d indicates either a single event centered at x = 47 mesh units which takes place over nearly 10 mesh units, or two closely spaced smaller events, depending upon the interpretation of the double peak of the variance, plus a second event centered at the end of the computational region.

An estimate of the propagation speed of significant turbulence events can be made by comparing the velocity distributions or distributions of other quantities at different time steps. In Figure 9 is shown the uv distribution along a streamwise coordinate line at 2 time steps with an interval of 80 time steps between. Even though the time interval is short, there is considerable change in the flow field. However, the feature appearing at $x = 27$ at the earlier time is apparently still present at the later time and has moved approximately 3 mesh units downstream. By comparing such data from many locations in a specific plane and at several times, an average value of the propagation speed can be calculated. For the data discussed here, the propagation speed of uv production events was found to be approximately 0.8 times the average velocity in the plane. All data were obtained in the plane at $y = 21$.

Another important factor in quantifying the turbulence is the mean distance between events. In an experimental situation, where a single probe would be inserted at a single point in the flow to obtain data as a function of time, this would be referred to as "burst frequency." A series of calculations was made to count the number of significant events occurring and the distance between the events. Six different criteria were used to detect the events. The criteria selected were as follows:

1. Localized variance of u > threshold
2. Localized variance of u > threshold and $du/dx < 0$.
3. Localized variance of u > threshold and $du/dx > 0$.
4. Localized variance of u > threshold and $uv < 0$ for the lower wall (or $uv > 0$ near the upper wall)
5. Localized variance of u > threshold, $uv < 0.0$ (or > 0.0 near the upper wall) and $|uv|$ > threshold
6. $uv < 0.0$ (or > 0.0 near the upper wall) and $|uv|$ > threshold

In order to evaluate the characteristics of the turbulence, the LES code was used to calculate 100 time steps. The flow fields were saved after every 10 steps. This is a short run, since the time for a particle of fluid traveling at the mean velocity in the channel to pass completely through the channel would correspond to

approximately 900 time steps. However, it was sufficient to provide a preliminary assessment of the characteristics of the flow and a test of the conditional sampling technique, as well as an evaluation of the detection criteria.

Some results for the six detection criteria are shown in Figure 10. The figure shows the cumulative number of times the various detection criteria were found to be separated by a certain interval along the streamwise coordinate lines in planes at y = 21. Data from time steps 0 and 3 and 10 through 90 at 10-step intervals were examined for each detection criterion. The results indicate a predominance of closely-spaced events, as indicated by five of the six criteria. The largest number of events appear to be separated by a distance of approximately five mesh units, or x = 314. In addition, several of the criteria yield other apparent characteristic spacings. The most prominent of such behavior is seen in the results from the sixth criterion, the Reynolds stress threshold test. This is consistent with the results of Bogard and Tiederman (Ref. 26) who found that the Reynolds stress threshold test was the one which correlated best with visual observations of the bursting process.

In subsequent analyses, only the Reynolds stress threshold test was used. This test was characterized by the occurrence of "ejections" consisting of fluctuations of normal velocity components away from the wall combined with negative fluctuations of the streamwise component. Thus, near the upper wall, the quantity used to detect ejections was a positive value of the local instantaneous uv composed of negative u and negative v. This quantity is compared with a specified threshold value to record the occurence of ejections.

The preliminary results of the conditional sampling technique were employed to determine a value of the spatial wavelength of an imposed velocity distribution which might be expected to interact with the turbulence. The results led to the selection of a wavelength equal to one-thirteenth of the length of the computational region. That analysis was based on the data for the spacing of ejections detected at a distance y = 20.5 from the wall measured at 10 computational steps chosen at 10 step intervals from the unperturbed case. Subsequently, the data base was expanded to include data from a total of 102 output steps calculated at 10-step intervals for 1020 steps of the unperturbed case.

From the expanded data base, the LES results for the distance between ejection events tend to approximate closely an exponential curve (Fig. 11). Since such a curve is a characteristic of randomly spaced events, it is concluded that the ejections are randomly distributed in the computational planes. An average spacing can be defined for the solution, but no one spacing stands out as "characteristic" of the calculated turbulence. However, the data approximate an exponential curve only for spacings above a certain threshold. That is, there are relatively few events found with spacing less than about three or four computational grid increments, so that the largest number of events are found to be spaced in the neighborhood of five mesh units apart, or one-thirteenth of the length of the computational region. On the other hand, the average spacing for all such events is around 17 mesh units or about one-quarter of the length of the computational region.

The results found from the calculated turbulence flow field are in very good qualitative agreement with the experimental results reported by Bogard and Tiederman (Ref. 26). They found that the average ejection period increased almost linearly with the threshold. The same appears to be true of the numerical results, as shown in Figure 12 where the average ejection spacing is seen to vary almost linearly with the threshold within a fairly wide range.

The value of the bursting frequency is further confused by a controversy that has existed for many years as to whether the mean time between bursts, T, scales with inner or outer variables. It became widely accepted (Ref. 27) that T scales with the outer layer variables, and that a universal constant exists such that

$$U_\infty T/\delta = 5 \qquad (6)$$

However, measurements of this quantity vary from 2.5 to 10, and more recent results indicate that no such universal relation exists.

For the channel flow, the distance between bursts is needed rather than the time between bursts or the frequency of bursts. A value for the mean distance between bursts is

$$\lambda = c\ T \qquad (7)$$

where c is the propagation speed, and T is the mean time between bursts. If Equation (6) is used, and the channel half-width and centerline velocity are substituted for the boundary layer thickness and free stream velocity,

$$\begin{aligned} \lambda &= (\ 0.8\ U_m)(5\ \delta/U_m) \\ &= 4\delta \\ &= 2560 \end{aligned}$$

In the channel solutions calculated by Moin and Kim (Ref. 23), the total length of the computational region was $2\pi\delta$ or 4021 wall units. Thus, from the observation that the mean distance between bursts from the numerical solution is about one-quarter of the channel length, the value is

$$\lambda = 1005$$

7. RESULTS FOR MODEL 1: TRAVELING WAVE DISTURBANCE.

In this section, the first of the flow models described previously is examined. The model consists of an unsteady disturbance imposed on one wall of the channel in the form of the normal and streamwise velocity components given by Equations (1) and (2).

The values required for the parameters in the boundary conditions for the calculations were obtained from the conditional sampling results described previously. The computation is performed using periodic boundary conditions in the streamwise direction. Therefore, in order to maintain the periodicity of the streamwise boundary conditions, the length of the computational region must be an integral number of wavelengths of the imposed disturbance. Therefore, the value to be used should be

$$\lambda = (2\pi\delta)/n \tag{8}$$

where n is an integer. For the calculations made with these boundary conditions, the value

$$n = 13$$

was chosen as representing the dominant burst spacing.

The next quantity to be specified is the amplitude of the disturbance. In a turbine, the velocity deficit in the wakes of stator blades is typically of the order of 10 percent of the mean flow velocity. This translates to an amplitude of approximately 5 percent of the mean velocity for the disturbance formulation discussed herein. Thus,

$$V_o = 0.05\ U_m$$

The propagation speed of the wall condition was defined to be slightly less than the mean flow velocity for the channel:

$$c = 15.14$$

Finally, the angle, θ, at which the hypothetical wake enters the channel must be specified. As a first approximation, an angle of 10 degrees was used.

The use of a periodic wall boundary condition such as the one discussed above raises the question of the validity of periodic streamwise boundary conditions on the turbulent channel flow. As long as the length of the computational region is an integral number of wavelengths of the boundary condition, periodic streamwise conditions are valid for the inviscid and purely viscous parts of the flow field, but what of the turbulent flow? The criterion for validity of periodic conditions in the turbulent flow, according to Rogallo and Moin (Ref. 17), is that the period be significantly greater than the separation distance at which two-point correlations vanish. Thus the validity of periodic streamwise conditions must be verified a posteriori in accordance with this criterion.

Several analysis techniques were employed as follows:

(1). Statistical analysis of LES solutions, consisting of comparison of plots of statistical quantities from the disturbed and undisturbed LES solutions. These plots

help to identify the characteristics of the flow in the mean. They are a useful basis for comparison since it is the long-time average flow which is of interest in Reynolds averaged calculation methods.

(2). Least-squares analysis of the LES solutions in which the periodic component of the disturbed flow field is subtracted from the flow field, and the remainder flow field compared with the undisturbed flow field. This approach yields information about how the periodic disturbance interacts with the instantaneous local turbulent flow field.

(3). Comparison of laminar and turbulent flows to determine if the occurrence of periodic disturbances could make a laminar boundary layer appear turbulent in terms of the quantities that would normally be measured.

7.1 Statistics

Samples of the comparison of statistical quantities are shown in Figures 13-15. First, in Figure 13, the mean streamwise velocity components are compared. The velocity normalized by the friction velocity is presented as a function of distance from the perturbed wall for the perturbed and the unperturbed cases. It is noted that the periodic disturbance imposed on one wall affects the mean velocity for some distance from the wall, even though the mean value of the disturbance at the wall is zero. It is also noted that the mean velocity is reduced by the disturbance, implying that the imposed wall flow generates a flow in the opposite direction. This point was examined further using the laminar Navier-Stokes code. The results of the laminar calculations will be discussed subsequently.

In Figure 14, the turbulence intensities (the rms values of the turbulence fluctuations) in the upper half of the channel are compared for the disturbed and undisturbed cases. The DELTA used to normalize the coordinates in these plots is the channel half-width. In these comparisons, it appears that the effect of the wall velocity disturbance is confined to a thin layer near the wall. Large fluctuations are produced in the streamwise, u, and normal, v, velocity components, while only small effects, if any, are notable in the spanwise component, w.

The turbulent shear stress distributions in the two flow fields are compared in Figure 15. The dashed line represents the theoretical shear stress distribution in the channel, while the symbols represent the distribution of uv averaged over each plane of the computational region and time. The slight deviation of the calculations from the theoretical line in the center of the channel indicates that the statistical sample is not quite complete. However, the deviation is small and has little effect near the walls, as observed in plots at earlier calculation steps. In particular, at the perturbed wall, the boundary condition is exact, and the effect seen in the flow field near the wall is consistent with the results shown in Figure 15 over the entire calculation. The imposed disturbance at the upper wall has a value of <uv> of -.35, where <> denotes the average over horizontal planes and time. Note that the negative value of <uv> is opposite the normal sign for <uv> for the turbulent boundary layer on the upper wall of a channel. However, as shown in Figure 15b, the resulting effect in the flow field is a sharp positive <uv> peak followed by a rapid decrease to the level of the normal solid-wall distribution. As with the intensities, the effect of the wall is apparently confined to a very thin layer near the wall.

It is noted that the effect of the imposed disturbance is present through most of the laminar sublayer and a portion of the buffer layer of the turbulent boundary layer. It is in this region and the lower part of the logarithmic region that the maximum production of turbulence kinetic energy occurs. Thus, while the thinness of the layer affected is at first somewhat disappointing in terms of simulating the conditions in the rotor-stator problem where a perturbation would be expected to exist across the entire boundary layer, it is nevertheless of interest to study the interaction between the imposed high-frequency oscillating velocity and the turbulent flow in this important inner region of the boundary layer.

Another aspect of the effect of the periodic disturbance on the turbulence is seen in the energy spectra calculated near the disturbed wall. In Figure 16, the spectra are shown for the streamwise direction at distances y = 3.85 and 38.2 from the disturbed wall. Strong perturbations are noted in the spectra of the u and v velocity components and the pressure at the wave number corresponding to the wall disturbance (K1 = 13). Significant perturbations are also noted in the u, v, and p spectra at the harmonic wave number 2*K1 = 26 at the y = 3.85 level, but only in the v and p spectra at the y = 38.2 level.

7.2 Least Squares Analysis

In order to expand the view of the interaction between the turbulent flow and the imposed oscillatory velocity disturbance, a least-squares analysis was applied to the calculated results in chosen planes of the flow field at the final time step of the series of 1020 steps. Examples of these results are shown in Figures 17 and 18. The u-component for the perturbed case is shown in Figure 17a, where the LES solution is presented as a solid line while the periodic function determined by least-squares is plotted, with the mean velocity included, as a dashed line. Similar plots for the v- and w-components are presented in Figures 17b and 17c. All of the plots show the streamwise variation of the quantities at an arbitrarily chosen spanwise location for a plane at a distance y = 38.2 from the perturbed wall. The periodic solution shown in the figures is the part of the flow field in the chosen plane which can be identified with the form of the input disturbance. A phase angle is included to account for a shift from the wall function.

The unperturbed case is compared with the perturbed case in Figure 18. In that figure, the unperturbed solution is presented as the solid line, while the dashed line represents the perturbed solution with the periodic perturbation subtracted. All three velocity components exhibit significant differences between the two flow fields.

If there was no interaction between the turbulence and the periodic disturbance, then the two flow fields represented in Figure 18 should be the same. However, the difference between the two curves shown in Figures 18a-18c is not necessarily the turbulence fluctuations alone. The usual approach that is taken is that the velocity field is considered to be composed of a combination of random fluctuations and periodic fluctuations, i.e.,

$$u = \tilde{u} + u'' \tag{9}$$

where $\tilde{u}$ is the periodic component and u'' is the random component. However, it is probable that the periodic component contributes to the production of turbulence, so that the random component is a function of the periodic component. The random component of the perturbed flow would then not be the same as that of the unperturbed flow.

The magnitude of the effect of the perturbation can be estimated by examining the distributions of the various turbulence intensities and the Reynolds stress. In Figure 19a, the distribution of the streamwise component of the turbulence intensity is compared for the unperturbed case, the perturbed case, and the difference between the two cases. The intensity of the difference field is defined as the rms value of the differences between the local instantaneous flow fields. The difference between the two fields is significantly greater than the superposition of the periodic component as determined by least squares would give. Similar results are noted for the v and w component intensities in Figures 19b and 19c and for the Reynolds stress in Figure 19d.

These results have no clear relationship to the turbulent burst frequency. The magnitude of the perturbations noted in the energy spectra suggests that the perturbation is a dominant feature of the near wall flow field. However, the sharpness of the wavenumber perturbations indicates that the spectrum of the turbulence was unaffected. The choice of the dominant burst spacing as the wavelength of the perturbation has had no profound effect.

7.3 Comparison of Laminar and Turbulent Flows.

This analysis is guided by two questions:

1. What is the effect of a periodic disturbance on a laminar flow?

2. What is the equivalent laminar flow to compare the effects of periodic and turbulent fluctuations?

The first question can be answered using any laminar flow. The second requires further specification. The aim of the second question is to determine whether a laminar flow with an oscillatory perturbation is qualitatively similar in the mean to a turbulent flow. Since laminar flow in a channel is completely determined by the boundary conditions, two choices are available for matching or comparing with a turbulent flow. The first possibility would be to establish a laminar flow with the same mean flow as the turbulent flow. The other choice is to match the friction at the walls. This means setting the channel pressure gradient to establish the same wall friction in the two flows.

For steady laminar channel flow, the momentum equation is

$$(U),yy = (P),x \tag{10}$$

so that

$$U = (1/2)(dP/dx)(y - h)\, y \tag{11}$$

where h is the total width of the channel. Integrating to calculate the mean velocity yields

$$U_m = -(1/12)(h)^2(dP/dx) \tag{12}$$

For turbulent flow in the channel,

$$dP/dx = -d\tau/dy \tag{13}$$

where τ is the shear stress, so

$$dP/dx = -2\, \tau_w/h \tag{14}$$

but

$$\tau_w = 1$$

so

$$dP/dx = -2/h \tag{15}$$

Substituting this relation into the equation for U_m gives

$$U_m = h/6 \tag{16}$$

For the case in point, h = 1280.5, so to match the wall friction, a laminar flow must have

$$U_m = 213.42$$

On the other hand, to match the mean flow, the laminar flow must have

$$\begin{aligned} dP/dx &= -12\, U_m/h^2 \\ &= -12\, (18.92)/(1280.5)^2 \\ &= -0.00013846 \end{aligned}$$

This corresponds to a smaller slope of the velocity profile at the wall. Thus,

$$\begin{aligned} (dU/dy)_w &= -(1/2)(dP/dx)h \\ &= 0.088649 \end{aligned}$$

For comparison, the value for the turbulent flow is

$$(dU/dy)_w = 1$$

Two test cases were set up for the laminar Navier-Stokes program.

1. Set conditions to match the turbulent case with the same wall velocity parameters, the same channel width in terms of the friction velocity, and the same friction boundary conditions.

This was originally set up as described except that the wall parameters were selected to correspond to a laminar flow at a lower Reynolds number. It was found that the variation of the velocity fluctuation intensities was qualitatively like the turbulent case. Also, while quantitative comparison could not be made, it was shown that for the laminar case, the omission of a mean flow through the channel, as produced by a prescribed pressure gradient, had neglible effect on the results obtained with the prescribed wall velocity perturbation.

2. Same conditions as in (1), but pressure gradient set to zero, producing zero imposed cross flow.

The resulting solution has a mean throughflow, varying from positive near the wall, becoming negative further away, then asymptotically going to zero (Figure 20). These results are consistent with the LES solution wherein it was noted that the mean velocity was reduced near the perturbed wall. A second run was made to investigate the source of the mean throughflow. That run had everything the same as the first run, except that the imposed u component was omitted. The results were very nearly the same. The difference was neglible for v, a maximum of 5 percent for u near the wall, and neglible elsewhere. The conclusion is that the wall u- component has nothing to do with the production of a net throughflow, but the mean flow is the result of the unsteady motion of the imposed disturbance and the nonlinear interaction between the convective terms and the pressure terms which produces a flow in the opposite direction from the motion of the imposed wave.

Comparisons were made between the laminar and turbulent solutions by plotting the resulting rms velocity fluctuations as functions of distance from the wall

in wall variables. The laminar results are included with the turbulent results in Figure 19. The laminar results have lower maximum values and extend less far into the flow field than those from the turbulent solution.

The results presented in this section indicate that some significant effects have been produced by the imposition of a periodic velocity field along one boundary of the steady turbulent flow. The magnitude of the effects obtained for laminar flow in the channel suggests that a rotor-stator interaction may be more like a turbulent flow even under laminar flow conditions, since the time averaged effects of the periodic disturbance on the wall shear stress and other quantities may resemble those of a turbulent flow. However, a more accurate appraisal of the effects of periodic disturbances on rotor-stator-like boundary layers requires a disturbance which will interact with more than a thin layer near the wall. The small effects on the turbulence noted in this section suggest that the disturbance must reach further into the turbulence producing layer. The analysis of the flow with an oscillating mean flow to be presented subsequently (in Section 9 of this report) will provide further insight into the effects of a disturbance which is confined to a thin wall layer and the properties of the flow and the disturbance which may affect the interaction.

8. RESULTS FOR MODEL 2: SIMULATED WAKE DISTURBANCES.

A sketch of the flow and boundary conditions in the channel for Flow Model 2 is presented in Figure 5. An example of the distribution of the normal velocity component along the channel at several vertical locations for laminar flow is shown in Figure 7. A similar set of velocity distributions for turbulent flow after 160 time steps is shown in Figure 21. The boundary distributions at that time have moved one-quarter of the length of the computational channel from the position at which they were initially imposed upon the undisturbed steady flow field. The data are presented at descending levels in the channel, beginning at a plane at $y = 3.85$ from the top wall. The perturbed flow is shown as a dashed line superimposed on the solid line representing the steady flow. It is clear that near the walls the normal flow is hardly affected by the perturbation imposed at the opposite wall. Also, further from the walls, the effect of the imposed disturbance spreads, creating

a shift in the turbulence profile due to the net crossflow, but only small effects on the turbulence fluctuations. In particular, the velocity distributions show no clear signs of being accelerated or decelerated by the moving disturbance, although there is a slight spreading of the turbulence near the lower wall where the upper blowing jet impinges. These distributions are at too early a time to conclude whether the turbulence "locks in" to the disturbance.

The mean streamwise velocity distributions across the channel at the two observation stations are shown in Figure 22 for several time steps. The first set of profiles corresponds to the station for which the upper boundary has a large blowing velocity. The first profile (Fig. 22a) is that for the undisturbed channel. Next, the profiles for 80, 120, 160, 320, and 480 time steps are shown in Figure 22b-f. The remaining profiles (Fig. 22g-l) correspond to the station for which the lower boundary has a large suction velocity. The corresponding steady flow solutions are included for steps 160, 320, and 480. The first thing that is evident from these profiles is that the effect of the boundary condition is transient. The boundary condition is imposed impulsively, and the channel flow requires some time to adjust. It does not appear that the flow has reached an equilibrium condition after 480 steps. It is doubtful that such a condition would be reached. The conditions in the channel at the wall opposite the blowing and suction were expected to be similar to the conditions on rotor blades in a turbine since the wakes of the preceding stator stage move along the blade after being impulsively imposed at the leading edge and impose a transient blowing or suction effect on the boundary layers.

Certain effects are obvious from the mean streamwise velocity distributions shown in Figure 22. First, near the lower wall opposite the upper wall blowing condition, the mean streamwise velocity is increased, accompanied by an increase in the velocity gradient and therefore the shearing stress at the wall. Second, near the upper wall opposite the suction on the lower wall, the streamwise velocity is decreased. For the first 320 time steps, the flow is well behaved and stable. At the 480th step, however, the mean velocity at the lower surface suction stations indicates a more violent deviation from the steady flow than previously.

A series similar to that of Figure 21 is presented in Figure 23. In that figure, the normal component distributions at k = 25 and time step 480 are shown. The results indicate a much more significant effect on the turbulence level in the regions near the solid portions of the walls.

The streamwise velocity distributions at the 480th step for the same planes and stations as the normal components are shown in Figure 24. These distributions show more spectacular effects than the normal velocity components. Near the upper wall at the lower wall suction station, the streamwise velocity is shifted only slightly, but the turbulent fluctuations are considerably smoother. Moving down, there is a region of sharp decrease in the streamwise component between the two boundary flows just above the channel centerline. This corresponds to the large increase in the normal component in the same region. Thus, the flow has become less well behaved, the cross flow tending to retain the form of a narrow jet which enters one wall and proceeds to bend in the direction of the exit on the opposite wall. It is believed that the flow that is developing at step 480 is of no further interest for the study of the turbulence. If the solution were to be continued, two things would happen. First, the cross flow would become more and more confined to a narrow curved region joining the inflow on the upper wall and the outflow on the lower wall. Second, the turbulence in the vicinity of the solid portions of the walls would become contaminated by the transient process of the cross flow development and the effects of jet impingement on the boundary layer could not be discerned explicitly.

Analysis of the results for turbulence intensities and turbulence kinetic energy indicates that the turbulence level at the stations opposite the input boundary conditions is decreased somewhat opposite the blowing and increased opposite the suction (Fig. 25). This result is consistent with the measurements of Binder et al (Ref. 21) who found very high turbulence intensities on the pressure side of rotor blades accompanying the passage of stator wakes. It will be recalled that the pressure side of the rotor blade corresponds to the upper channel wall opposite the lower wall suction region for the flow model used herein.

The interaction that is of most interest is that between the wake flow field and the boundary layer. This interaction occurs mostly in the outer part of the

boundary layer and has two aspects. First is the interaction between the boundary layer turbulence and the mean flow field of the wake. Next is the interaction between the turbulence of the boundary layer and the turbulence of the wake. Referring to Figure 5, the regions of interest are generally between the centerline and the walls and centered on the solid segments of the walls. The velocity imposed at the boundary is necessarily of a large magnitude in order to produce an effect of appropriate magnitude in the region of interest. It has been observed that the vertical velocity at the centerline has only a small variation from the mean along the channel. Therefore, the most important requirement of the boundary conditions is that they have a mean value that is appropriate for the study of the wake/turbulence interaction. The velocity defect in a wake is generally 5 to 10 percent of the free stream velocity. The boundary velocity distributions for the channel simulation were adjusted to produce a normal flow with a mean value of 5 to 10 percent of the undisturbed channel centerline velocity. With regard to the two aspects of the interaction mentioned previously, the boundary conditions shown in Figure 5 produce a flow field which attempts to model the mean flow/turbulence interaction. At the same time, as the normal jet flow enters the channel, it interacts with the turbulence that already is present and modifies it. The turbulent flow field at the centerline is then quite different from that of the channel alone. The boundary conditions could be modified by adding a random disturbance to the basic distribution if necessary to increase or otherwise modify the simulated wake turbulence. This would introduce new turbulence components which would interact with the boundary layer turbulence. Comparison of the two simulations, with and without the additional boundary turbulence, should yield useful information about the effect of the wake on the boundary layer. Even though the interaction will occur mostly in the outer part of the boundary layer, it is expected that some effects would be felt at the wall as well. Such a comparison could not be made within the scheduled funding and time limits of this investigation.

In summary, the results of Flow Model 2 indicate that turbulence models for rotor boundary layers must account for two effects of the passage of stator wakes through the rotor cascade. The wake region acts as a defect region on the pressure side of the rotor blades, causing the mean flow to be drawn away from the wall, and, as an impinging jet on the suction side of the rotor blade, causing the boundary layer to be pressed closer to the wall. These effects result in

amplification of the turbulence intensity on the pressure side of the rotor blade and decrease of the turbulence intensity on the suction side. Because of the periodic nature of the blade-passing flow fields, turbulence models must acknowledge the fact that the rotor blade boundary layers alternate between undisturbed flow regions between the stator wakes and the disturbed regions of the wakes.

9. RESULTS FOR MODEL 3: OSCILLATING FLOW IN A CHANNEL.

Ramaprian and Tu (Ref. 1) identified five ranges of frequency that are of importance for the interaction between a turbulent pipe flow and an oscillatory mean flow. In the present work, the frequencies that were possible for the oscillatory flow were in the ranges which Ramaprian and Tu identified as the "high frequency regime" and the "rapid-oscillation regime." In the high frequency regime, according to their analysis, the time-mean velocity is affected and can exhibit an inflective profile near the wall. The periodic flow will also be affected but the effect is confined to a thin region near the wall beyond which the flow oscillates like a solid mass. They say that the turbulence structure will exhibit total departure from equilibrium, that the turbulence intensity remains practically frozen across the outer part of the shear layer, and quasi-steady turbulence modeling breaks down completely.

In order to examine the type of flow studied by Ramaprian and Tu in greater detail than was possible in the experiments, the large-eddy-simulation channel code was used with three values of oscillation frequency for the mean flow rate. The oscillation frequencies and other pertinent parameters are listed in Table 2. A simultaneous calculation for steady mean flow was performed to provide direct information on the effect of the oscillation. For Case 1, the frequency of the imposed oscillating mean flow rate was determined from the observation that a typical turbulent burst would move approximately one-quarter of the channel length before becoming undetectable. (This also was the average distance between bursts at a distance from the wall corresponding to the lower part of the logarithmic region.) The value of the oscillation frequency for Case 2 was lower than the first and was determined from observations of the results of Case 1. The value for Case 3 was a still lower value chosen on the basis of the results of the previous two frequencies.

The length of a calculative time step was specified to be as large as possible within the constraints of the CFL condition. After some trial and error, a value which appeared to be satisfactory for all anticipated calculations was chosen as

$$DT = (U_\tau/\delta)dT = 0.0005$$

The corresponding time required for the fluid to completely pass through the channel was estimated to be

$$T = 640\ DT$$

The frequency of an oscillation with a period roughly equal to the life time of a typical burst is thus

$$\begin{aligned} \omega\delta/U_\tau &= 2\pi/(160\ DT) \\ &= 78.54 \end{aligned}$$

or, in the notation of Reference 1,

$$2\omega\delta/U_\tau = 157.08$$

This value corresponds to the "rapid-oscillation regime" defined by Ramaprian and Tu.

The amplitude of the oscillations for all three cases was 20 percent of the mean flow velocity. A test case made for Case 1 using 10 percent amplitude produced results that were virtually identical to the 20 percent amplitude results.

The initial condition for all calculations was as described previously. Results were calculated at several instantaneous time steps at which various statistical quantities were averaged over the planes parallel to the walls of the channel. Such averages correspond to time-phase averages of experimental data. The individual time steps are defined so as to divide each period of the imposed disturbance into an equal number of segments. For Case 1, the data were output and statistics calculated every 20 time steps. This produced eight output steps for every cycle of the prescribed disturbance.

The variation of the mass flux through the channel is shown in Figure 26 to indicate the phase relationship to the input disturbance of the results to be shown subsequently. In Figure 27, the mean velocity profiles at time step 920, corresponding to a phase angle of 270 degrees in the sixth cycle of the mean flow oscillation, are shown. The result for the steady case is shown in Figure 27a, while the unsteady case is shown in Figure 27b. The instantaneous value of the wall shear stress is used to normalize the velocity and normal coordinate. From these figures, it appears at first that there is a difference between the two cases. The unsteady case, having a different wall shear velocity, is displaced from the steady solution. However, when the data are averaged over all output time steps, which span six complete cycles of the periodic disturbance, the differences in the time average velocity profiles are negligible.

Another valuable comparison for evaluating the effect of the mean flow oscillation and the accuracy of the simulation is the two-point correlation function

$$R_{ii}(y,r_1) = \frac{\langle u''_i(x,y,z)u''_i(x+r_1,y,z)\rangle}{\langle u''_i{}^2(x,y,z)\rangle} \tag{17}$$

This is the quantity used to justify the use of periodic boundary conditions for the channel code. The two-point correlation profiles show that, in general, for small separation distances, the correlation for the velocity in the direction of the displacement is larger than the corresponding transverse correlations. The two-point correlations produced by the large-eddy-simulation code were discussed in some detail by Moin and Kim. That discussion will not be repeated here. The interesting comparison for the present work is between the steady and the unsteady cases. Figure 28 indicates that for the high frequency case, the two-point correlations are unaffected by the oscillation. Both the steady and the unsteady solutions have the same distribution for all three components of the correlation functions. Also, the small values of the correlation functions at the ends of the computational range indicate that the periodic boundary conditions are appropriate for the unsteady case as well as for the steady case.

In the experiments of Reference 1, the quantity which most clearly revealed the nature of the turbulence/oscillating flow interaction was the periodic component

of the time mean velocity field with the time mean value determined by averaging the measured values at the same phase point in an ensemble of oscillation cycles. The corresponding quantity in the numerical simulation is the periodic component of the planar averaged velocity where the planar average at any instant is analogous to the ensemble of experimental measurements at different times. The periodic component was determined by subtracting at a given time step the time averaged velocity of the steady flow solution. The distribution of the periodic component of the velocity field through the oscillation cycle is displayed in Figure 29, where the solutions at several phase angles in the oscillation cycle are plotted as a function of distance from the wall in wall units based on the steady flow wall shear stress. The data are taken from the sixth cycle of oscillation. Comparison with previous cycles revealed that the oscillatory behavior of the solution reached an essentially periodic status after one complete cycle. A total of six cycles were calculated to ensure either that periodicity would be achieved in the time variation or that nonlinear effects would be evident. In Figure 29a the acceleration phase of the oscillation is shown, while Figure 29b shows the deceleration phase. Also shown in the figures are the corresponding exact solutions of the linearized Navier-Stokes equations for a channel with oscillating mean flow. This solution is identical to that of the classical Stokes solution for viscous flow relative to an oscillating flat plate. In the notation of this report, the Stokes solution is given by

$$U/U_{max} = -\exp[-\sqrt{W/2}y]*\sin[wT-\sqrt{W/2}y] + \sin[wT] \qquad (18)$$

where $w = \omega\delta/U_\tau$ and $W = w/\delta^+$ where δ refers to the dimensional quantity and the $^+$ denotes non-dimensionalization. The small phase difference between the turbulent solution and the Stokes solution is attributable to the use of the average steady solution instead of the steady solution for the corresponding time step in determining the turbulent periodic component since the steady solution undergoes small deviations from the mean value as the time integration proceeds.

Thus, the periodic component of the calculated turbulent flow for the frequency of these calculations differs only slightly from a laminar flow. The important features of the variation of the periodic flow are the phase lag near the wall and the nearly constant values (no variation with y) further away. Observations of the turbulence intensities and Reynolds stress variations reveal that

the turbulence appears to be "frozen." In other words, the planar averaged (or ensemble averaged) turbulence statistics are not affected by the oscillation.

These results are consistent with the experimental results of Ramaprian and Tu for their high frequency case. However, the calculated results of this work are more in agreement with the Stokes solution than are the experimental data of Ramaprian and Tu. This discrepancy is explained by the fact that the frequency used in the present calculations is higher in the same nondimensional variables than the high frequency of Ramaprian and Tu. The reasons for this conclusion will become clearer when the results for a lower frequency are presented.

The results presented so far are the same kind of results that can be obtained experimentally. Another perspective can be obtained from the numerical solution by examining the instantaneous velocity components for both the unsteady solution and the steady solution which were started from identical initial conditions and integrated forward in time using the same time increments. These results reveal that the turbulence is indeed "frozen" in the sense that the velocity fluctuations of the two flow fields are identical even after six cycles of oscillation. The exception to this observation is near the wall in the region where the phase lag occurs. However, for the frequency of the results shown in Figure 29, the deviation of the unsteady flow from the steady flow is very slight. Thus, for high enough frequency, the turbulence appears to remain the same as for the steady mean flow.

A clue to the reason why the turbulence is not affected by the high frequency oscillation is provided by the distribution of the turbulence production term of the turbulence kinetic energy equation. This quantity is presented in Figure 30 where the production of turbulence at both walls of the channel for the unsteady case is compared with the steady case at the time step corresponding to the maximum phase velocity. The corresponding variation of the periodic component of the planar averaged velocity is also shown in the figure. This distribution reveals that the variation of the periodic velocity component is confined to a thin layer below the region where the majority of the turbulence production occurs. The velocity gradient is an important factor in the production of turbulence. Except for the thin Stokes layer, the velocity gradient is the same in both the steady and the unsteady flows because of the constancy of the periodic component with distance from the

wall. Since the velocity gradient is only affected where little turbulence is being produced, there is little effect on the turbulence generally at the frequency of Case 1.

The observation that the major effects of the influence of the wall may be related to the proximity to the wall of the major production of turbulence is an aspect of the flow that has not been mentioned by previous investigators. Since the region of wall influence increases with decreasing frequency, the Stokes solution was used to estimate a value of the frequency which would produce a thicker "Stokes layer," thus allowing the wall influence to be extended further into the region of turbulence production.

In Figure 31, the results for the periodic velocity of Case 2 with frequency one-third that of Case 1 after a single cycle of oscillation indicate a behavior similar to that of Case 1. The slightly greater deviation from the Stokes solution observed in Figure 31 is believed to be due in part to the shorter run time. However, the turbulence production shown in Figure 32 indicates that somewhat more interaction is occurring at the lower frequency. This result is as expected on the basis of the previous analysis, since the variation of the periodic component extends into the region of significant turbulence production. The instantaneous velocities also show the influence of the interaction since there are small but measurable differences between the velocities of the steady and unsteady flows as far from the wall as $y = 200$.

In order to elucidate further the effects of frequency, an even lower frequency case (Case 3) was calculated using a frequency one-tenth the frequency of Case 2. In Figure 33, the results for the periodic velocity component of Case 3 for the first quarter cycle are presented. Again, as for Case 2, the deviation from the Stokes solution may be partly due to the short calculation in terms of the length of the oscillation cycle. However, it is noted that Case 3 includes a total of 1200 integration steps, compared to 640 for Case 2 and 960 for Case 1. The fact that more turbulence interaction is occurring in Case 3 than in either of the other two cases suggests that agreement with the Stokes solution would not be achieved by an extended calculation. For this frequency the theoretical Stokes layer extends well into the region of maximum turbulence production (Fig. 34). After a calculation of

one quarter cycle, there is clear evidence that the turbulence is being strongly influenced by the changing periodic component of the flow as seen by small differences in the calculated turbulence kinetic energy and shear stress between the unsteady flow and the steady flow at the same time step (Figs. 35 and 36).

The evidence gathered in the calculations discussed herein points to the conclusion that there is a high frequency cut-off where the thickness of the viscous Stokes layer becomes less than a certain limit which is a function of the Reynolds number of the mean flow. When the perturbations to the mean velocity profile are confined to a layer which is below the level where the main production of turbulence occurs, the turbulence is unaffected.

Another factor that must be examined is the relationship of the Stokes calculations to the bursting frequency. In a previous section of this report, a bursting frequency was determined by taking the results of spatial distributions and converting them into temporal distributions using Taylor's Hypothesis. The Stokes results tend to indicate that the relevant frequencies are not related to the frequency obtained from that technique. The range of frequencies over which the effects apply seems more likely to be a function of the frequency alone at the high end of the scale since the effects appear to be dominated by viscosity. At the lower end of the scale, the turbulence would logically be important because the turbulence will determine how the wall effect propagates across the channel. As Ramaprian and Tu pointed out, the disturbance diffuses faster in the turbulence than in a laminar layer, so that, in the intermediate frequency range where the effects of the oscillation are confined to a layer thinner than the entire channel (or boundary layer), the turbulent "Stokes layer" would be much thicker than the viscous Stokes layer.

The main thing that can be done with these results is to more clearly define the regions that Ramaprian and Tu called the high frequency and rapid oscillation regimes. In the rapid oscillation regime, the calculated results show that the turbulence is not affected, even close to the wall. The situation can be quantified by using the Stokes solution to determine the frequency at which the Stokes layer is thinner than the level of maximum turbulence production. If the production is affected, so, too, is the dissipation (Fig. 37). If these quantities are affected, then

the effects will spread to be seen further away from the wall. Eventually, for low enough frequency, the effects can be expected to extend across the entire layer, and the flow will enter the low frequency regime wherein the turbulence is quasi-steady even though the flow is unsteady and must be calculated as a time dependent flow.

A rough quantitative estimate of the high frequency limit can be derived by examining the simple Stokes solution [Eq. (18)]. The plots presented in Figures 29, 31, and 33, show the damped wave nature of the solution. As the flow oscillates, a wave is produced at the wall which propagates into the flow. The location of the peak of the waveform is found where $du/dy = 0$. The wave damping is high so that the greatest disturbance to the flow occurs in the first wave near the wall. In each phase of the oscillation, the greatest distortion of the mean flow velocity profile would occur in the range of $-\pi/4 < \omega T < \pi/4$ or $5\pi/4 < \omega T < 7\pi/4$ since in those ranges the periodic velocity component has both positive and negative directions. If the profile at $\omega T = \pi/2$ is taken as the limiting profile, and a value of $y = 15$ is taken as a criterion for the limit of interaction with the turbulence, then a high frequency limit for the flow oscillations can be defined as

$$\omega = 13\ U_\tau/\delta$$

where both U_τ and δ are the values for the steady mean flow.

The results of this section have implications for the interpretation of the previous results discussed in Section 7. In that case, a traveling wave condition was imposed on one wall of the channel, with a wavelength of approximately 309 wall units and a propagation speed of 15.14. This corresponds to an oscillation frequency at a fixed point on the wall of

$$\begin{aligned} \omega\delta/U_\tau &= 2\pi c\delta/\lambda \\ &= 197 \end{aligned}$$

This value is almost three times the highest frequency used in the oscillating flow study. Thus, the frequency of the imposed wave was in the high range in which little effect is found on the turbulence.

Another implication of the results of this section applies to the study of compliant walls conducted by Kuhn et al (Ref. 16). That study found that only small effects on the drag of a turbulent flow though a channel were produced by a traveling wave on a flexible wall. However, the propagation speed and the wavelength of the wall conditions used were similar to those used in Section 7 of this study. The results of the oscillating flow study discussed herein suggest that a longer wavelength, corresponding to a lower frequency might be expected to produce more effect on the turbulence of the flow, which would in turn have a greater effect on the drag of the wall. Whether the effect would be a drag reduction or increase must be determined by performing the calculations.

Finally, the results of the oscillating flow offer insight regarding the importance of the burst frequency in the interaction of periodic external disturbances with the turbulence. It is clear that in the high frequency regime, there is no interaction between an oscillating mean flow and the turbulence, and hence the burst frequency is of no significance. Also, at frequencies in the intermediate range where the flow is neither frozen nor quasi-steady, the burst frequency would seem to be an effect of the flow environment and not a property of the flow which can interact with external disturbances. This view is supported by examination of the distribution of bursts in the lowest frequency case as compared to the steady flow case in Figure 38. The first two parts of the figure (Fig. 38a and b) show the burst statistics for the two cases at a level of 20.5 wall units from the lower wall, and the final two parts show the same comparison at 20.5 units from the upper wall. In both cases, the oscillating flow has a slight decrease in the number of bursts found in the plane at the time step of the count, and the average burst spacing is shifted slightly to a larger value. Although this result is not quantitatively conclusive, it demonstrates that the burst distribution is influenced by the oscillation of the main flow.

These results suggest that the bursting phenomenon is affected by the stability of the near wall flow. For very high frequency oscillations, the wall effects are completely damped within the laminar sublayer. For somewhat lower frequencies, the perturbations reach the layer where the turbulence originates from the breakdown of the stable layer. The perturbations increase the instability and produce a new mode of turbulence production.

10. TURBULENCE MODELS FOR PERIODICALLY PERTURBED FLOWS

Starting at a high frequency, the viscous perturbation is confined to a very thin layer at the wall. As frequency is reduced, the perturbed layer thickens until it eventually begins to interact with the turbulence. The calculations suggest that significant interaction requires that the perturbed (Stokes) layer be comparable in thickness to the region wherein the maximum turbulence production occurs, approximately $y = 20$. Interaction of the oscillatory component with the turbulence appears to commence at a frequency for which the viscous phenomenon begins to perturb the velocity gradients in the region where turbulence is produced and to continue to lower frequencies until the entire channel is affected. On the low frequency end there is probably not a clear boundary between the quasi-steady regime and the high frequency regime when the Stokes layer begins to cause a variation of the wall effect across the channel as described by Ramaprian and Tu. With regard to turbulence models for Reynolds averaged calculations, it is necessary to quantify the effects of these phenomena by making several calculations which cover several cycles of the imposed oscillation for several frequencies in the range beginning with the lowest frequency used to date and at least one order of magnitude smaller. The difference between the turbulence models in the three regions is as follows: in the quasi-steady regime, the turbulence model at each step is that which would apply for a steady flow with the driving conditions equal to the instantaneous conditions of the unsteady flow; in the high frequency region, the turbulence model is that of the mean flow; for the intermediate region, the turbulence model is modified to account for a transition between the mean flow in the center of the channel and a time dependent model in the modified layer near the walls. It would be expected that with decreasing frequency the turbulence model would approach asymptotically the quasi-steady model, and with increasing frequency the turbulence model would approach asymptotically the mean flow model.

Previous experimental studies of oscillating flows have concluded that the turbulence is "frozen" in the center of a pipe or channel, that is the turbulence remains at some mean state throughout the oscillation at high frequencies and that the interaction between the oscillation and the turbulence is somehow related to the characteristic "burst" frequency of the turbulence. The calculated results confirm that the turbulence is "frozen" in the sense that the statistics of the turbulence

remain the same throughout the oscillation in certain regions of the flow at high frequencies. The calculations also reveal that the frozen statistics are the result of the fact that the instantaneous velocity fluctuations are not changed from those of a steady mean flow. Furthermore, the interaction between the turbulence and the oscillations of the mean flow apparently depends upon the rate at which the disturbance produced by the wall can propagate across the viscous layer, independently from the rate at which turbulence bursts are produced.

One of the fundamental questions that was the impetus for the present research was whether a resonance could be excited between the turbulent flow and a time-dependent periodic disturbance. An approximate analysis using the one-dimensional Navier-Stokes equations and Fourier series representation of the velocity field indicates that for interaction to occur, the input disturbance should be equal to the fundamental frequency of the turbulence. If such a conclusion is applicable to the full Navier-Stokes equations, it is not clear that a resonance condition can be excited since the turbulence spectrum is continuous and the turbulence is distributed randomly in space as well as in time.

From the point of view of an observer at a fixed point on a rotor blade, the blade is subjected to a periodic flow which varies from an undisturbed boundary layer to a boundary layer with a moving disturbance. The observer would first see only the boundary layer flow, then the wake would be seen as an increasing (or decreasing) velocity as the wake moved through the blade channel. Standard turbulence models are based on data from equilibrium boundary layers in which there is no periodic motion or only motion which is very slow relative to the characteristic time of the turbulence. Furthermore, the data upon which such models are based generally do not contain the normal velocity component that is present in the wakes. Thus, the rotor boundary layer is undisturbed and disturbed in an alternating fashion, the relative length of each segment of the period depending on the stator blade spacing and the relative rotation rate. For closely spaced stator blades, the rotor blade boundary layers will be subject to the normal velocity disturbance most of the time. Turbulence models must account for this in order to accurately predict the boundary layer properties.

Since the stator wakes move along with the rotor boundary layer flow, and consequently along with the turbulent eddies, the boundary layers on the rotor blades are really several different boundary layers appearing periodically. From the point of view of an observer moving with the flow, the situation will depend upon the location of the observer. If the observer is in the flow field between stator wakes where the flow is mainly inviscid except in the rotor blade boundary layer, the observer will see an ordinary boundary layer. If the observer is moving with the external flow but is within the stator wake flow field, the boundary layer on the rotor blade will be seen to come under the influence of the wake flow and there will be relatively little interaction between the boundary layer flow that is subject to the wake influence and the boundary layer flow that is subject to the quiescent flow between wakes.

11. CONCLUDING REMARKS

Turbulent flows subjected to various kinds of unsteady disturbances were studied using numerical simulation techniques for flows in simple channels. Three flow models were designed to provide insight into the underlying physical processes governing the boundary layer flow in rotor-stator interactions. The first model attempted to model the effects of a velocity disturbance of short wavelength moving along the wall. Parameters were chosen which produced a disturbance with a scale on the order of the lower limit of turbulent burst spacing. The second model attempted to model the effect of wakes of stator blades passing through a rotor cascade. The third model considered oscillations of the mean channel throughflow.

The most enlightening results were achieved from the third flow model. It was demonstrated that the turbulence is not affected by oscillations of the mean flow at frequencies above a certain threshold where the effect of the no-slip wall is confined to a layer thinner than the laminar sublayer. It was concluded that the appropriate turbulence model for a flow with such a high frequency oscillation would be the turbulence model for the steady mean flow. Thus, turbulence models for oscillating flows must fall into three categories. For low frequencies, including frequencies where the time history of the flow field requires solution of the time-dependent equations, the turbulence is quasi-steady. At intermediate frequencies, the

turbulence structure is strongly affected. At high frequencies, the turbulence structure is not affected and remains the same as for the steady flow.

The most interesting of the three flow models from the point of view of the rotor-stator environment is the second model wherein an attempt was made to simulate the effects of stator wakes impinging on the pressure and suction surfaces of rotor blades. The results from this model demonstrate that two effects must be accounted for in turbulence models. The first effect is the effect of the mean flow in the wake acting as an impinging jet on one surface of the rotor blade, forcing the boundary layer flow closer to the blade, and as a sink flow on the other surface of the rotor, sucking the boundary layer away from the surface. The second effect is the amplification or suppression of the turbulence in the rotor boundary layer. This effect is probably a combination of the compression or stretching of the turbulence by the mean wake flow and interaction between the wake turbulence and the boundary layer turbulence.

This investigation has demonstrated the use of a numerical simulation technique to provide a generic environment for the study of turbulence. Quantitative results were obtained which agree with experiments in pipes and channels. Qualitative results were obtained which identify aspects of turbulent flow fields which must be accounted for in the development of turbulence models for Reynolds averaged flow calculations.

Several questions regarding the nature of turbulent flows and time-dependent disturbances remain at least partially unanswered. For example, since the disturbances imposed in this study were two-dimensional and periodic, can any effects be identified as turbulence-turbulence interaction? Does the absence of effects far from the wall at high frequencies imply that such interaction is low? Also, does the absence of any sign of the turbulence "locking in" to the imposed disturbance frequency imply that there would be no interaction between two random fields? Another question is, with effects of oscillating mean flow apparently traced to the laminar sublayer, how does a high frequency oscillation affect the stability of the laminar layer to cause a change in the production of turbulence?

With the results of the three flow models recorded in this report, the following recommendations can be made regarding the development of turbulence models for turbine or compressor rotor or stator blades. First, a turbulence model for oscillating flow could be determined computationally by performing a series of calculations covering several cycles of oscillation at several frequencies in the range shown in this study to produce significant effects. Secondly, the effects of amplification or supression of turbulence by the normal flow field of cut-off wakes need to be quantified more concisely by either an experiment or a computational model in which the inflow and outflow boundary conditions allow the modeling of a single vertical jet impinging on the boundary layer and moving with it.

REFERENCES

1. Ramaprian, B. R. and Tu, S. W.: Fully Developed Periodic Turbulent Pipe Flow, Part 2. The Detailed Structure of the Flow, J. Fluid Mech., Vol. 137, 1983, pp. 59-81.

2. Mizushina, T., Maruyama, T., and Shiozoki, Y.: Pulsating Turbulent Flow in a Tube, J. Chem. Eng. Jpn, Vol. 6, 1973, p. 487.

3. Mizushina, T., Maruyama, T., and Hirosawa, H.: Structure of the Turbulence in Pulsating Pipe Flows, J. Chem. Eng. Jpn, Vol. 8, 1975, p. 210.

4. Kirmse, R. E.: Investigation of Pulsating Turbulent Pipe Flow, Trans. ASME, Paper No. 79-WA/FE-1, 1979.

5. Ramaprian, B. R. and Tu, S. W.: An Experimental Study of Oscillatory Pipe Flow at Transitional Reynolds Numbers, J. Fluid Mech., Vol. 100, Pt 3, 1980, pp 513-544.

6. Ramaprian, B. R. and Tu, S. W.: Study of Periodic Turbulent Pipe Flow. IIHR Report No. 238, University of Iowa, Iowa City, 1982.

7. Tu, S. W. and Ramaprian, B. R.: Fully Developed Periodic Turbulent Pipe Flow, Part 1. Main Experimental Results and Comparison with Predictions, J. Fluid Mech., Vol. 137, 1983, pp. 31-58.

8. Cousteix, J., Houdeville, R., and Javelle, J.: Response of a Turbulent Boundary Layer to a Pulsation of the External Flow With and Without Adverse Pressure Gradient, in Unsteady Turbulent Shear Flows, ed. by R. Michel, J. Cousteix, R. Houdeville (Springer, Berlin, Heidelberg, New York, 1987), p. 120.

9. Parikh, P. G., Reynolds, W. C., and Jayaraman, R.: Behavior of an Unsteady Turbulent Boundary Layer, AIAA Journal, Vol. 20, 1982, p. 769.

10. Carr, L. W.: A Review of Unsteady Turbulent Boundary-Layer Experiments, In Unsteady Turbulent Shear Flows, ed. by R. Michel, J. Cousteix, R. Houdeville (Springer, Berlin, Heidelberg, New York, 1981), p. 3

11. Doorly, D. J., Oldfield, M. L. G., and Scrivener, C. T. J.: Wake-Passing in a Turbine Rotor Cascade, AGARD CP-390-Heat Transfer and Cooling in Gas Turbines, 1985.

12. Wittig, S., Dullenkopf, K., Schultz, A., and Hestermann, R.: Laser-Doppler Studies of the Wake-Effected Flow Field in a Turbine Cascade, Trans. ASME, J. Turbomachinery, Vol. 109, April 1987, pp. 170-176.

13. Hanratty, T. J., Abrams, J., and Frederick, K. A.: Flow Over Solid Wavy Surfaces, IUTAM Symposium on Structure of Complex Turbulent Shear Flows, Marseille, 1982, Dumas, R. and Fulachier, L., Eds., Springer, Berlin, 1983.

14. Chapman, D. R. and Kuhn, G. D.: The Limiting Behavior of Turbulence Near a Wall, J. Fluid Mech., Vol. 170, 1986, pp. 265-292.

15. Kim, J. and Moin, P.: Application of a Fractional-Step Method to Incompressible Navier-Stokes Equation, NASA Technical Memorandum 85898, March 1984.

16. Kuhn, G. D., Ferziger, J. H., Moin, P., and Kim, J.: Large Eddy Simulation of Turbulent Flow in Channels with Wavy Walls Including Both Compliant Walls and Walls with Prescribed Motion, Nielsen Engineering & Research, Inc., NEAR TR-325, July 1984.

17. Rogallo, R. S. and Moin, P.: Numerical Simulation of Turbulent Flows, Annual Review of Fluid Mechanics, Vol. 16, 1984, pp. 99-137

18. Giles, M. B.: Calculation of Unsteady Wake/Rotor Interactions, AIAA Paper No. 87-0006, AIAA 25th Aerospace Sciences Meeting, January 12-15, 1987, Reno, Nevada.

19. Dring, R. P., Joslyn, H. D., Hardin, L. W., and Wagner, J. H.: Turbine Rotor-Stator Interaction, ASME Paper No. 82-GT-3, April 1982.

20. Hodson, H. P.: An Inviscid Blade-to-Blade Prediction of a Wake-Generated Unsteady Flow, ASME Paper 84-GT-43, Presented at 29th International Gas Turbine Conference and Exhibit, Amsterdam, The Netherlands, June 4-7, 1983.

21. Binder, A., Forster, W., Kruse, H., and Rogge, H.: An Experimental Investigation Into the Effect of Wakes on the Unsteady Turbine Rotor Flow, ASME Paper No. 84-GT-178, Presented at 29th International Gas Turbine Conference and Exhibit, Amsterdam, The Netherlands, June 4-7, 1983.

22. Willmarth, W. W.: Pressure Fluctuations Beneath Turbulent Boundary Layers, Annual Review of Fluid Mechanics, Vol. 7, 1975, pp. 13-38.

23. Moin, P. and Kim, J.: Numerical Investigation of Turbulent Channel Flow, J. Fluid. Mech., Vol. 118, 1982, pp. 341-377.

24. Kim, J.: On the Structure of Wall-Bounded Turbulent Flows, NASA Technical Memorandum 84313, April 1983.

25. Blackwelder, R. F. and Kaplan, R. E.: J. Fluid Mech. Vol. 76, 1976, pp. 89-112.

26. Bogard, D. G. and Tiederman, W. G.: Burst Detection with Single-Point Velocity Measurements, J. Fluid Mech., Vol. 162, 1986, pp. 389-413.

27. Bandyopadhyay, P.: Period Between Bursting in Turbulent Boundary Layers, Phys. Fluids, Vol. 25, No. 10, October 1982, pp. 1751-1754.

TABLE 1.

Flow Models for Unsteady Turbulence

Model 1. Traveling Wave on Upper Channel Wall

$$V = V_o \sin[2\pi/\lambda(x - ct)]$$
$$U = - V \tan(\theta)$$
$$c = 0.8U_m$$
$$\theta = 10 \text{ degrees}$$
$$\lambda = 1005$$

Model 2. Wake-like Disturbances.

For $0 < x\text{-}ct < \pi\delta$, on the upper wall,

$$V = V_o \{\cos[2(x\text{-}ct)/\delta] - 1\}$$

and on the lower wall,

$$V = 0$$

For $\pi\delta < x\text{-}ct < 2\pi\delta$, on the lower wall

$$V = V_o \{\cos[2(x\text{-}ct)/\delta] - 1\}$$

and on the upper wall,

$$V = 0.$$

where

$$V_o = 2.0$$

and

$$c = 19.6.$$

Model 3. Oscillating Mean Flow in Channel

$$U_m = A \sin \omega^* T + B$$

$$A = 3.78$$

$$B = 18.92$$

TABLE 2.

Parameters of Oscillating Flow Model

Case	Frequency $\omega\delta/U_\tau$	Amplitude V_o/U_m	Length of Calculation (Time Steps)	Length of Calculation (Cycles)
1	78.54	.2	960	6.0
2	26.18	.2	640	1.33
3	2.618	.2	1200	.25

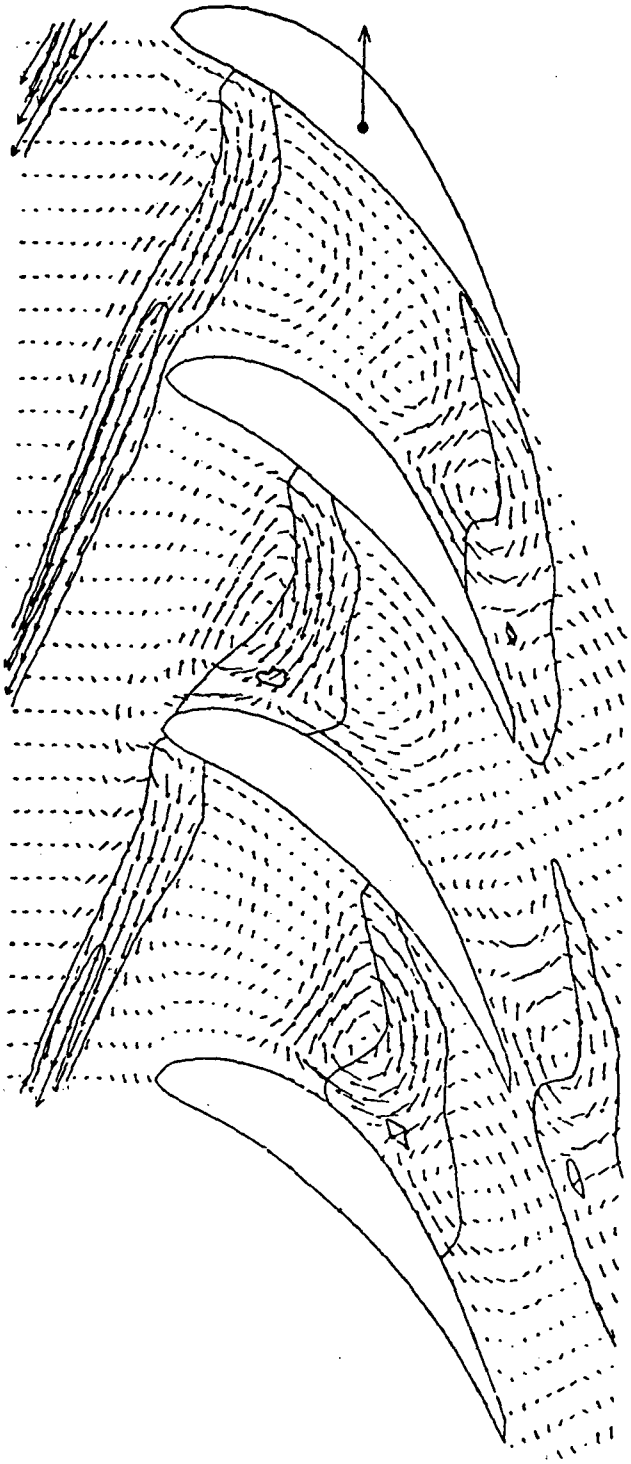

Figure 1.- Unsteady velocity vectors in a turbine rotor cascade; Hodson's calculation (Ref. 20) from Reference 18.

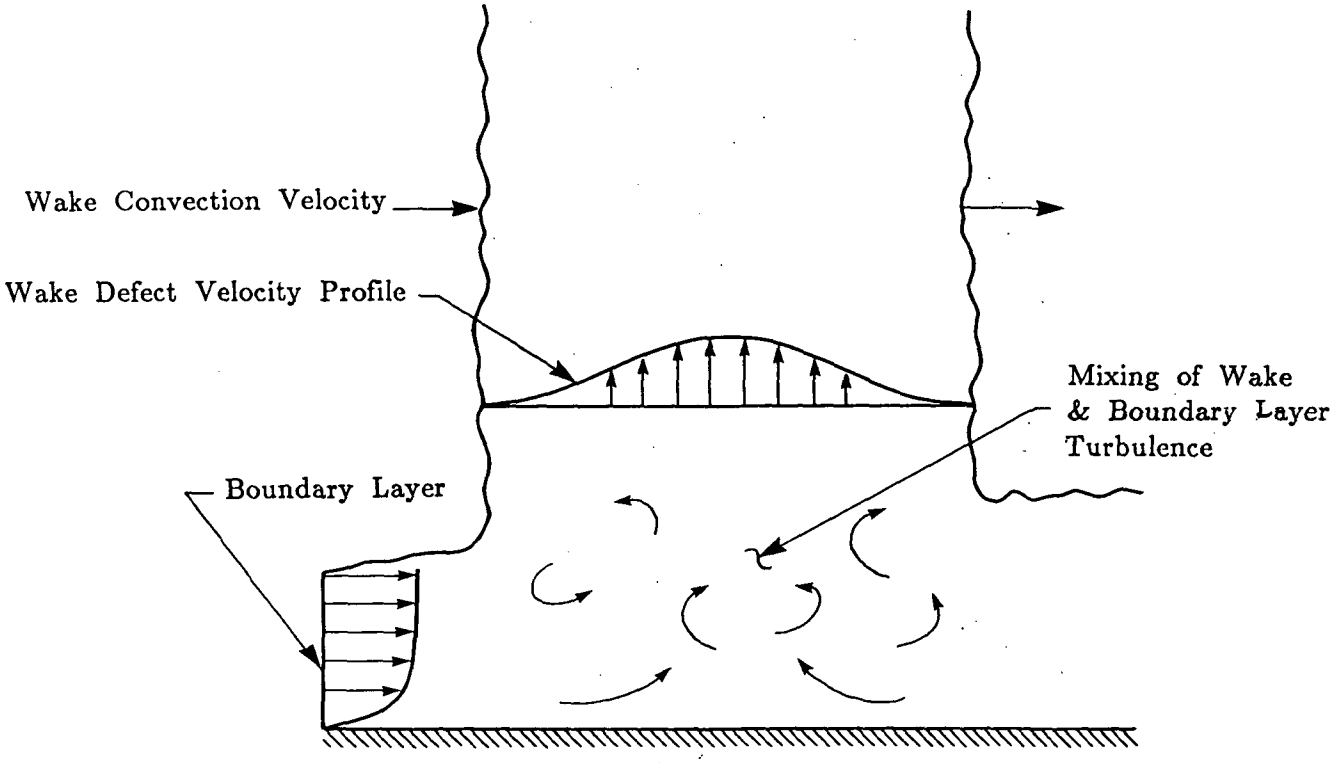

Figure 2.- Schematic of wake/boundary layer interaction

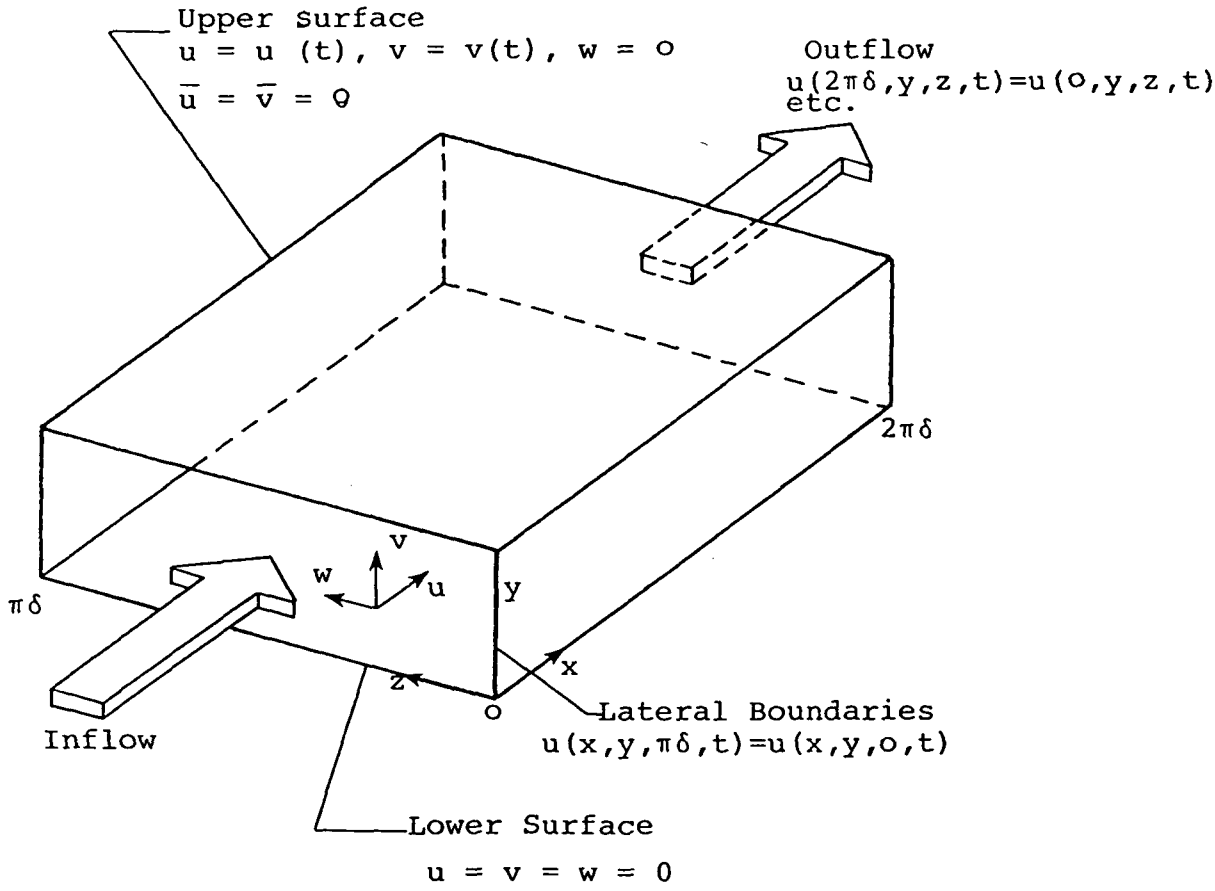

Figure 3.- Sketch of computational region and boundary conditions for calculation of flow in a channel

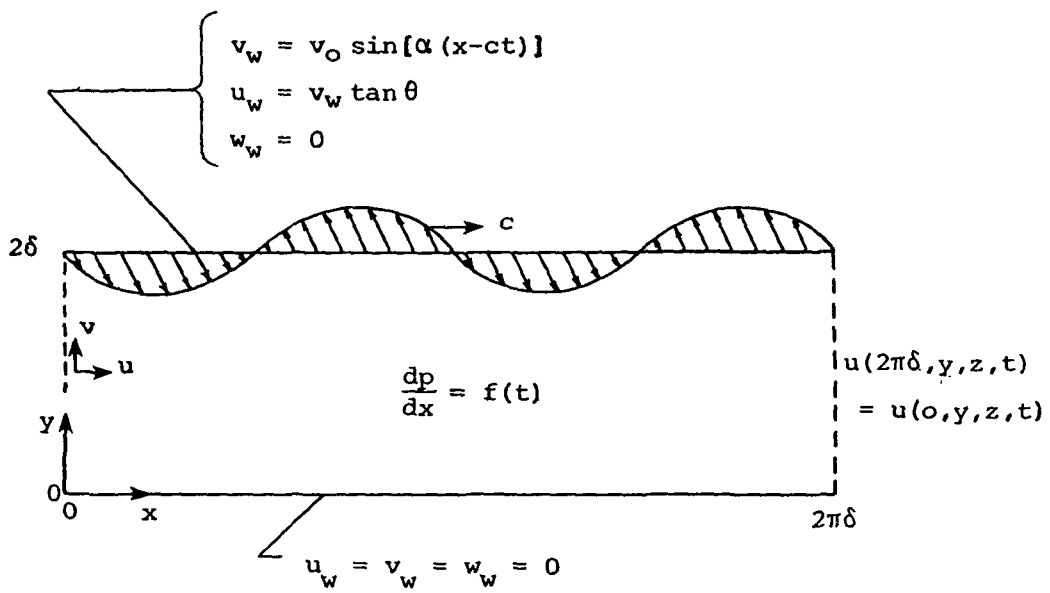

Figure 4.- Sketch of unsteady velocity vectors at the boundary of the channel

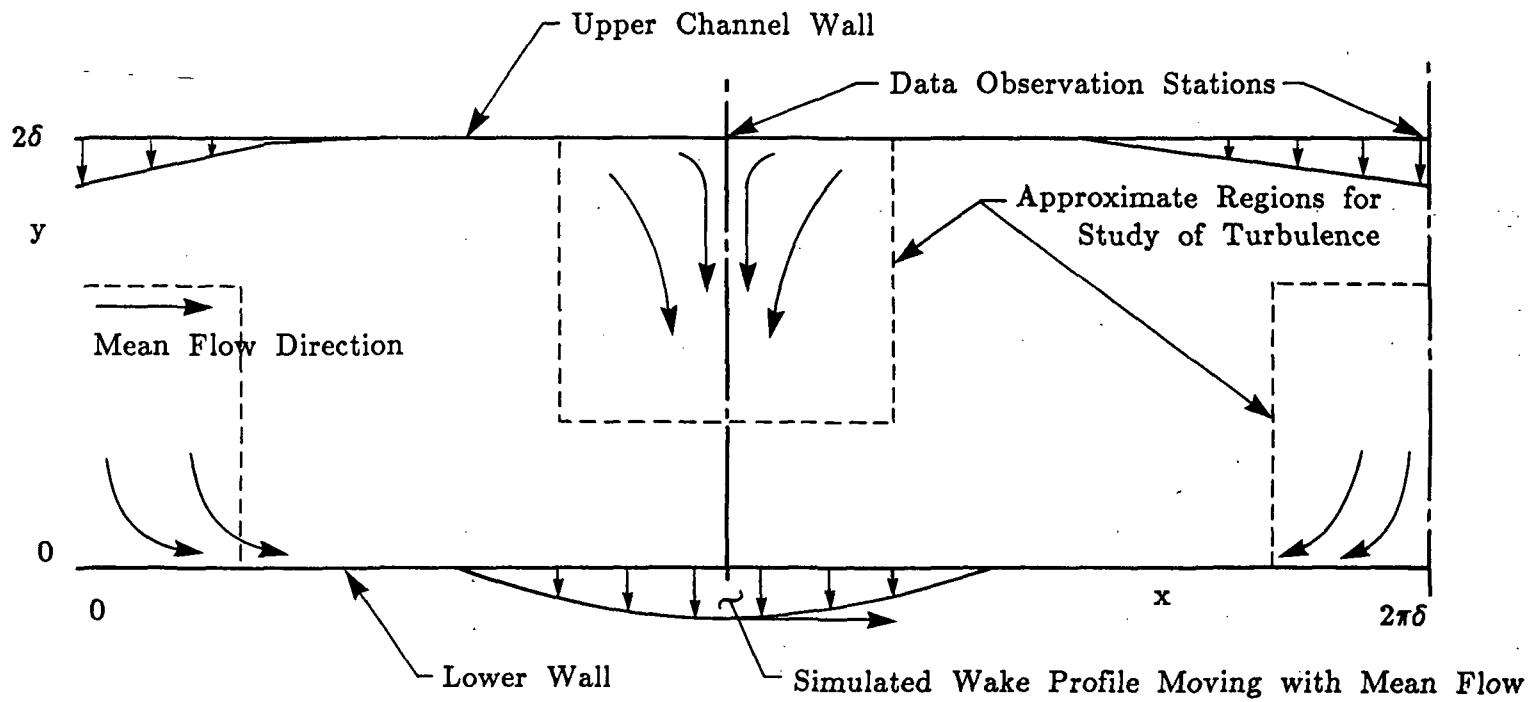

Figure 5.- Sketch of simulated wake flow relative to near channel flow.

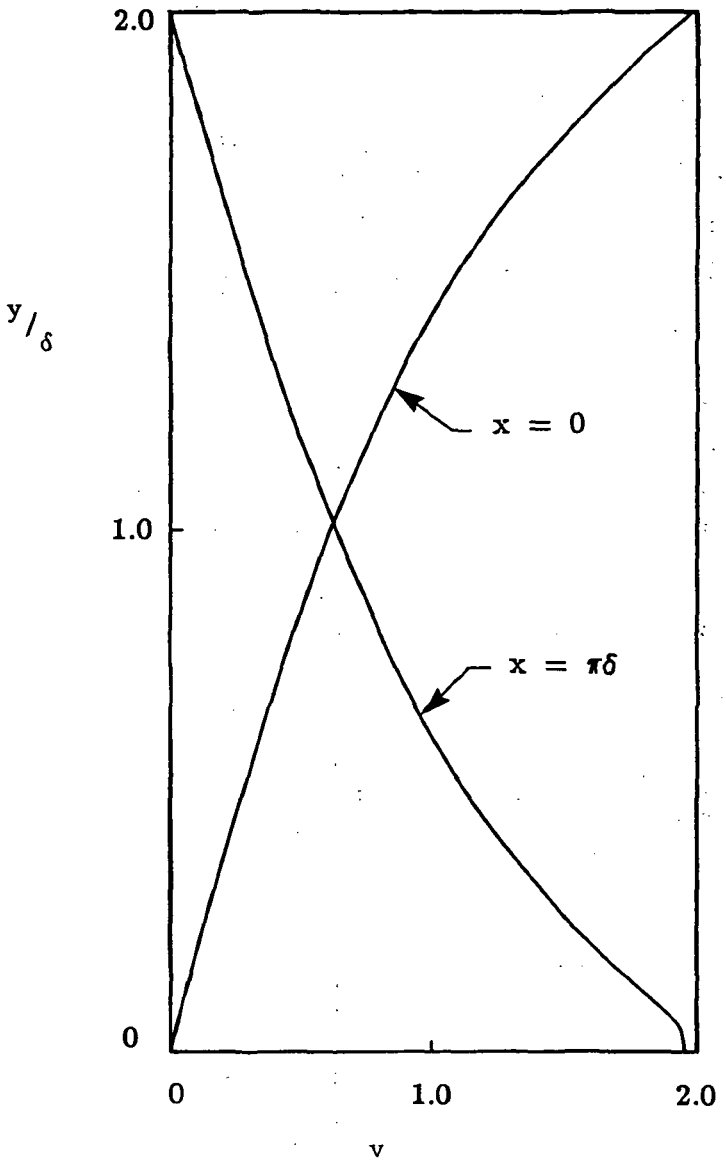

Figure 6.- Variation of normal velocity across channel.

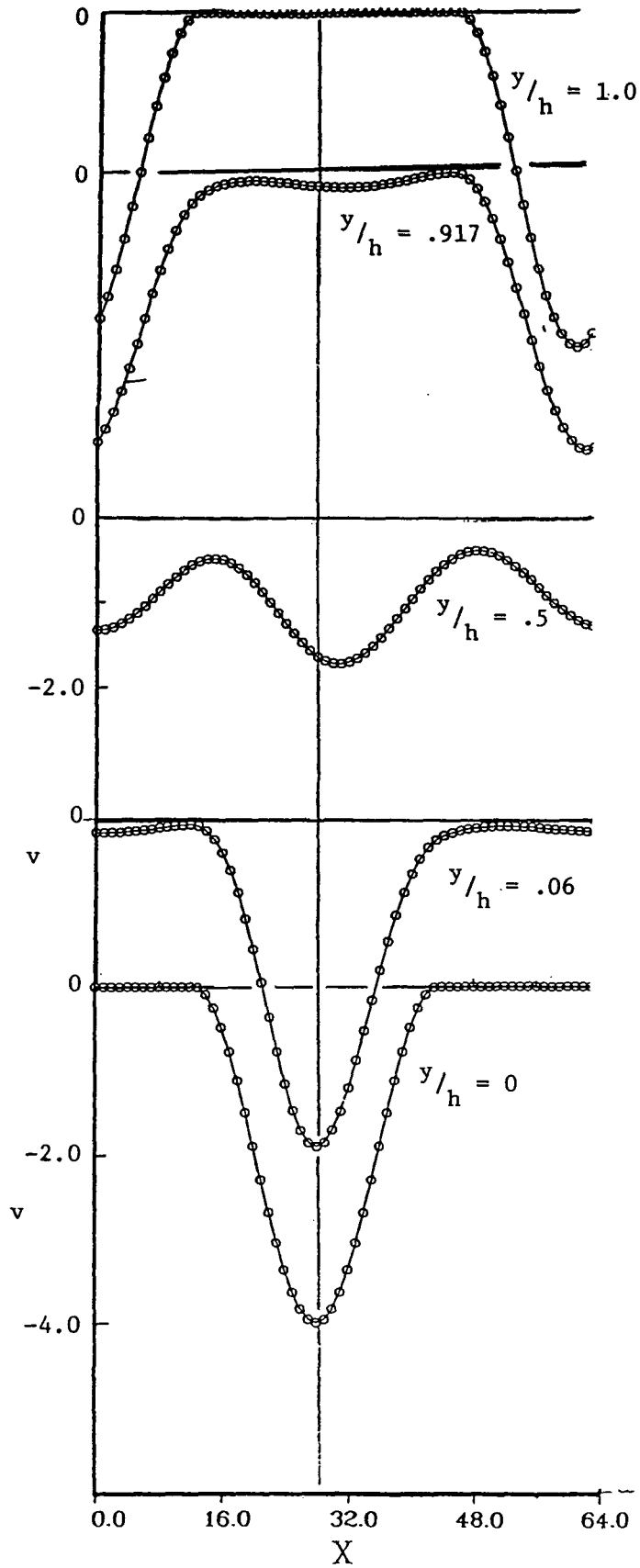

Figure 7.- Normal velocity in channel at several cross-channel levels for laminar flow.

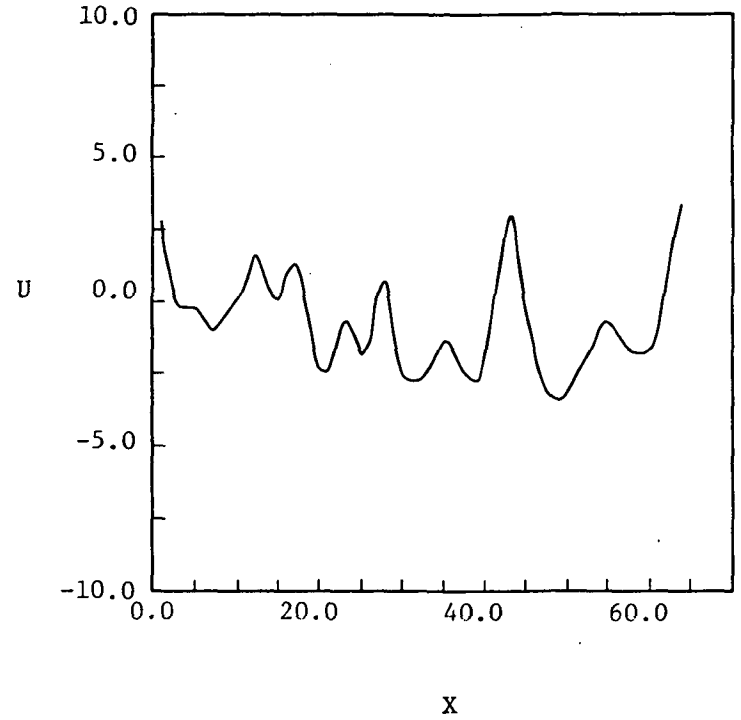

(a) Streamwise component of velocity fluctuation, u.

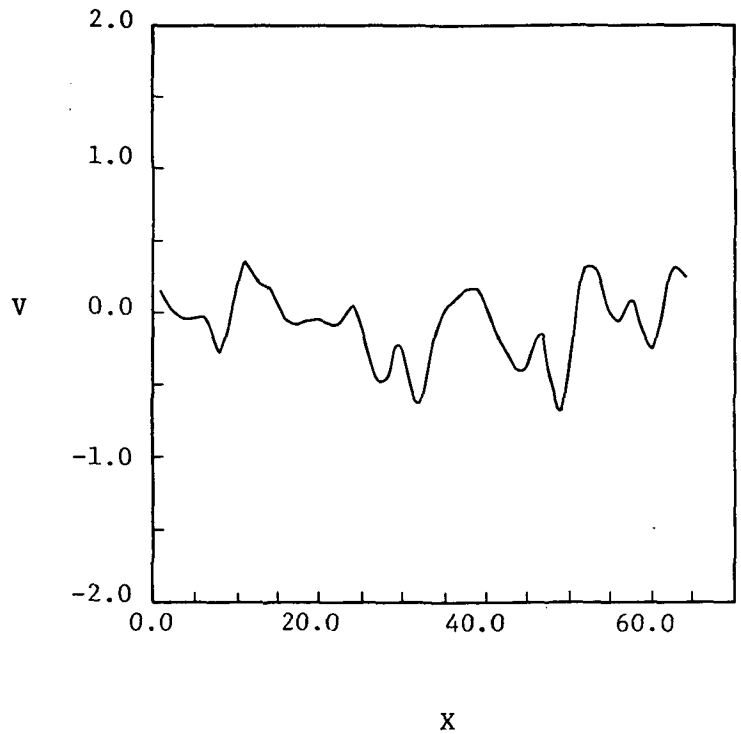

(b) Normal component of velocity fluctuation, v.

Figure 8.- Distributions of turbulence quantities along a streamwise coordinate.

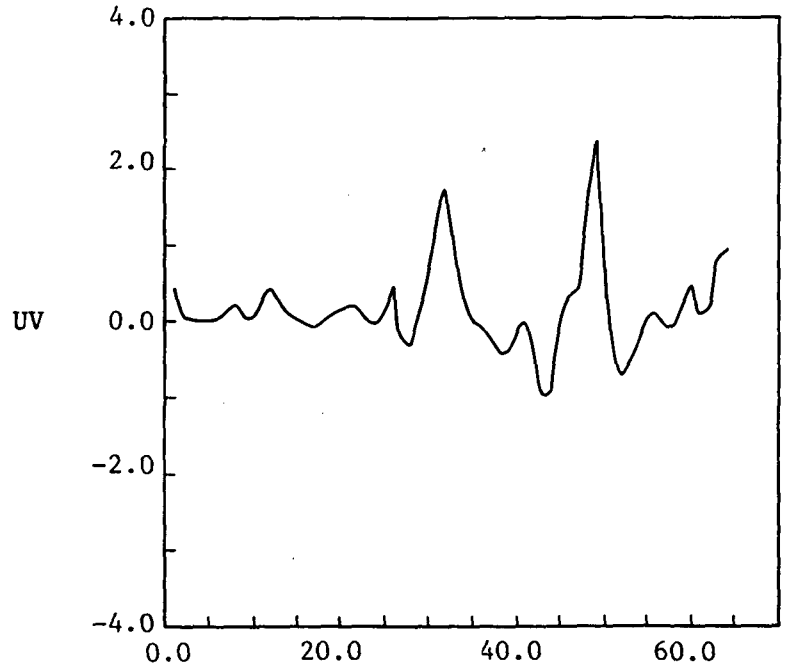

(c) uv

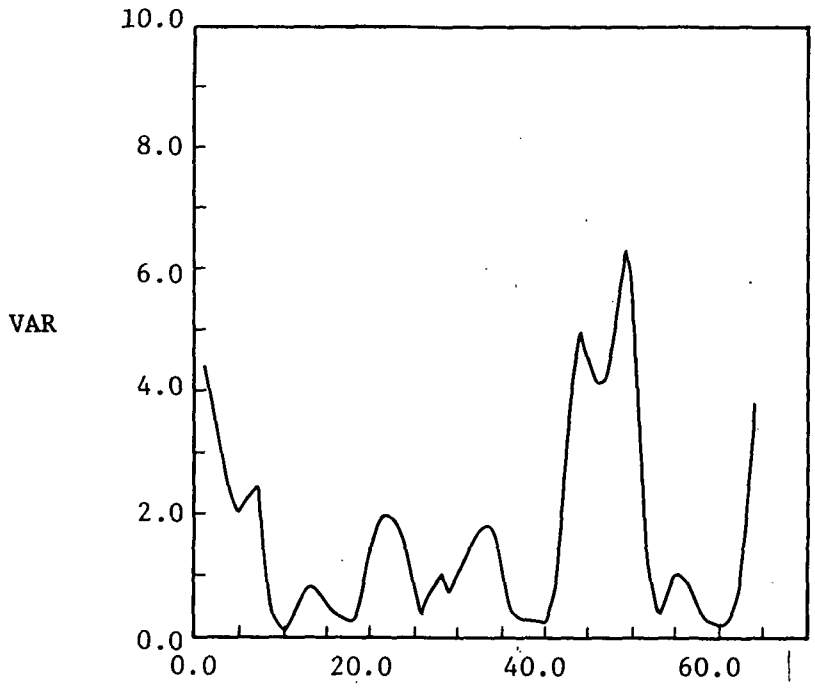

(d) Localized variance of u

Figure 8.- Concluded.

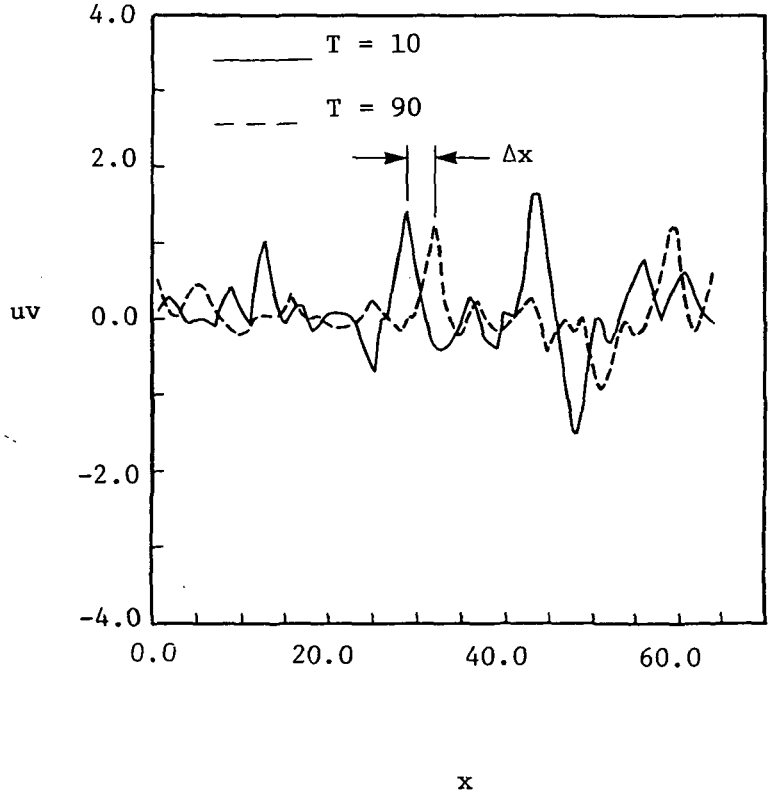

Figure 9.- Distribution of uv along a streamwise coordinate line at y = 21 at time steps 10 and 90.

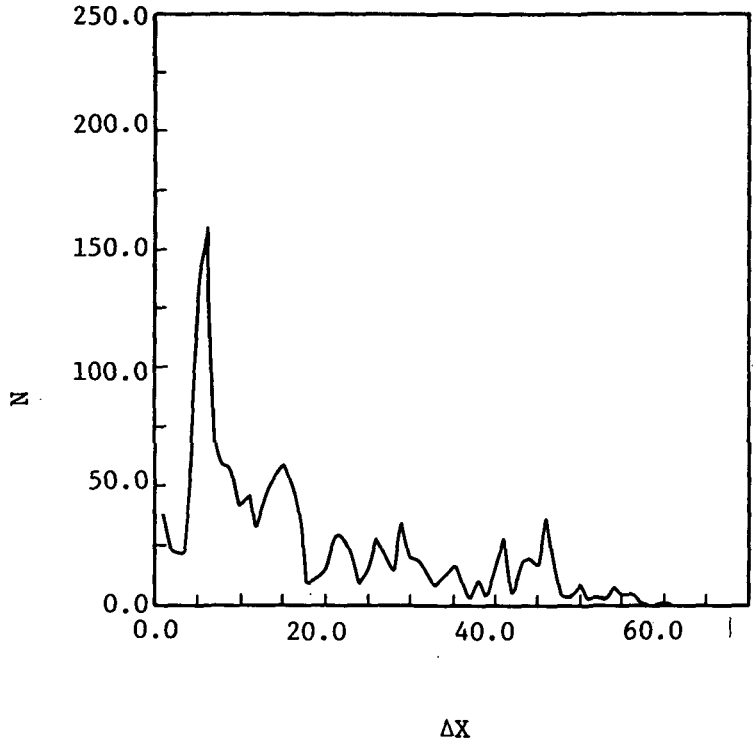

(a) Localized variance of u > threshold

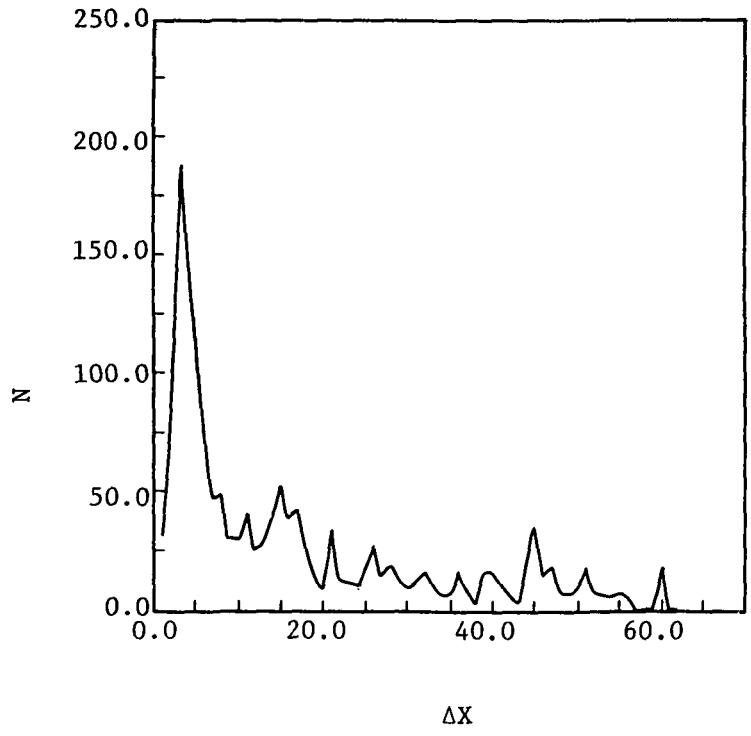

(b) Localized variance of u > threshold and du/dx < 0.

Figure 10.- Statistics of streamwise distance between significant turbulence events for six different event criteria.

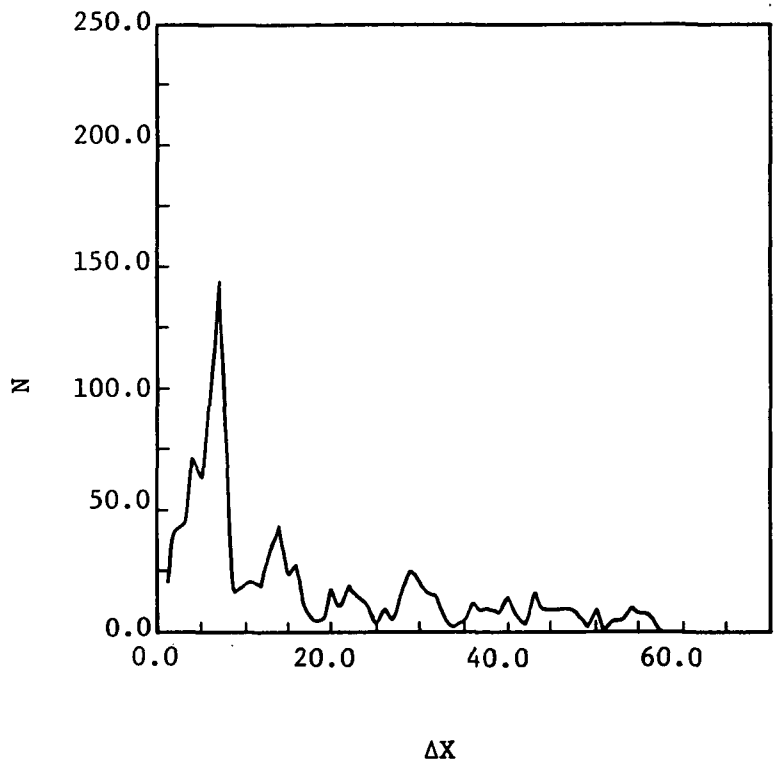

(c) Localized variance of u > threshold and du/dx > 0.

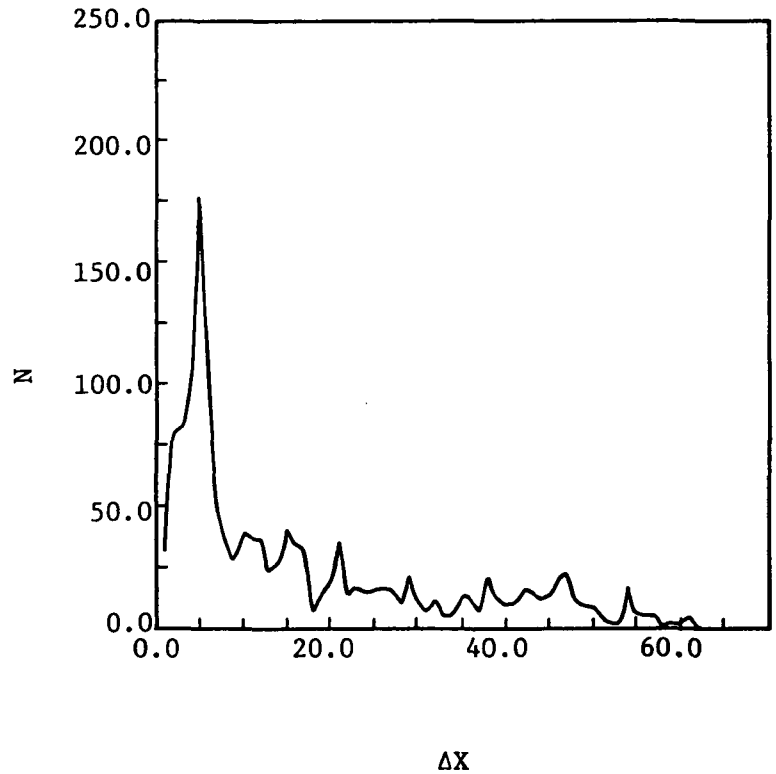

(d) Localized variance of u > threshold and uv < 0 for the lower wall (or uv > 0 near the upper wall)

Figure 10.- Continued

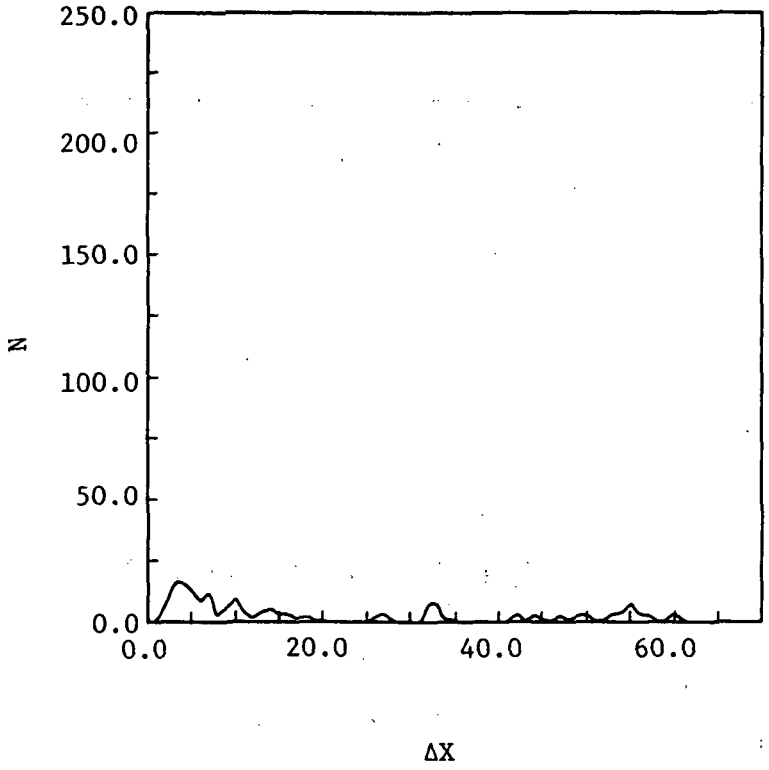

(e) Localized variance of u > threshold, uv < 0.0 (or > 0.0 near the upper wall) and |uv| > threshold

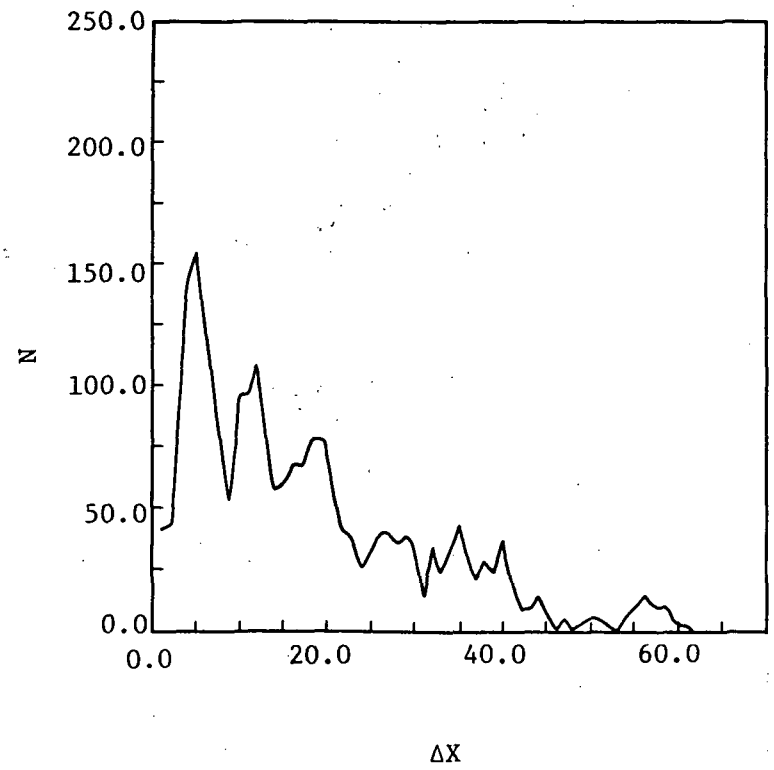

(f) uv < 0.0 (or > 0.0 near the upper wall) and |uv| > threshold

Figure 10.- Concluded.

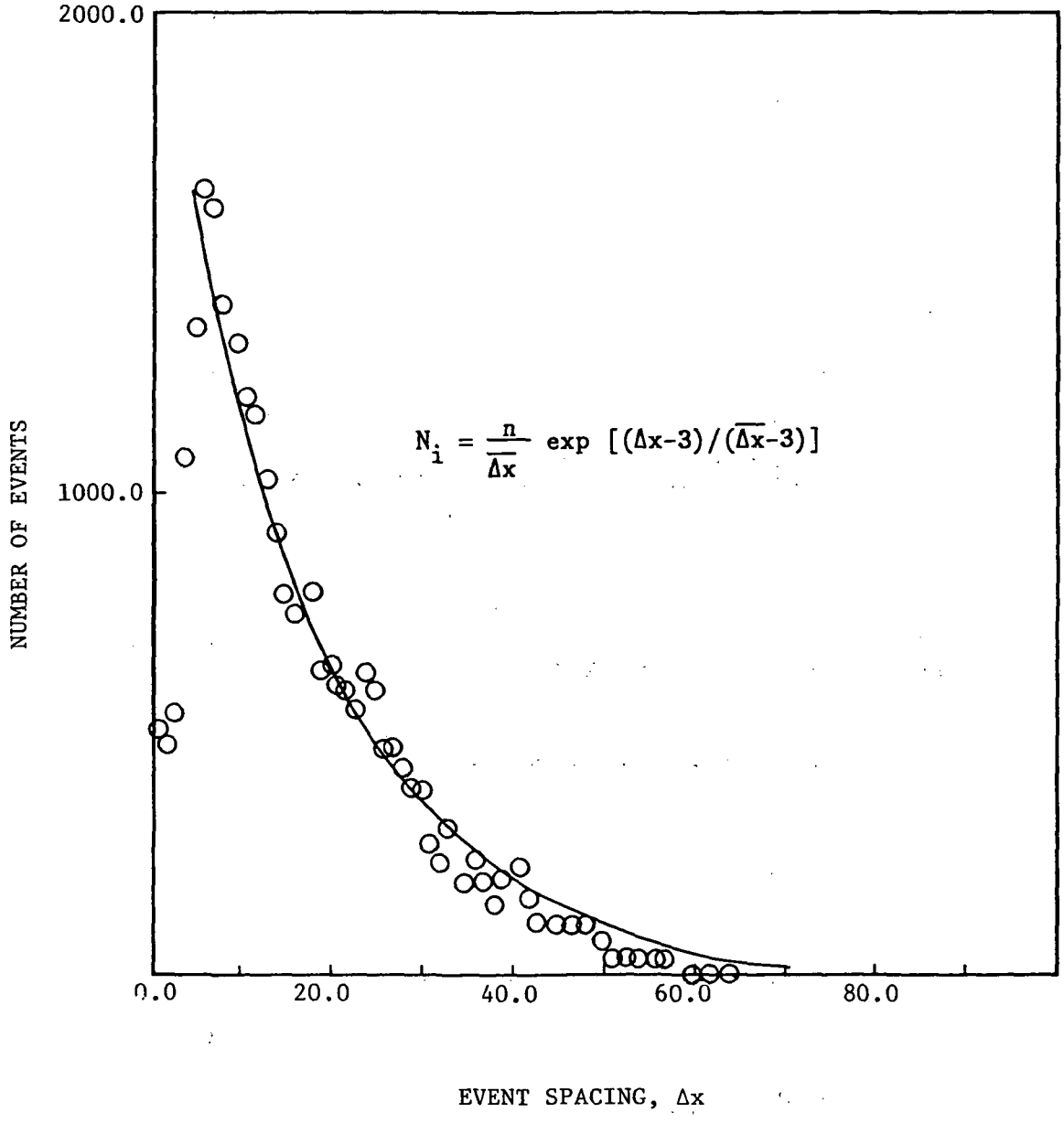

Figure 11.- Distribution of ejection spacing from unperturbed LES solution

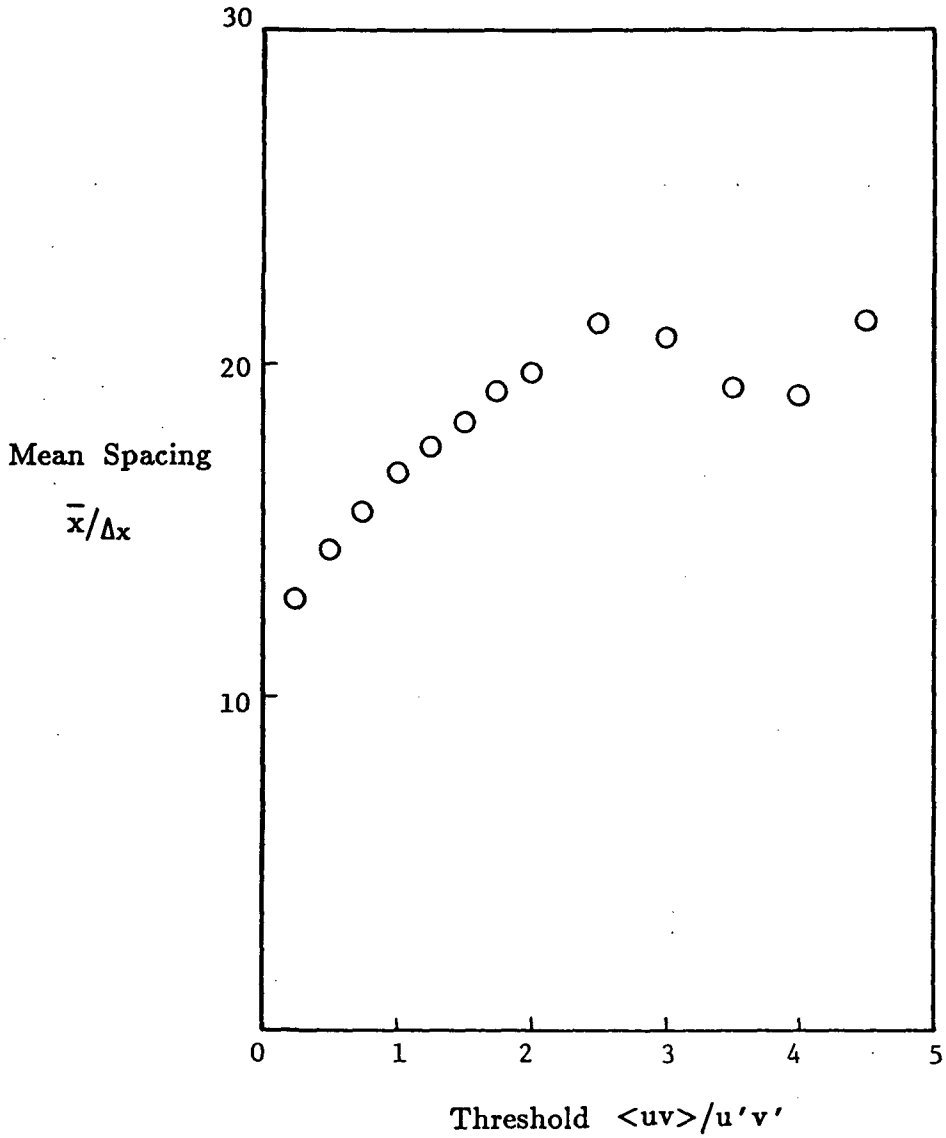

Figure 12.- Mean distance between turbulent bursts as a function of reynolds stress threshold

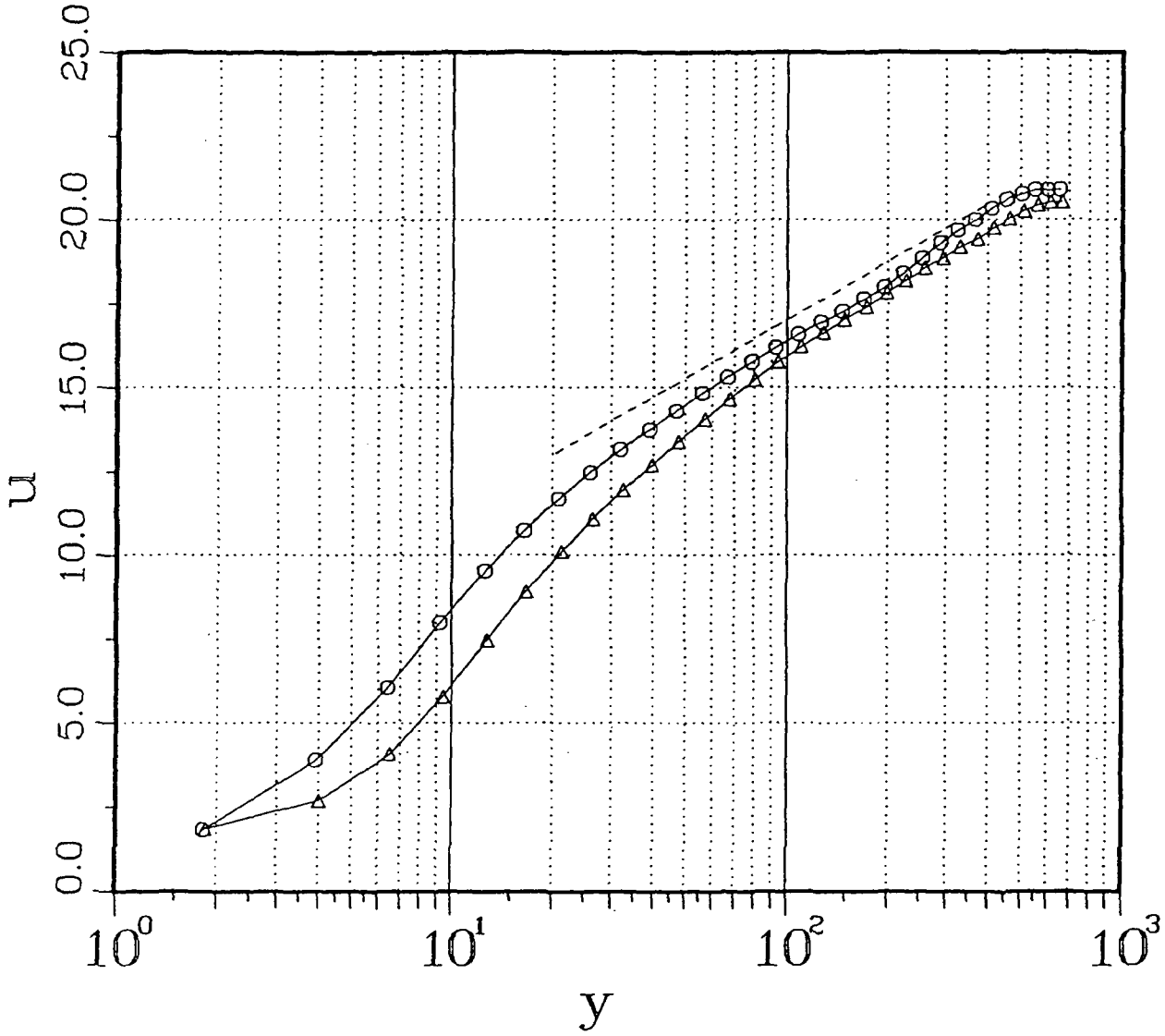

Figure 13.- Comparison of mean streamwise velocity components for perturbed and unperturbed turbulent flows at time step 1020.
○ Unperturbed, △ Perturbed

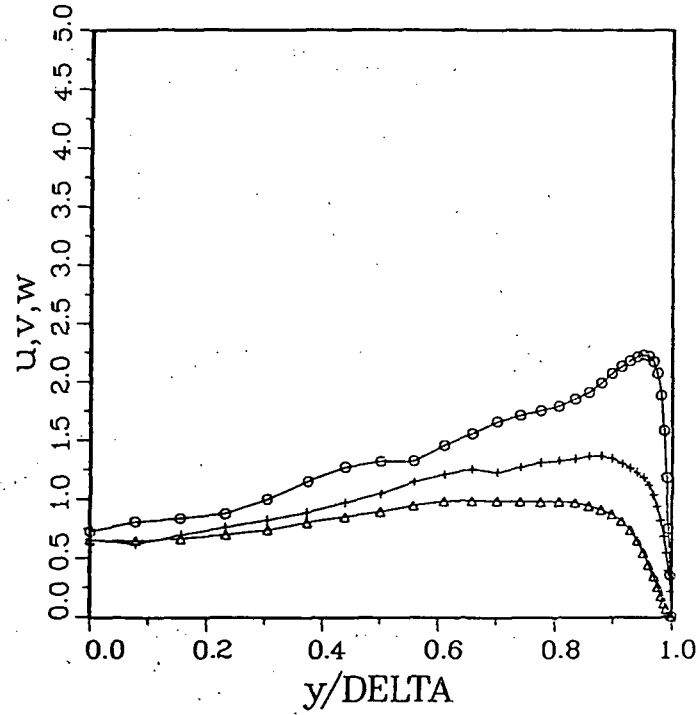

(a) Unperturbed case

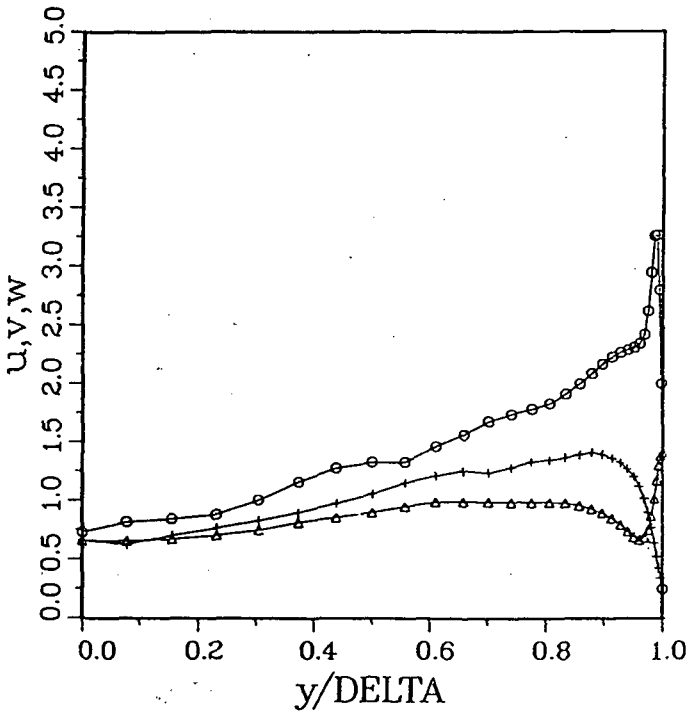

(b) Perturbed case

Figure 14.- Comparison of turbulence intensities near the perturbed wall. o-u, δ-v, +-w

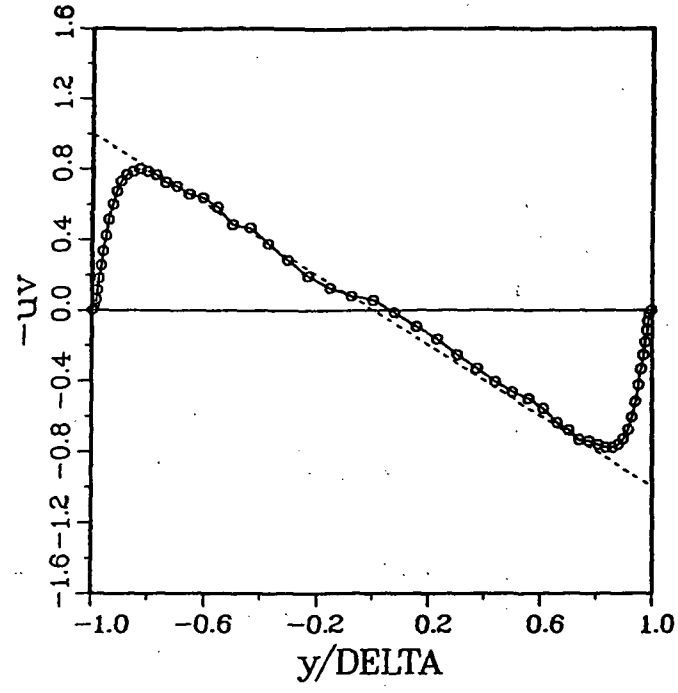

(a) Unperturbed case

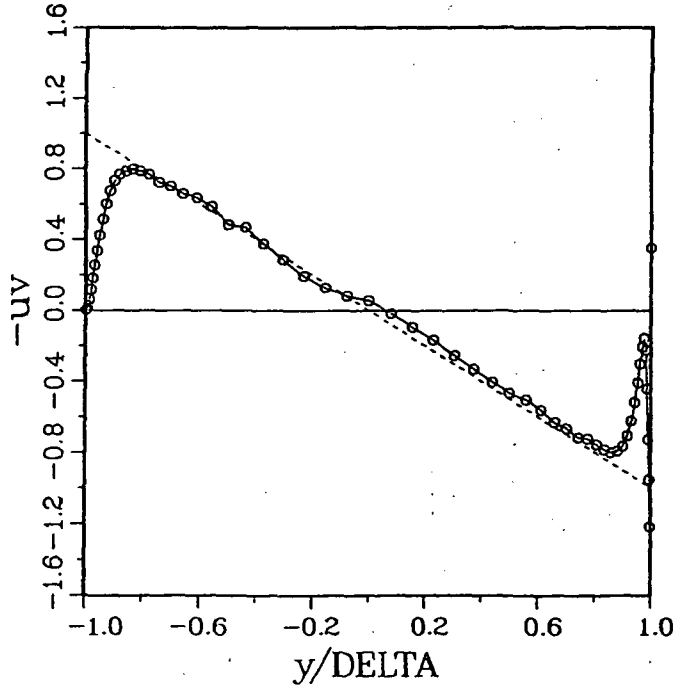

(b) Perturbed case

Figure 15.- Comparison of turbulent shear stress for perturbed and unperturbed channels.

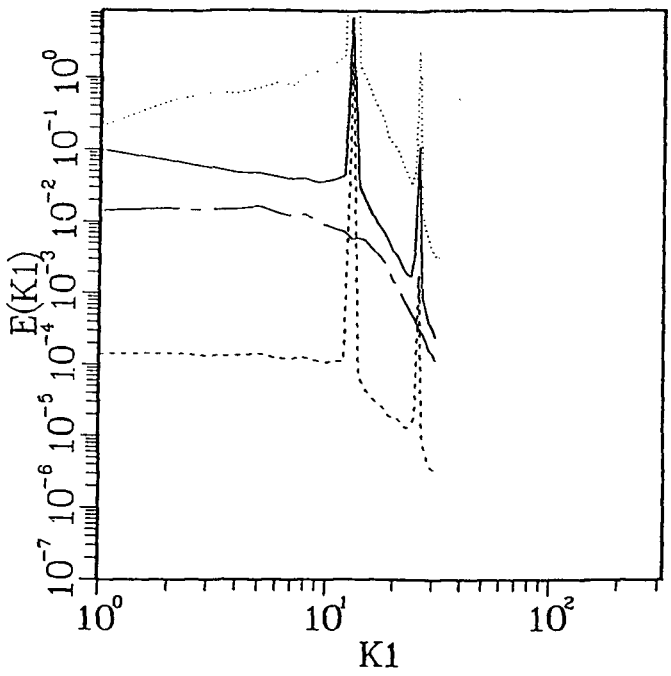

(a) y = 3.85 from perturbed wall

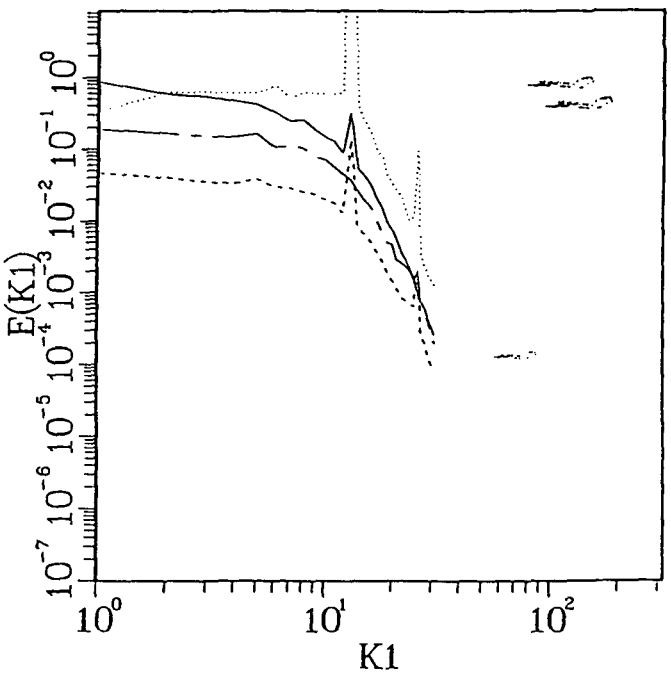

(b) y = 38.2 from perturbed wall

Figure 16.- Energy spectra for turbulent flow with periodic wall velocity perturbation. ——— u, _ _ _ _ _ v, ——— _ ——— w, ... p

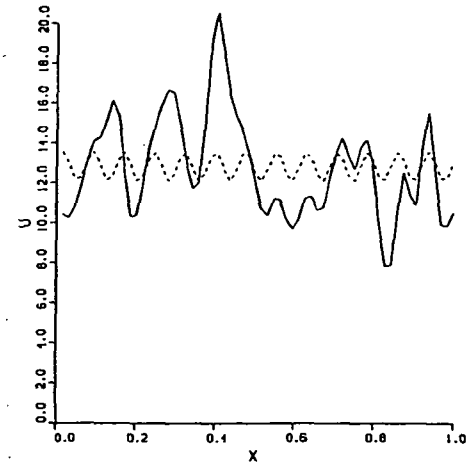

(a) u component

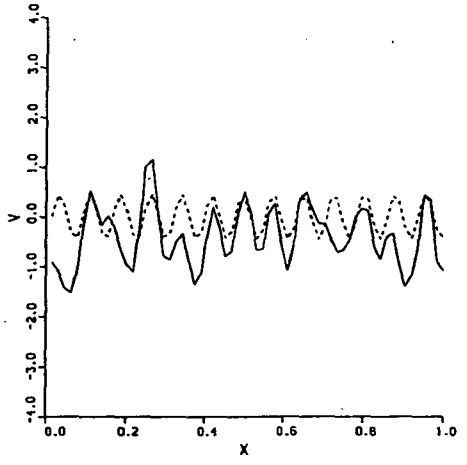

(b) v component

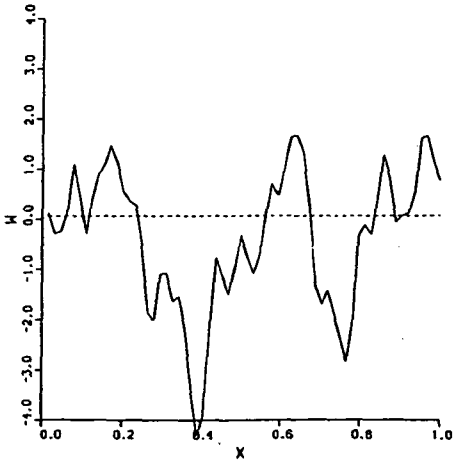

(c) w component

Figure 17.- Velocity distributions for perturbed channel flow and periodic component from least square. _____ instantaneous velocity _ _ _ _ _ periodic component + mean velocity

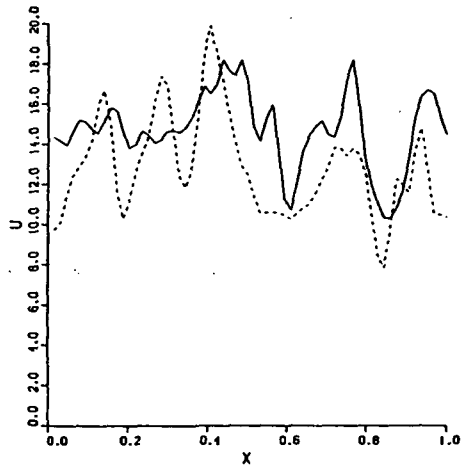

(a) u component

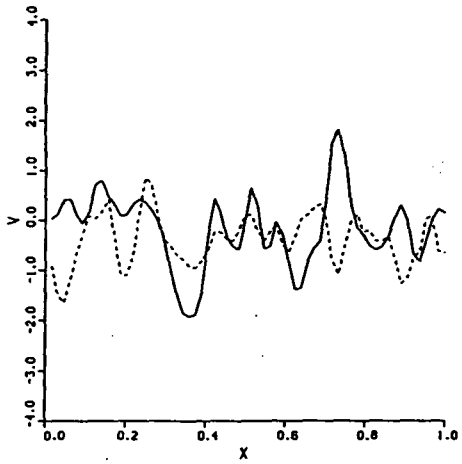

(b) v component

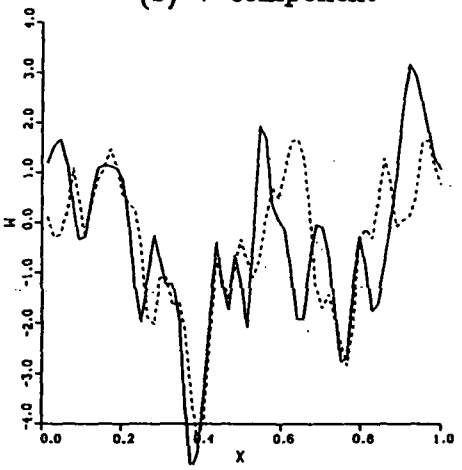

(c) w component

Figure 18.- Comparison of unperturbed velocity solution with perturbed solution after removal of periodic component. _____ unperturbed solution _ _ _ _ _ perturbed solution - periodic component.

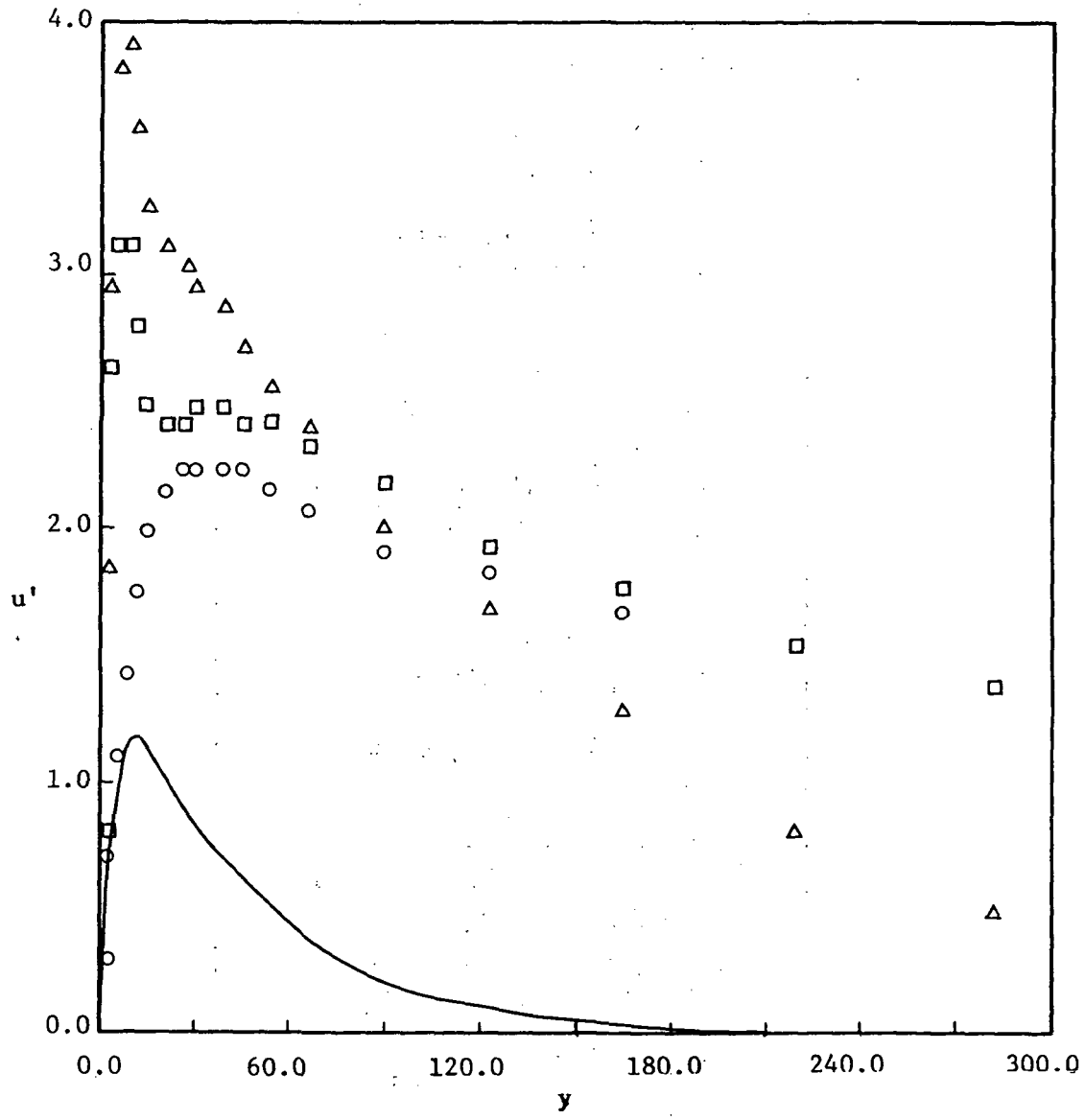

(a) u'

Figure 19.- Comparison of perturbed and unperturbed turbulence intensities and perturbed laminar fluctuation intensities ○ unperturbed turbulent, □ perturbed turbulent, △ difference, _____ laminar.

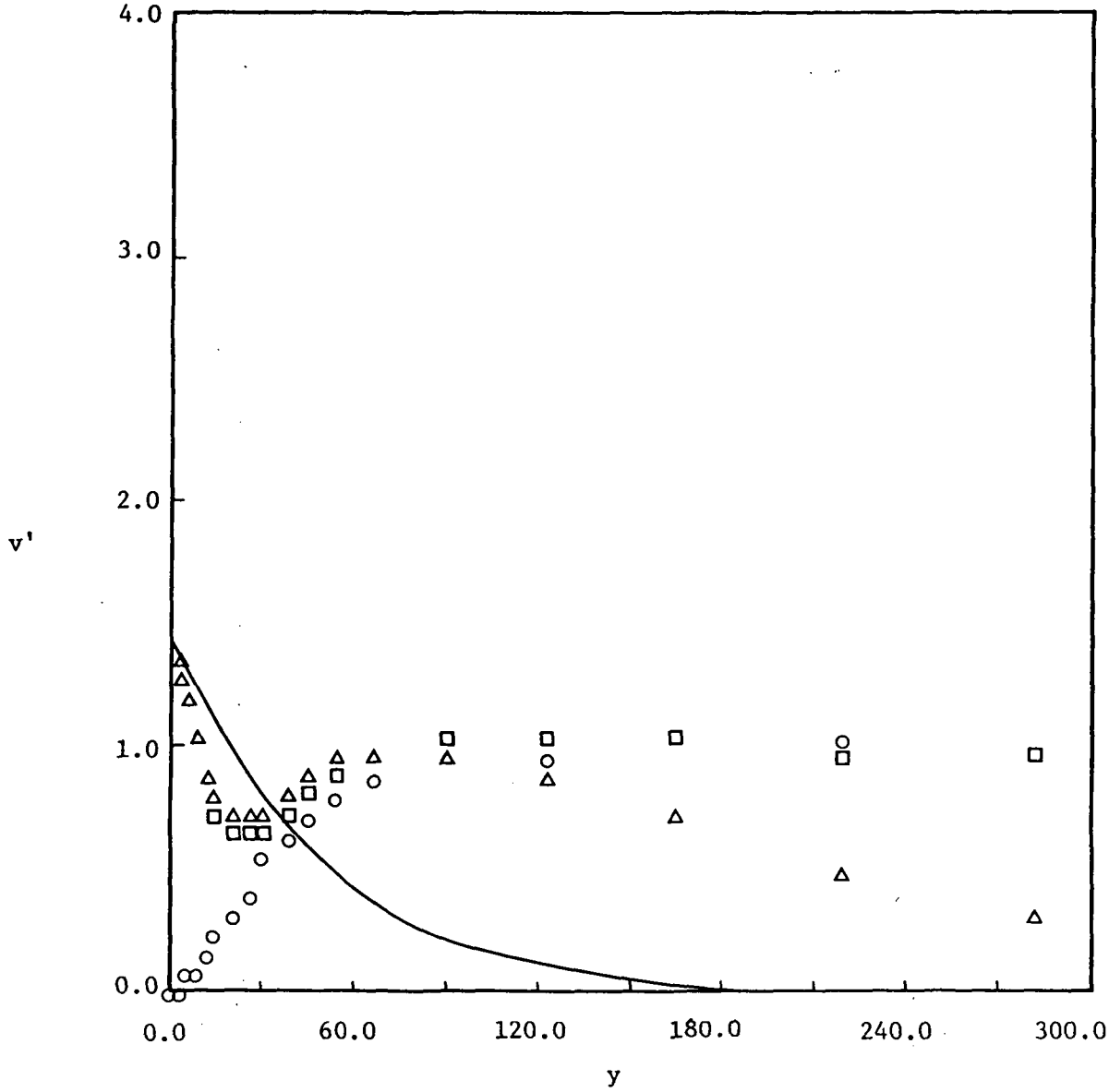

(b) v′

Figure 19.- Continued.

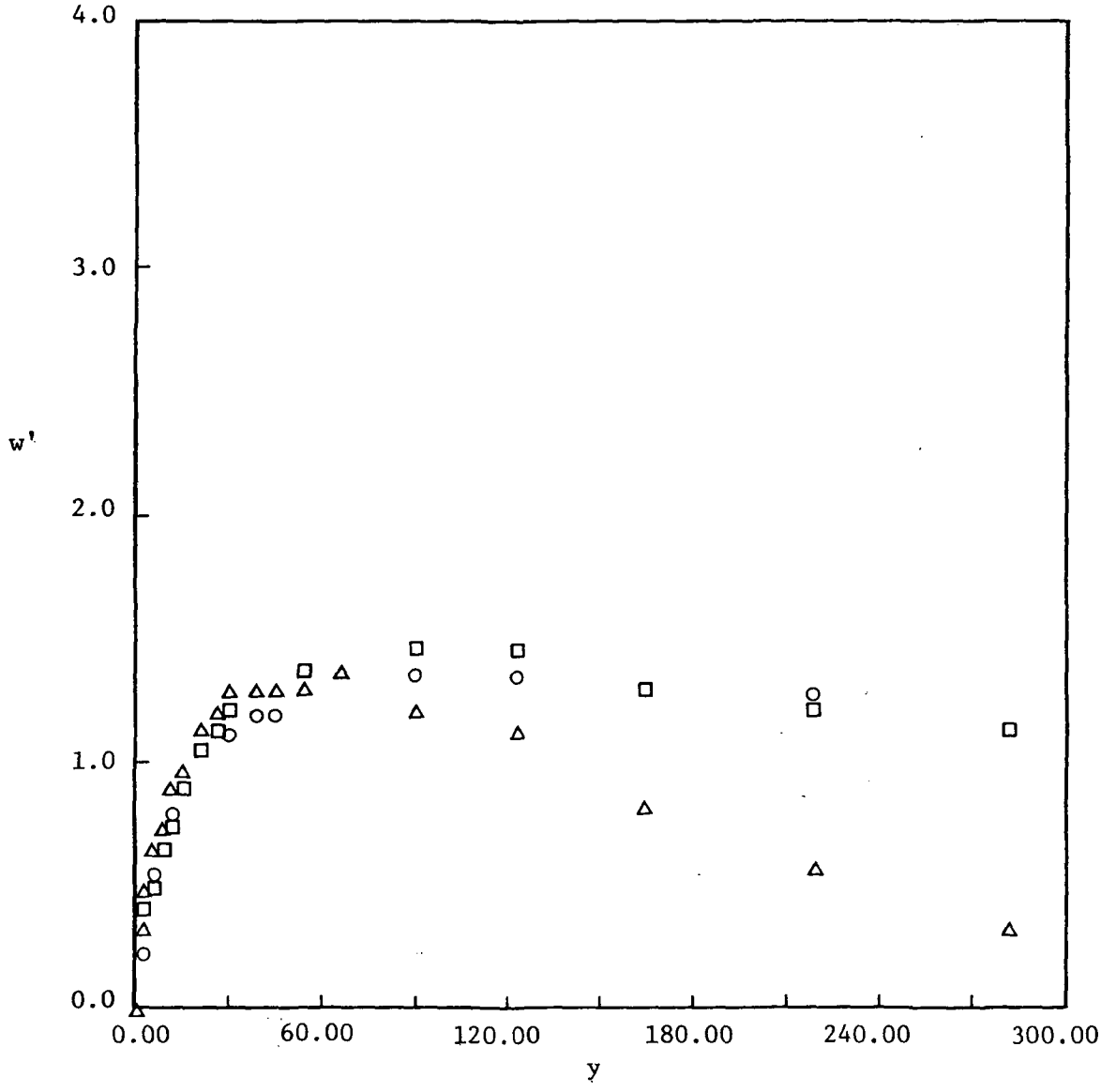

(c) w'

Figure 19.- Continued.

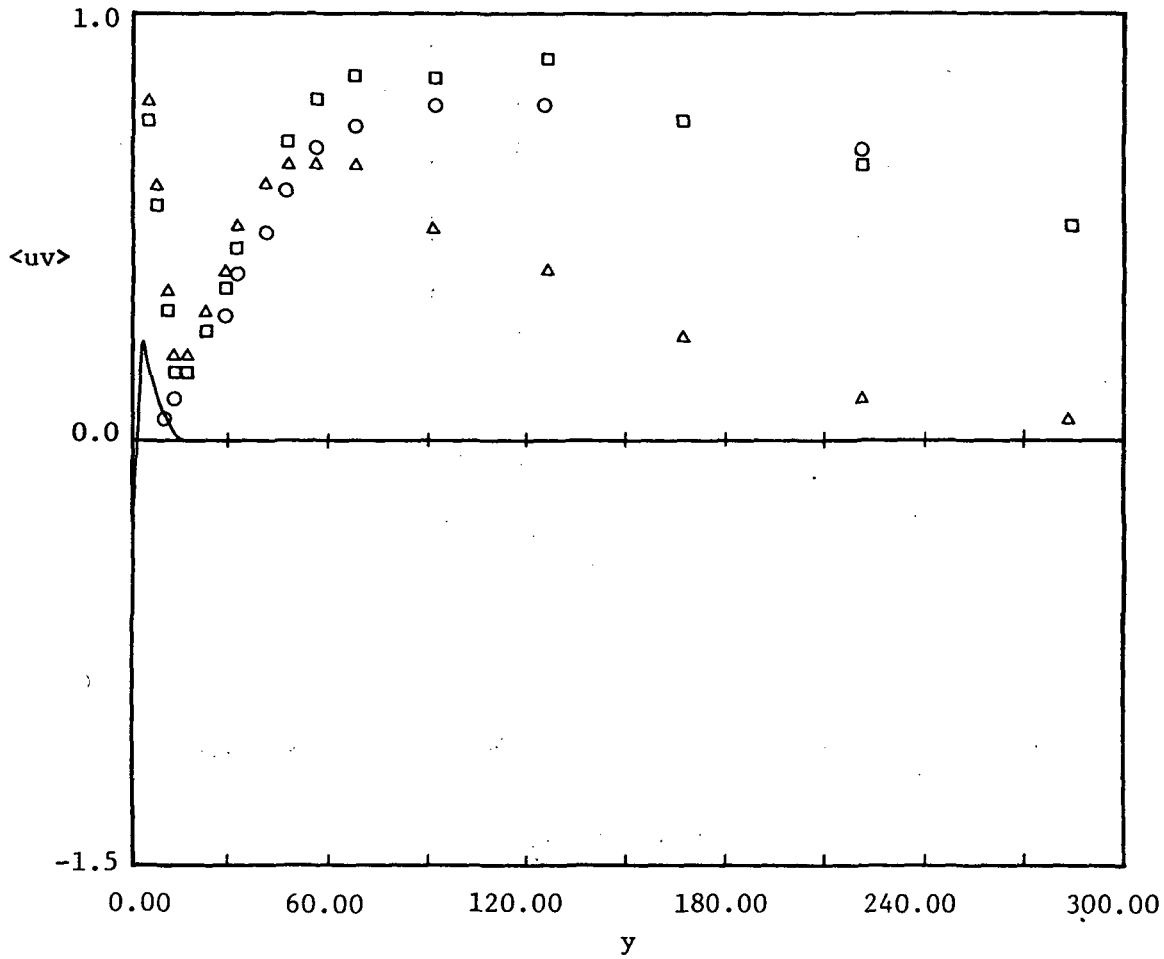

(d) <uv>

Figure 19.- Concluded.

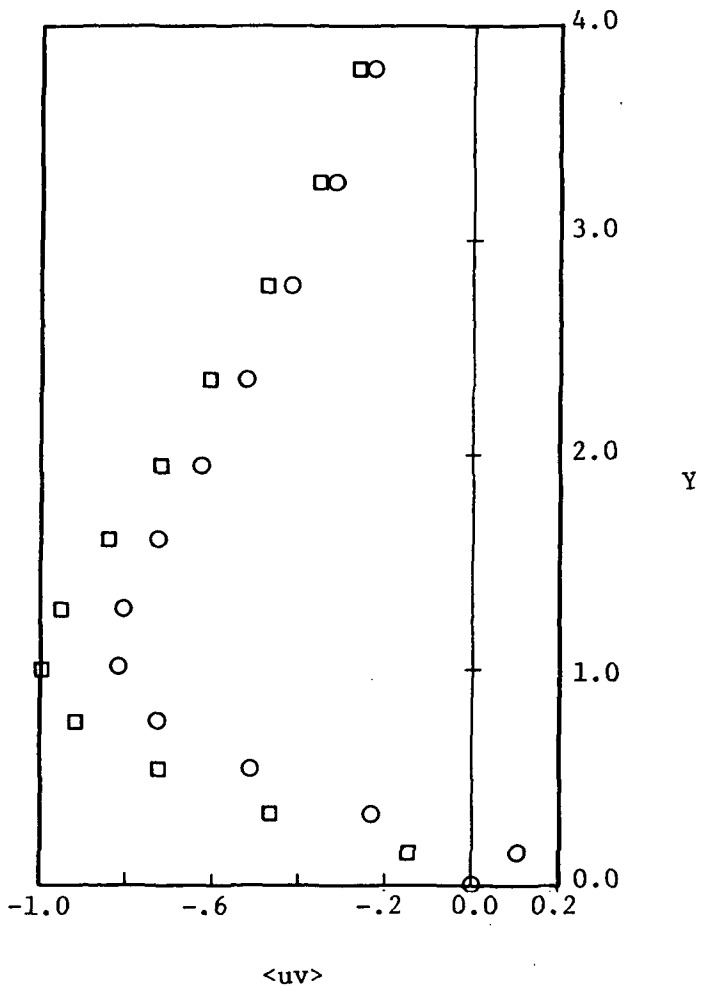

Figure 20.- Mean flow through a channel with periodic velocity on one wall.

○ $-V = V_o \sin[(2\pi/\lambda)(x-ct)]$, $u = V\tan(10°)$

□ $-V = V_o \sin[(2\pi/\lambda)(x-ct)]$, $u = 0$

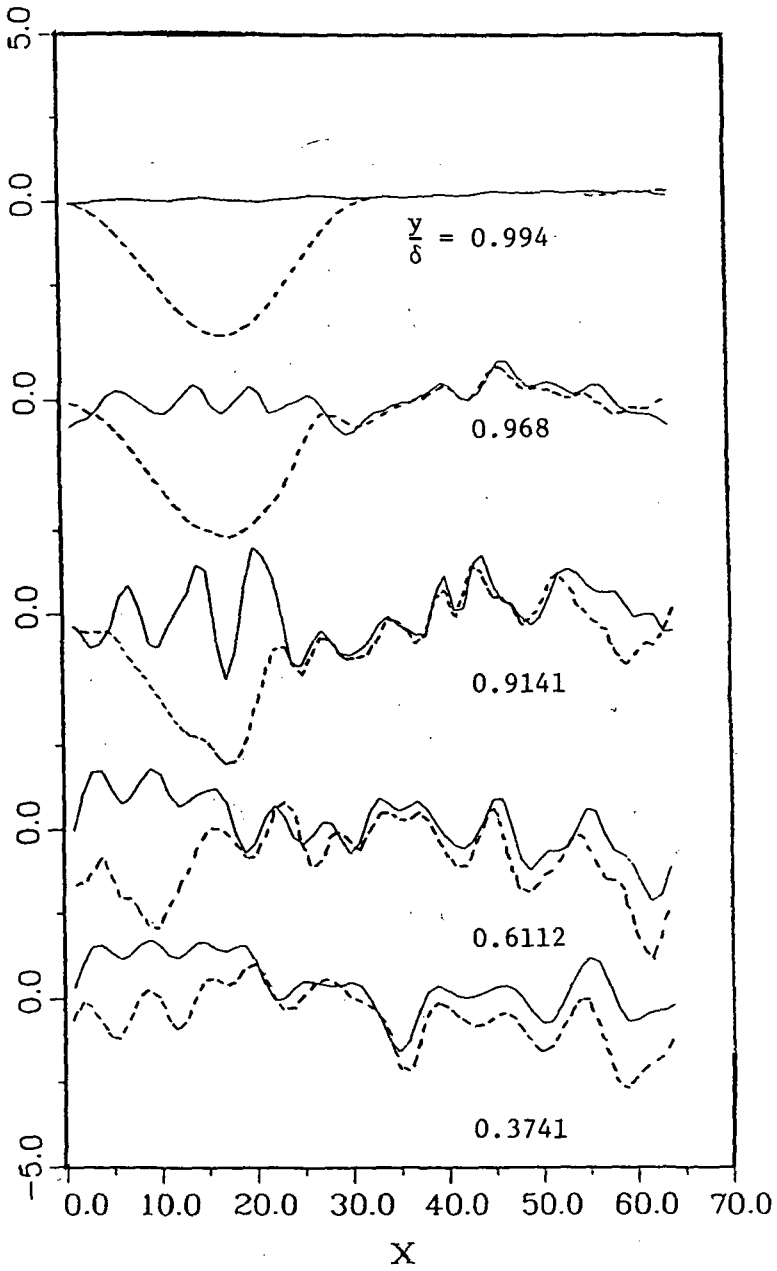

(a) Upper part of Channel

Figure 21.- Comparison of steady flow turbulence distributions with those from flow perturbed by staggered blowing/suction at channel walls after 160 time steps.

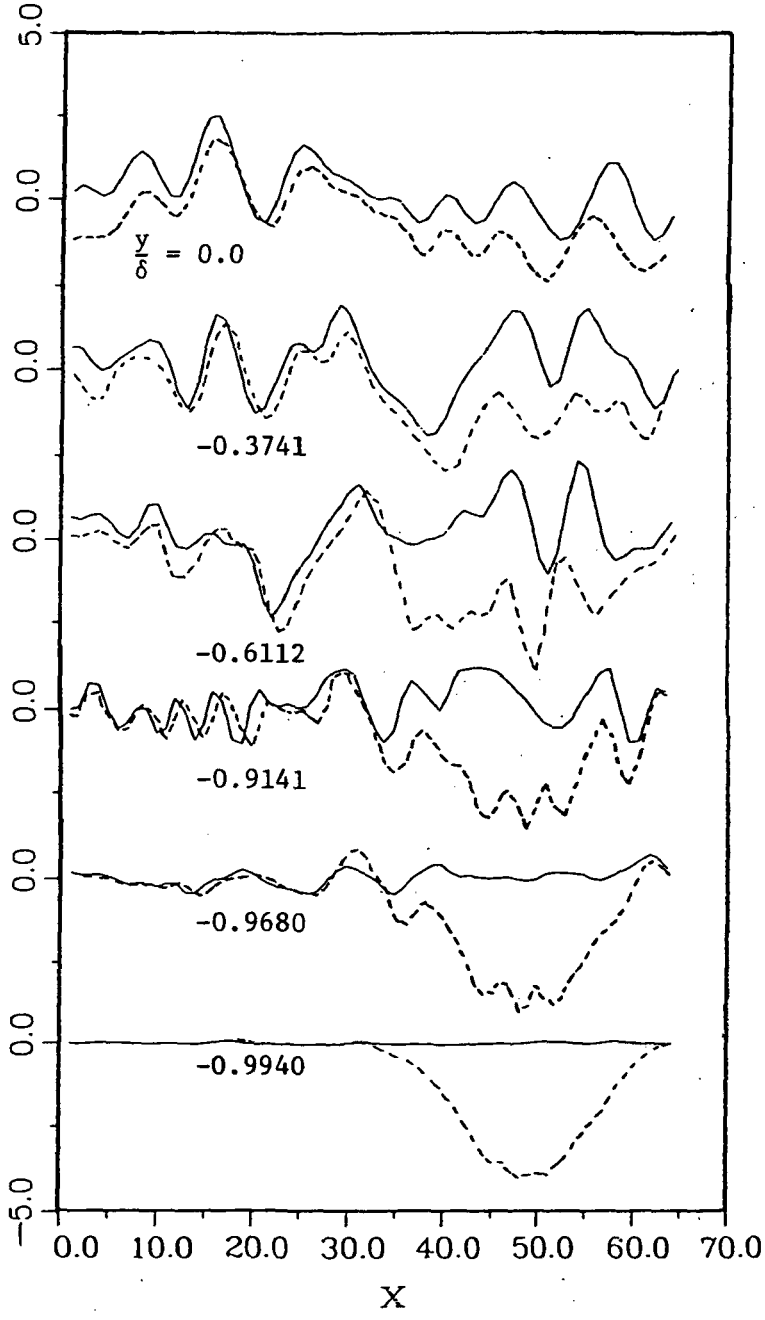

(b) Lower part of Channel

Figure 21.- Concluded.

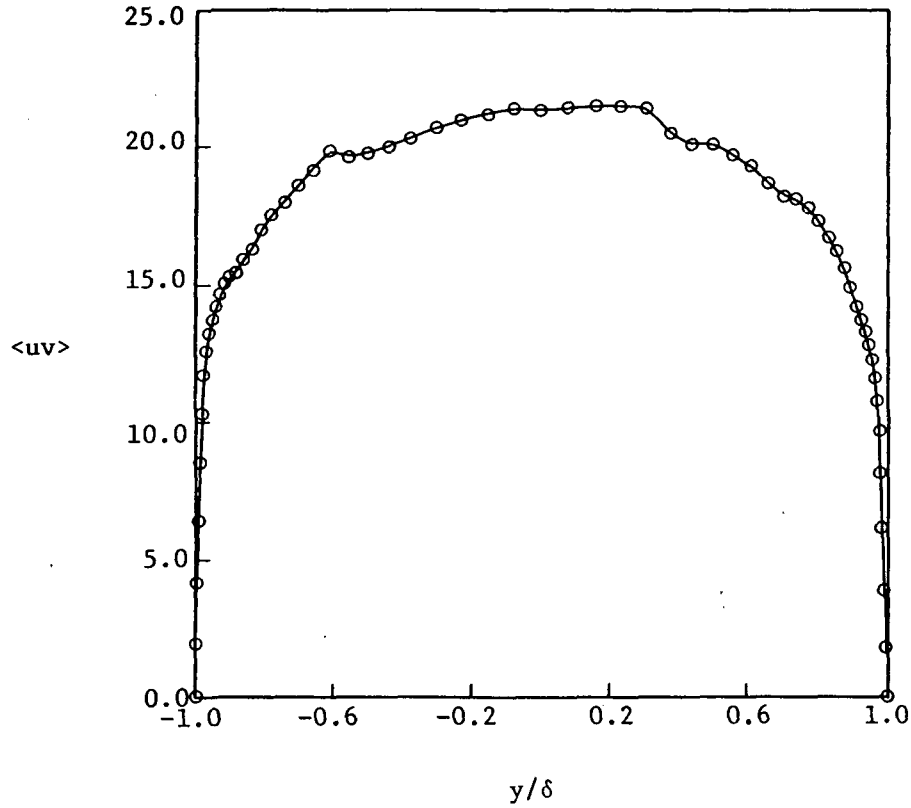

(a) Initial profile at upper wall blowing (UWB) station

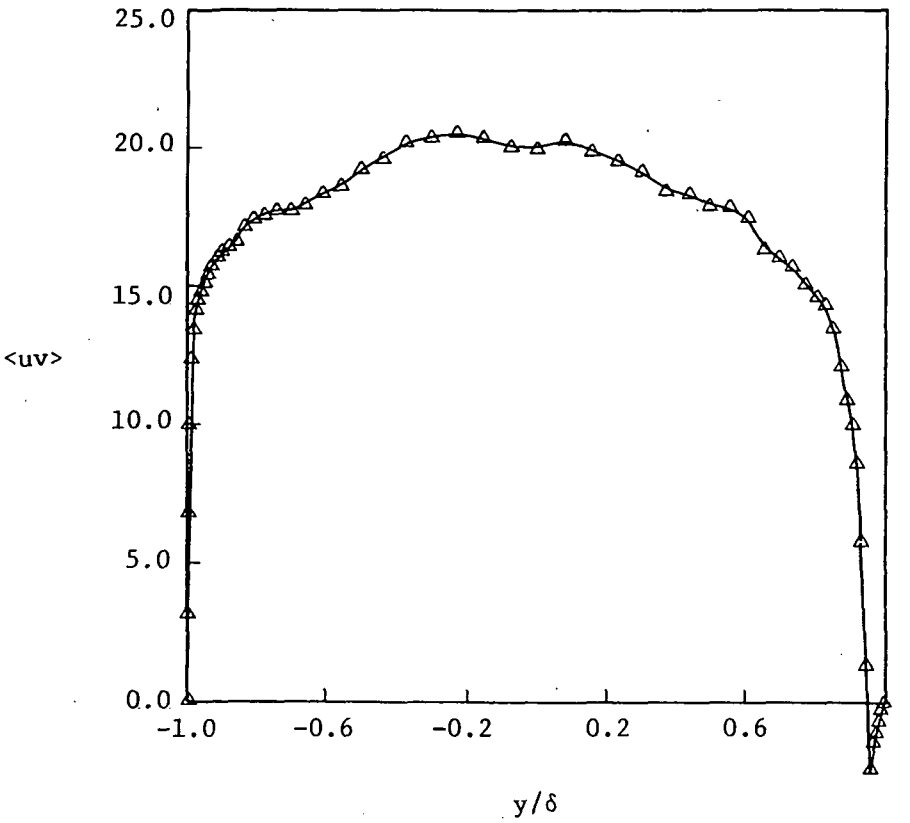

(b) Profile after 80 steps at UWB station.

Figure 22.- Mean velocity profiles at observation stations for blowing/suction boundary conditions.

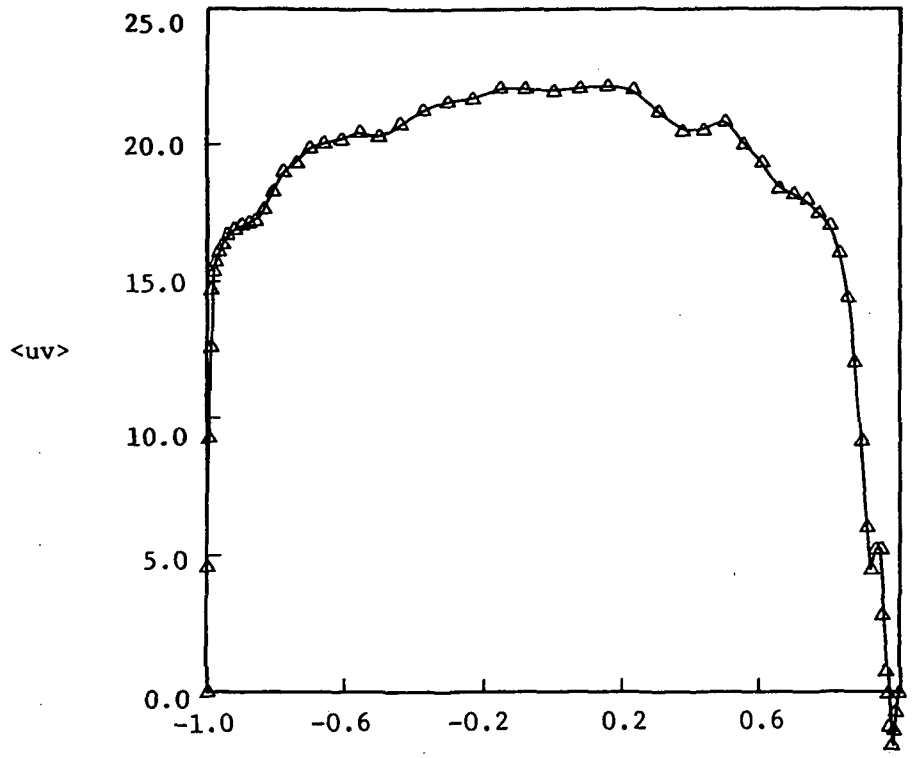

(c) Profile after 120 steps at UWB station

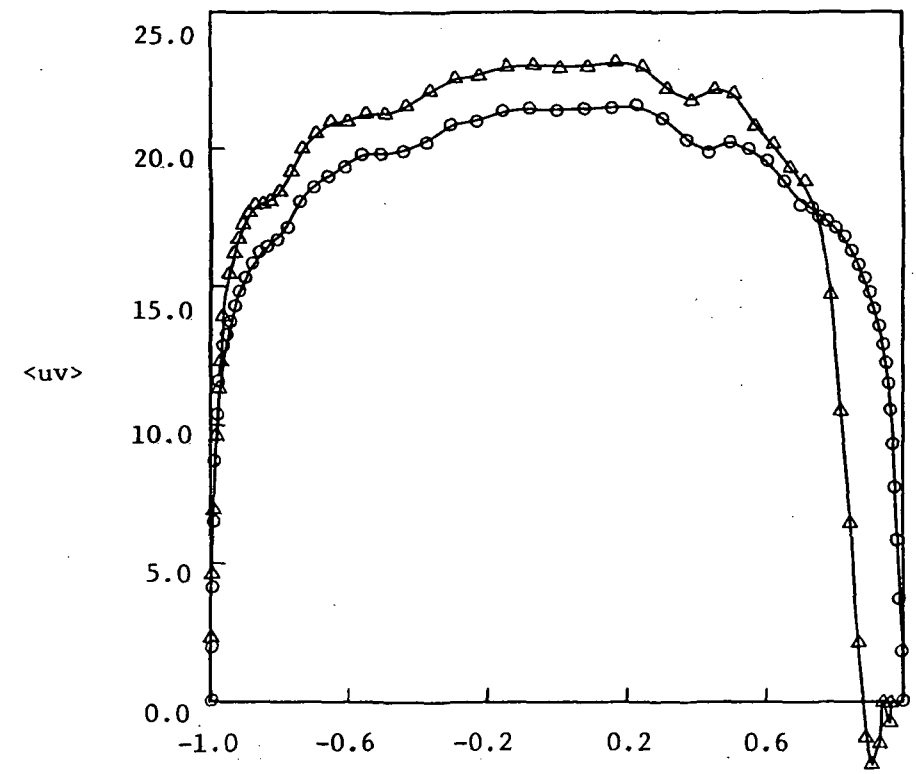

(d) Profile after 160 steps at UWB station

Figure 22.- Continued.

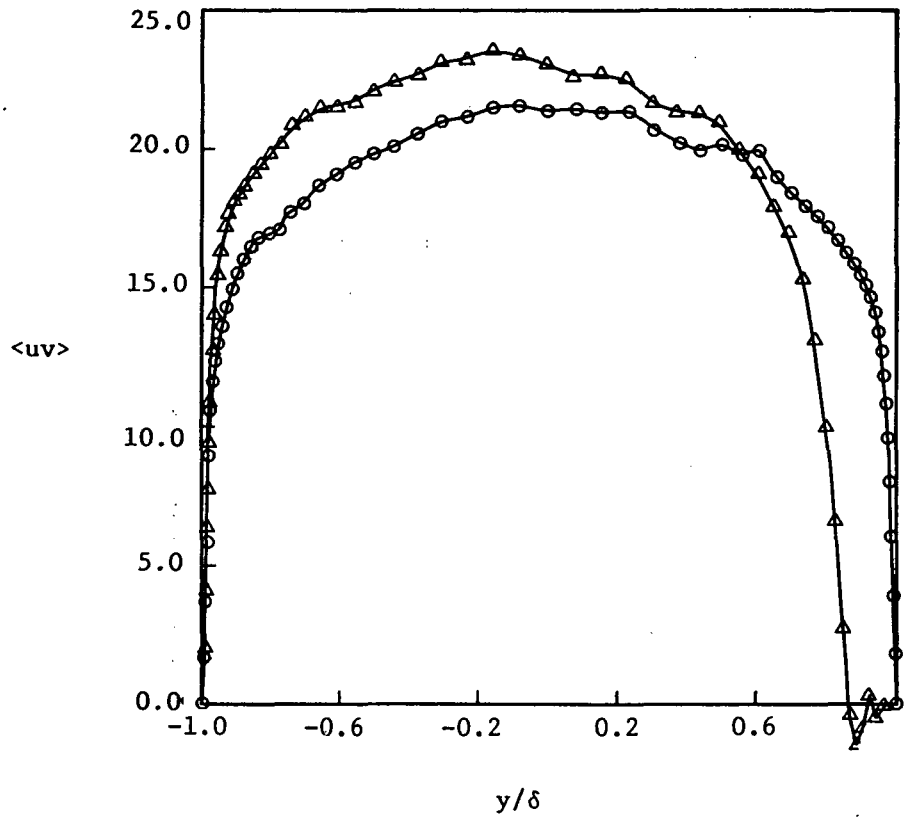

(e) Profile after 320 steps at UWB station

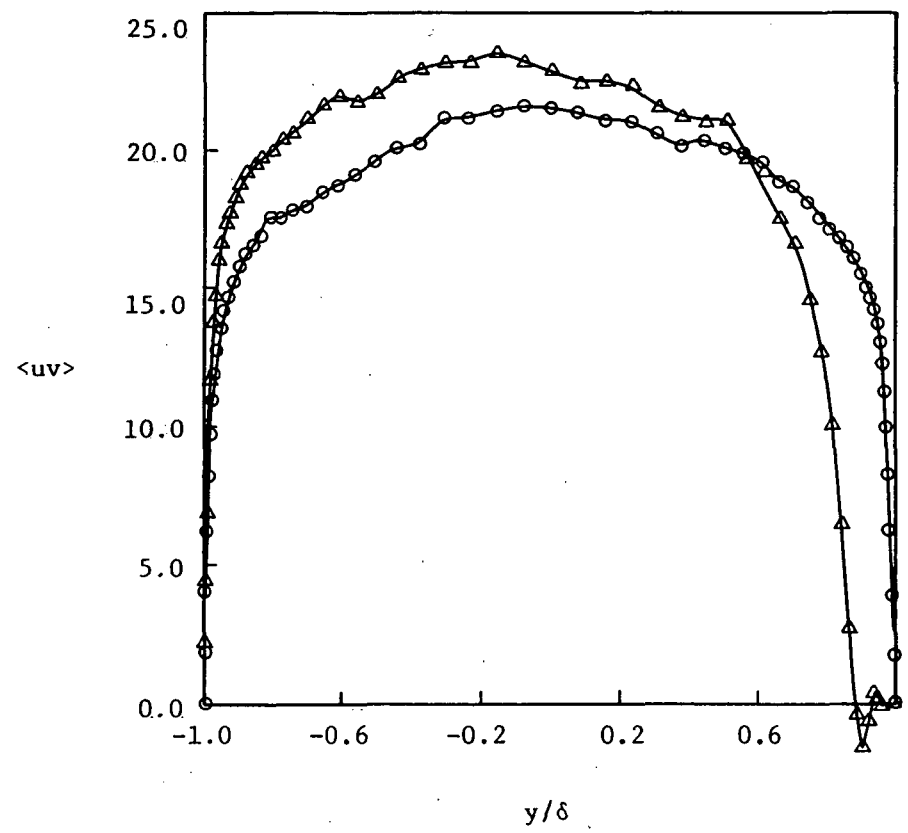

(f) Profile after 480 steps at UWB station

Figure 22.- Continued.

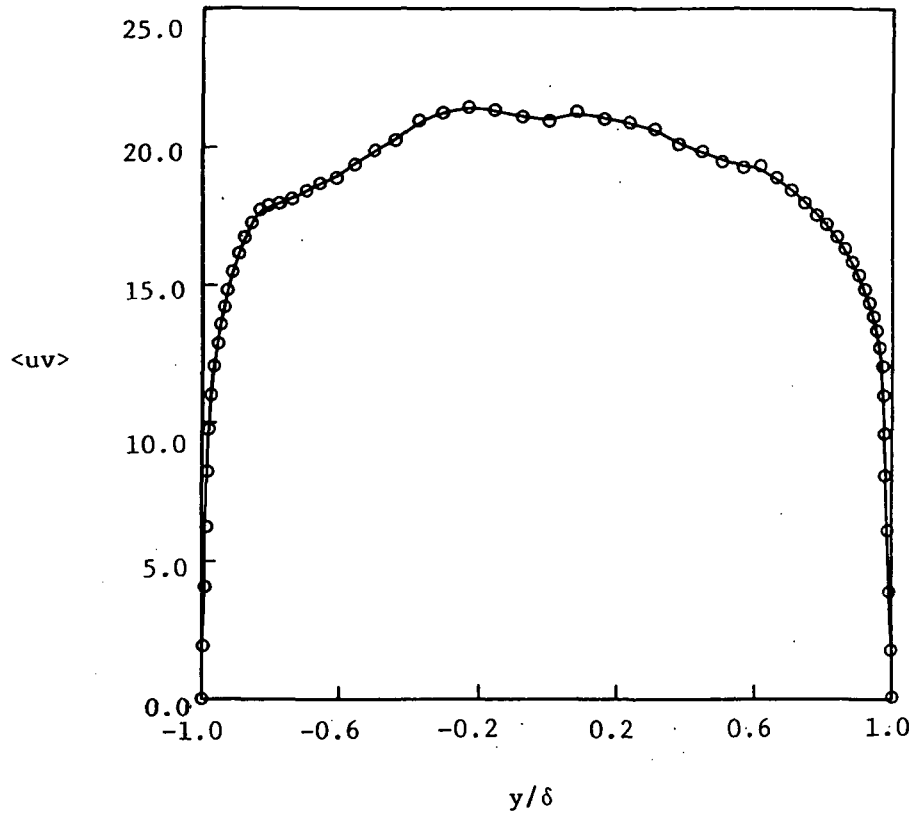

(g) Initial profile at lower wall suction (LWS) station

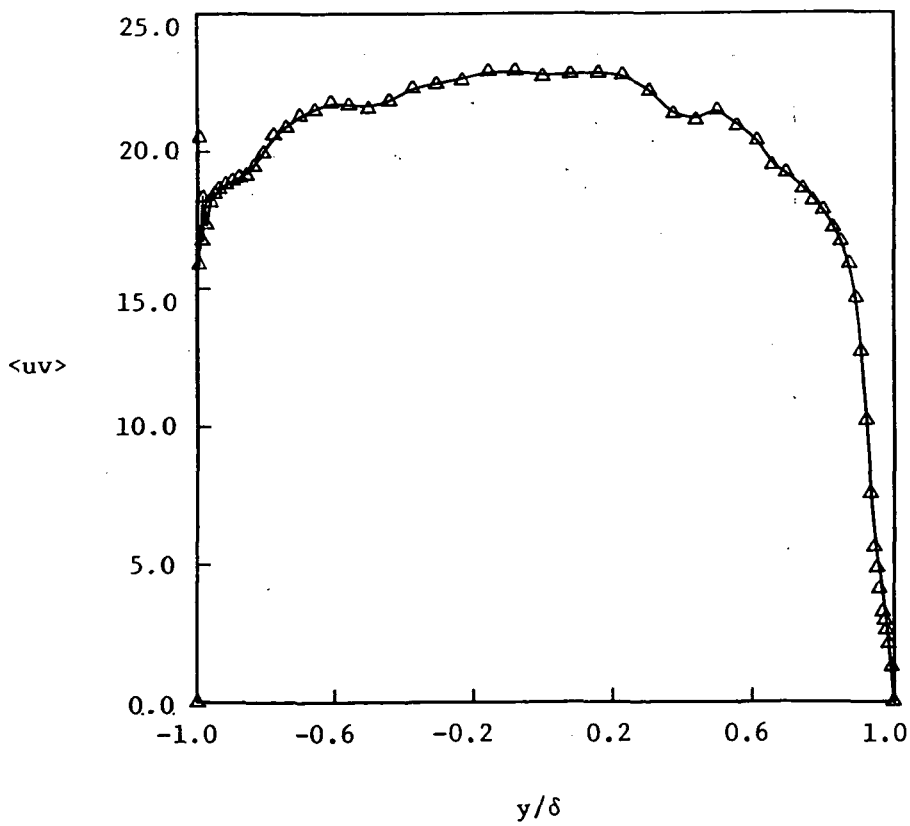

(h) Profile after 80 steps at LWS station

Figure 22.- Continued.

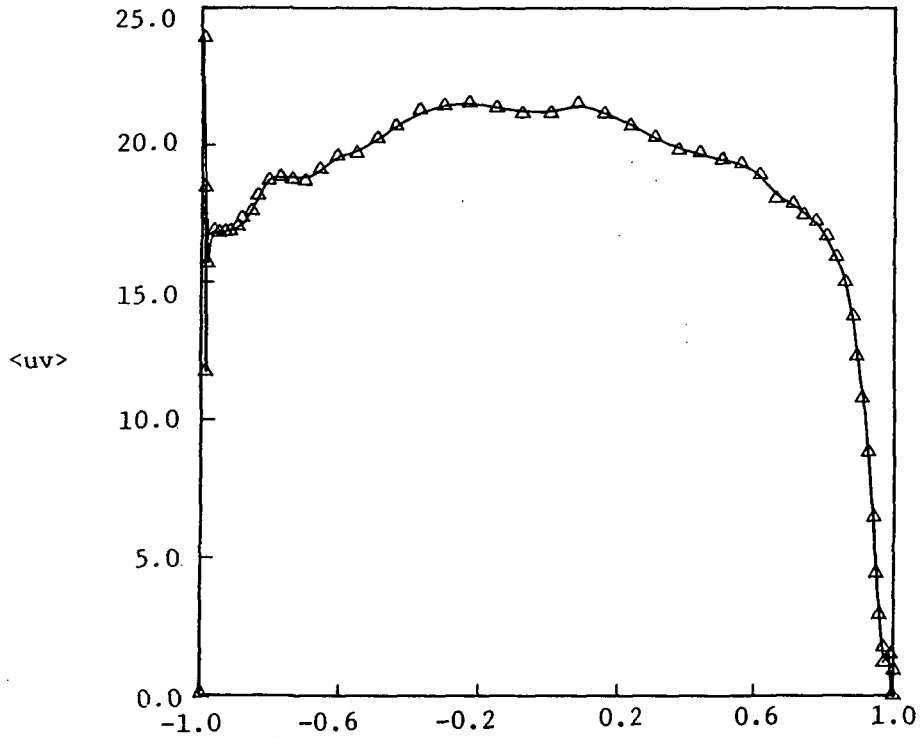

(i) Profile after 120 steps at LWS station

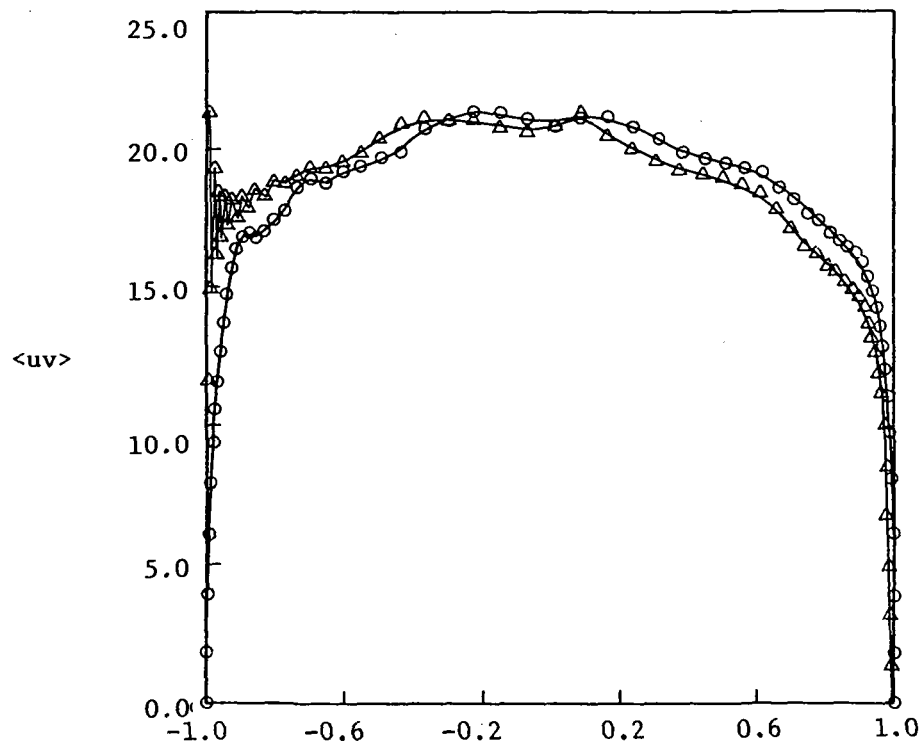

(j) Profile after 160 steps at LWS station

Figure 22.- Continued.

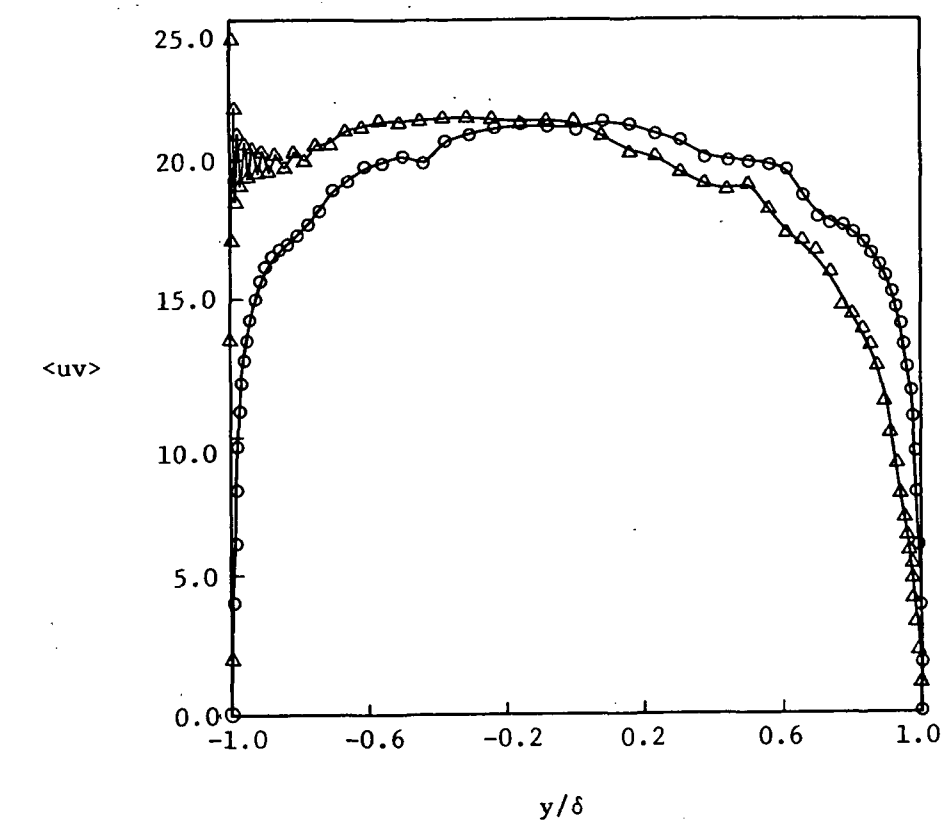

(k) Profile after 320 steps at LWS station

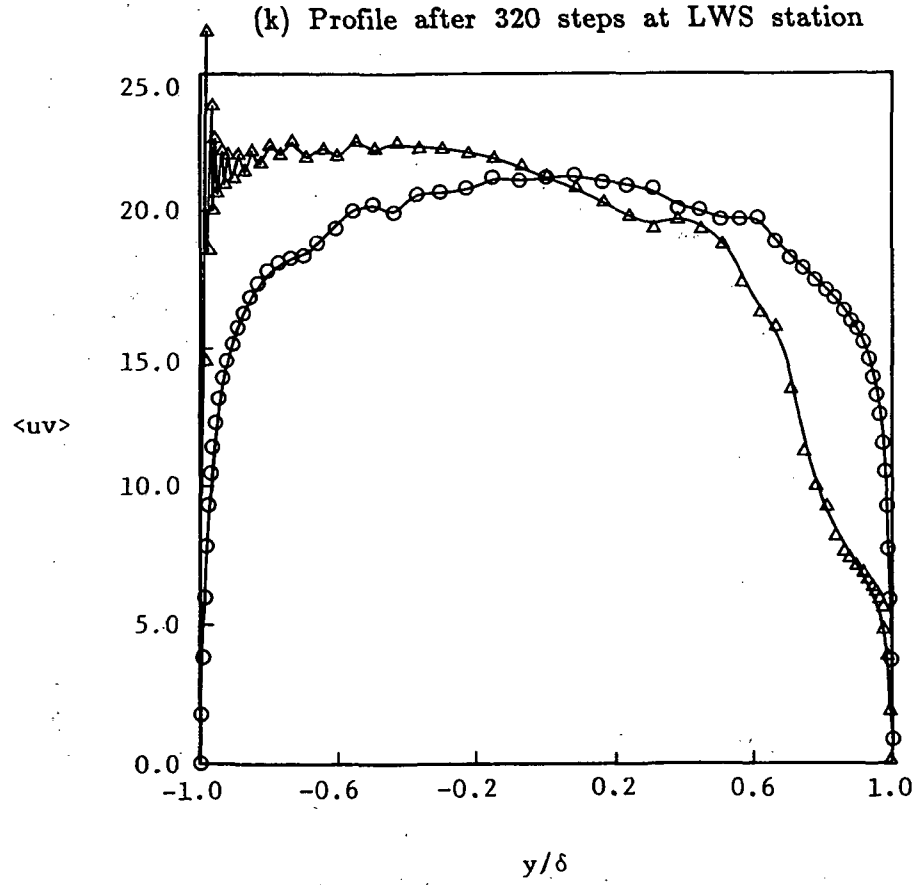

(l) Profile after 480 steps at LWS station

Figure 22.- Concluded.

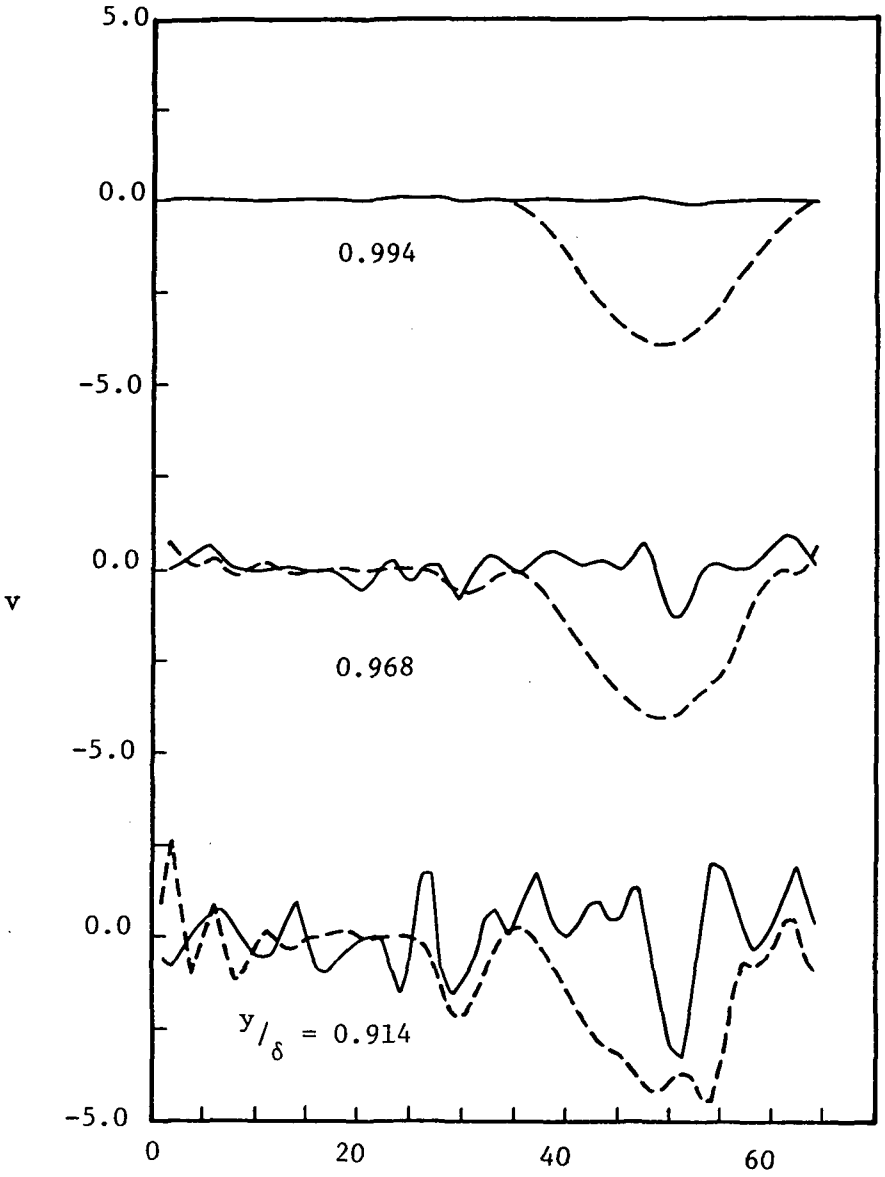

(a) Upper part of channel

Figure 23.- Comparison of vertical component of turbulence for steady mean flow and for flow perturbed by staggered blowing/suction distributions after 480 steps.
_____steady, _ _ _ _ _perturbed

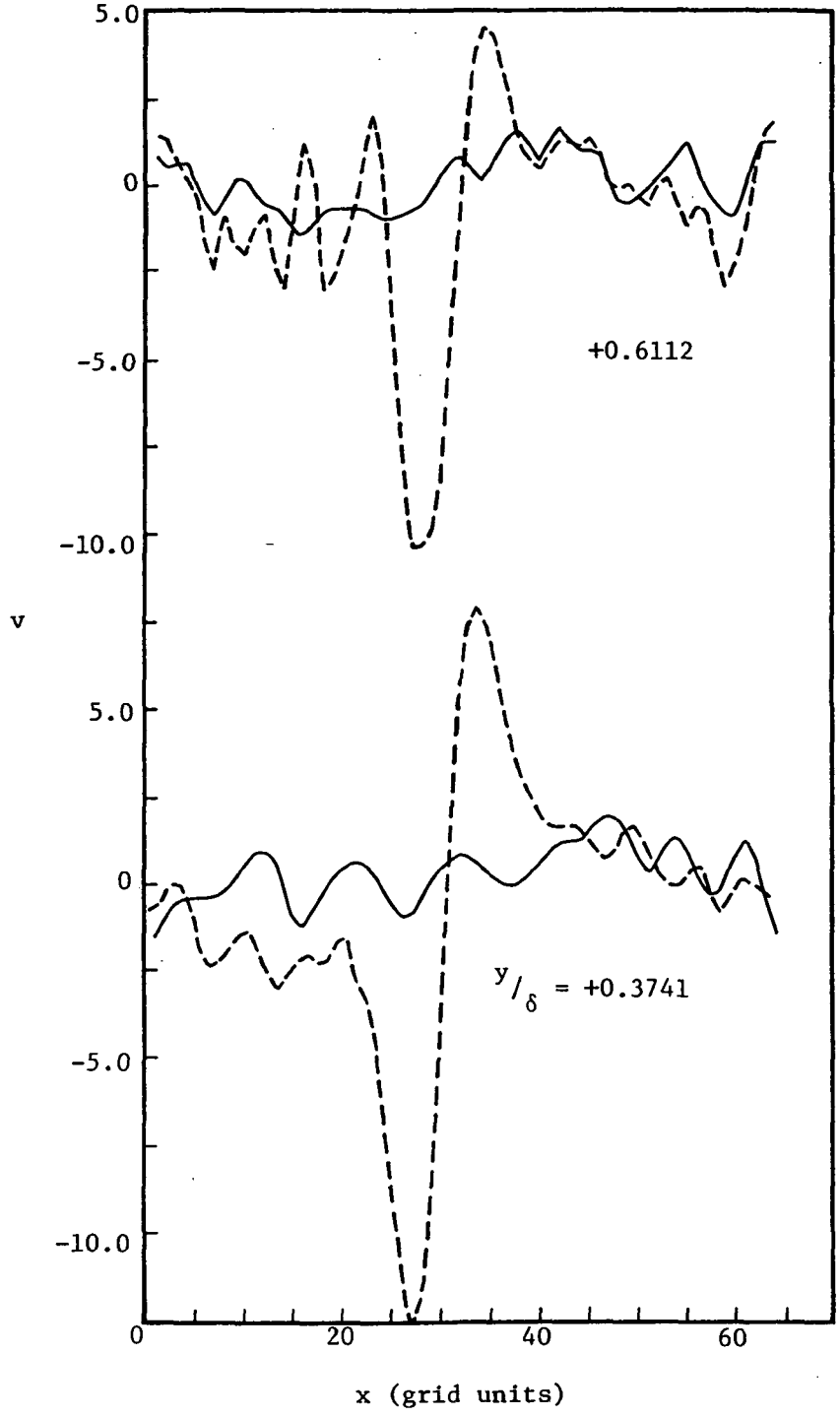

(b) Central part of channel

Figure 23.- Continued

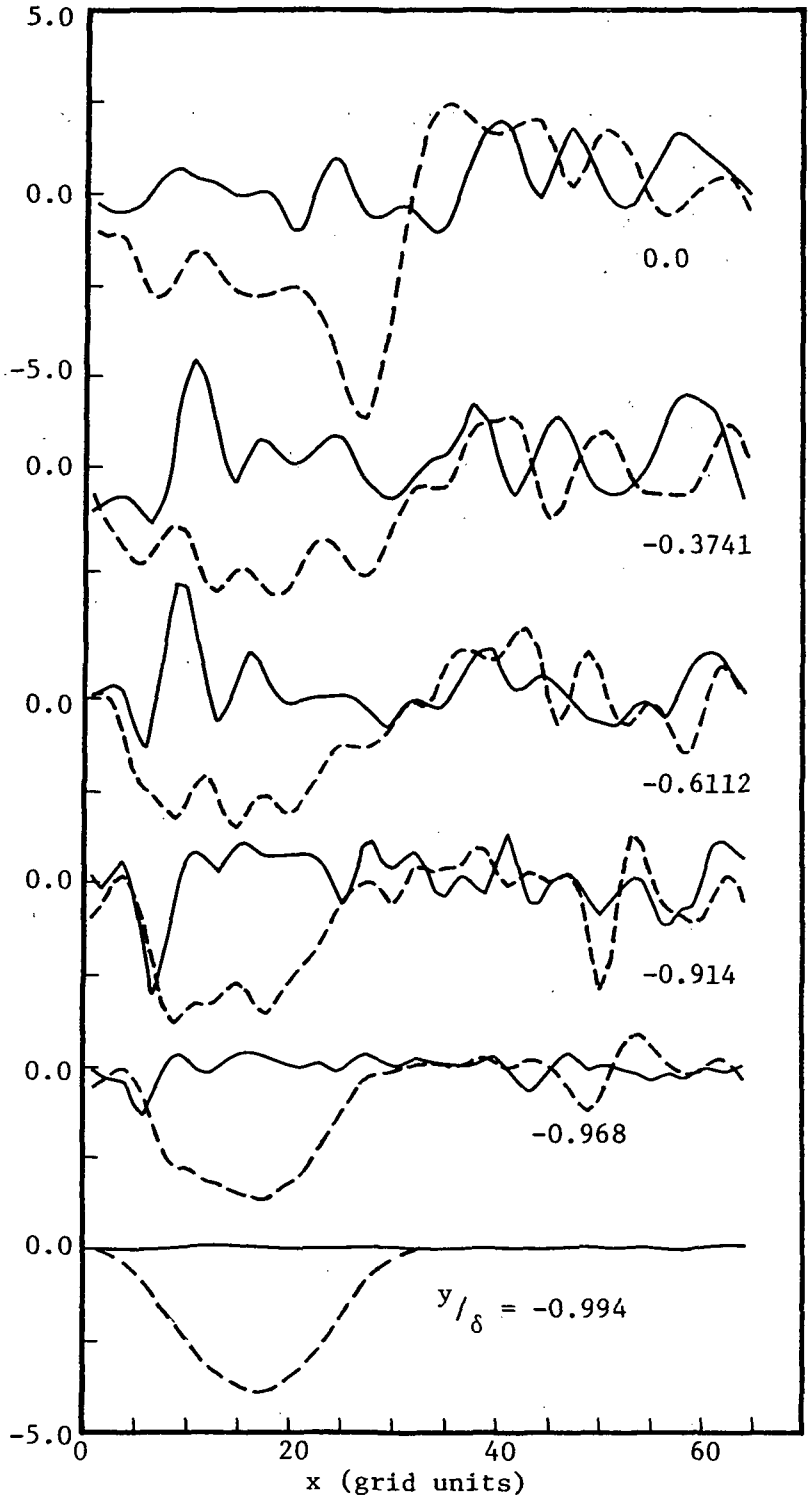

(c) Lower part of channel

Figure 23.- Concluded

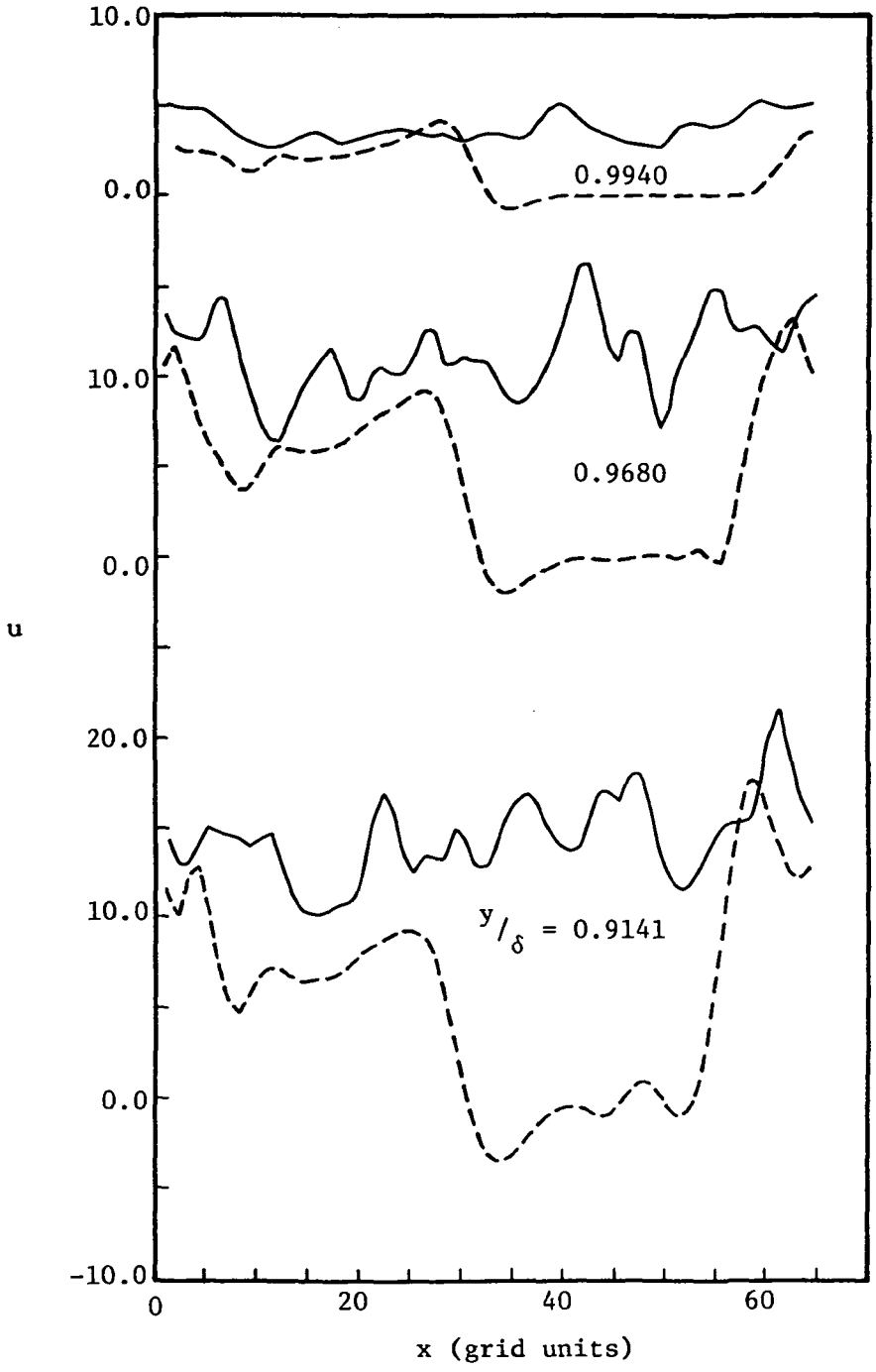

(a) Upper part of channel

Figure 24.- Comparison of streamwise component of turbulence from steady flow and for flow perturbed by staggered blowing/suction distributions after 480 steps. _____steady, _ _ _ _ _ perturbed.

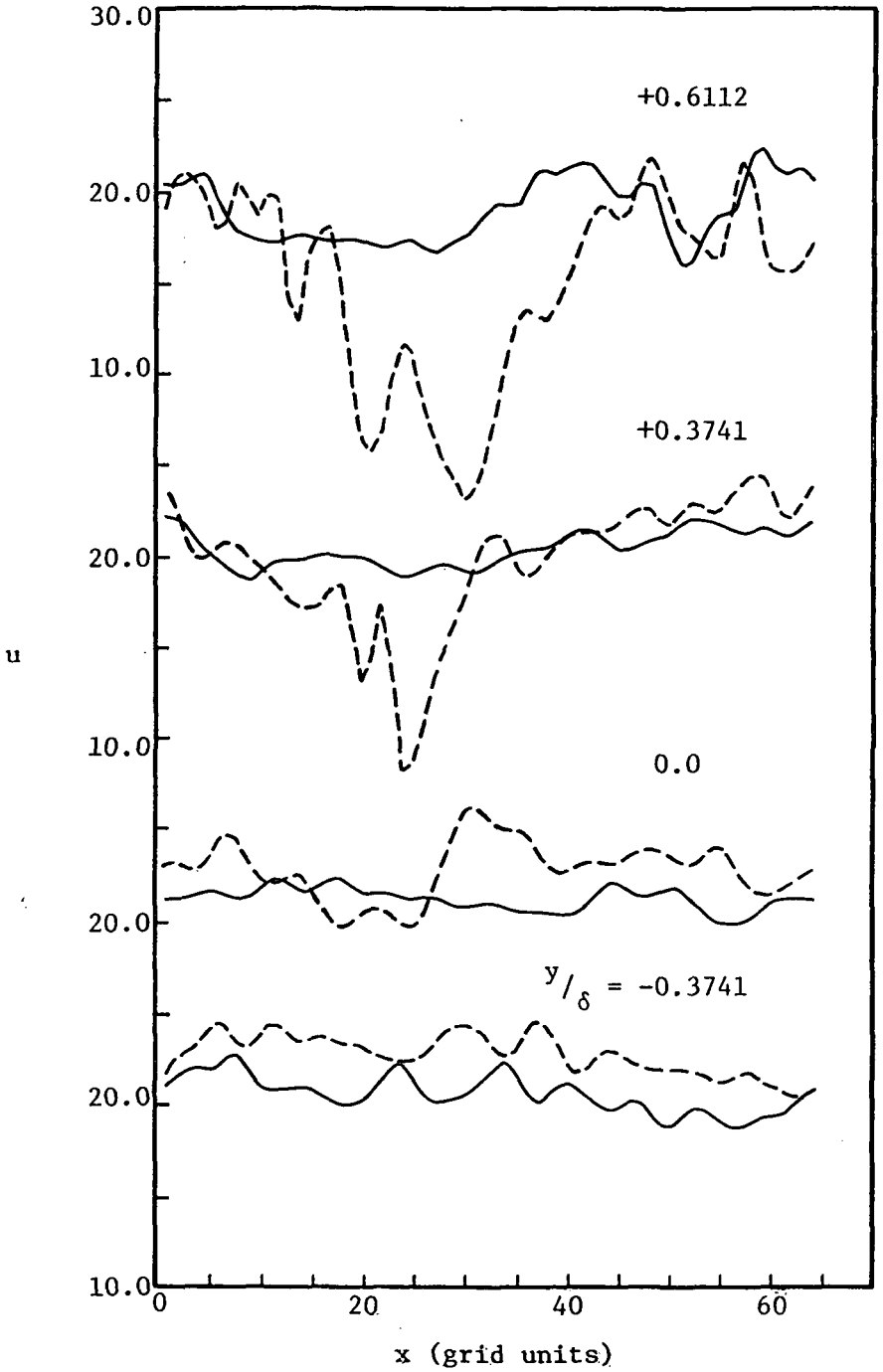

(b) Central part of channel

Figure 24.- Concluded.

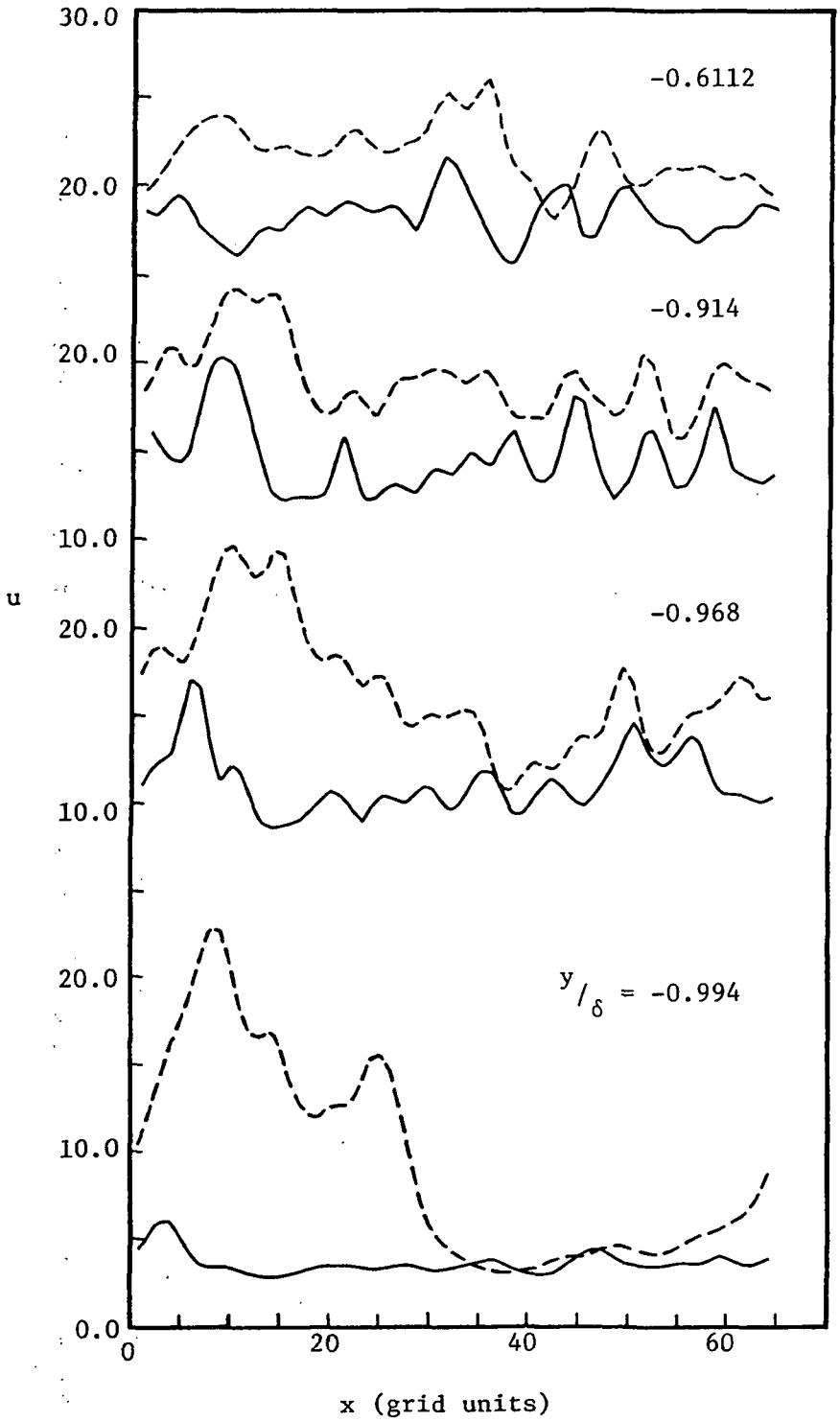

(c). lower part of channel

Figure 24.- Continued.

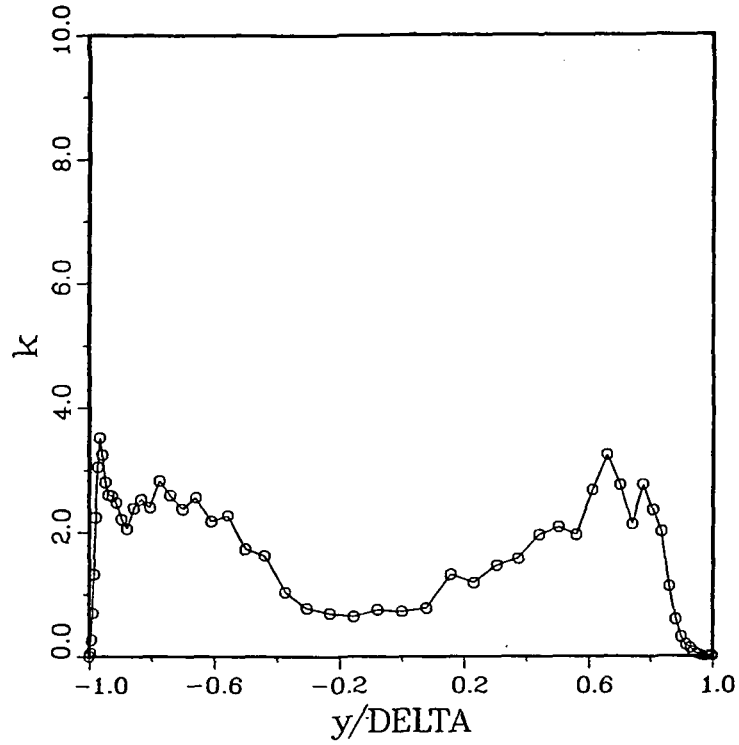

(a) Perturbed solution at UWB station

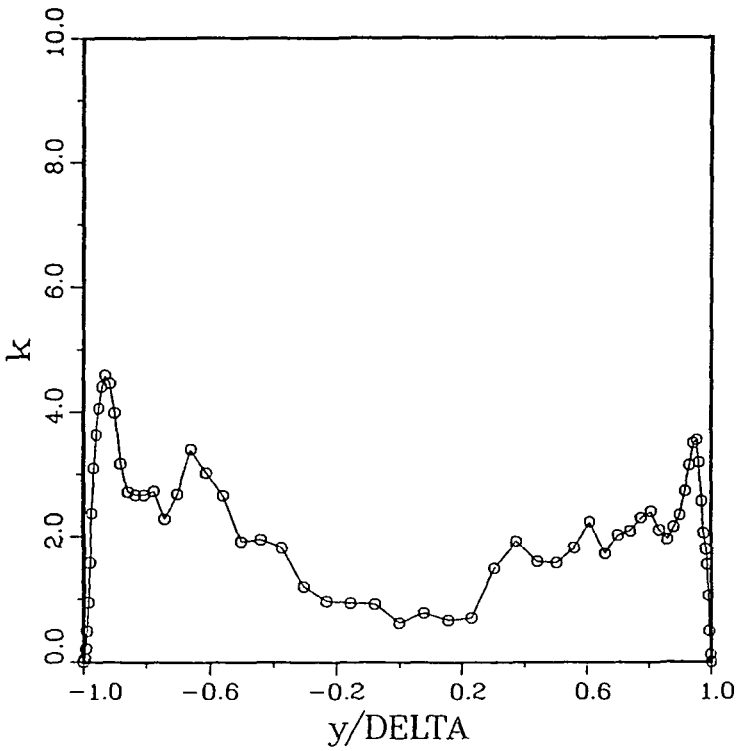

(b) Unperturbed solution at UWB station

Figure 25.- Turbulence kinetic energy at blowing/suction stations after 320 steps.

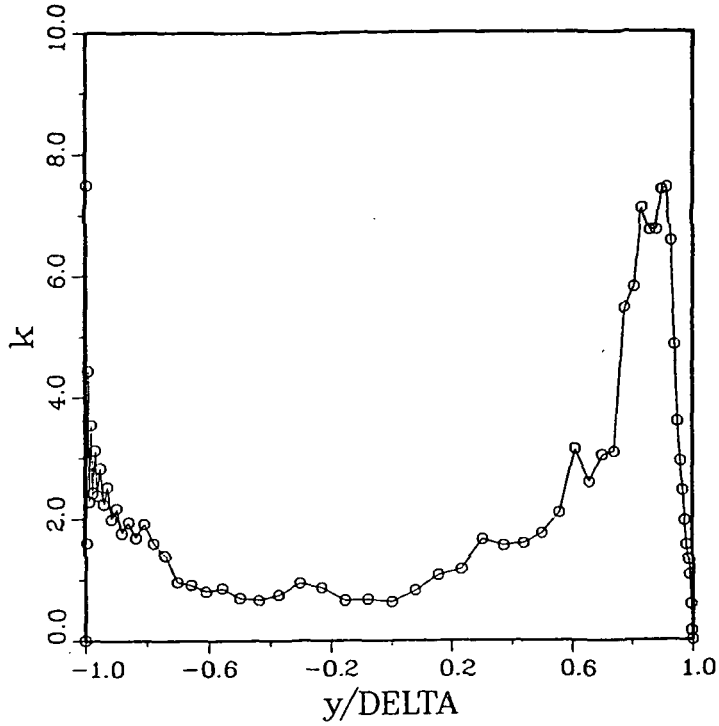

(c) Perturbed solution at LWS station

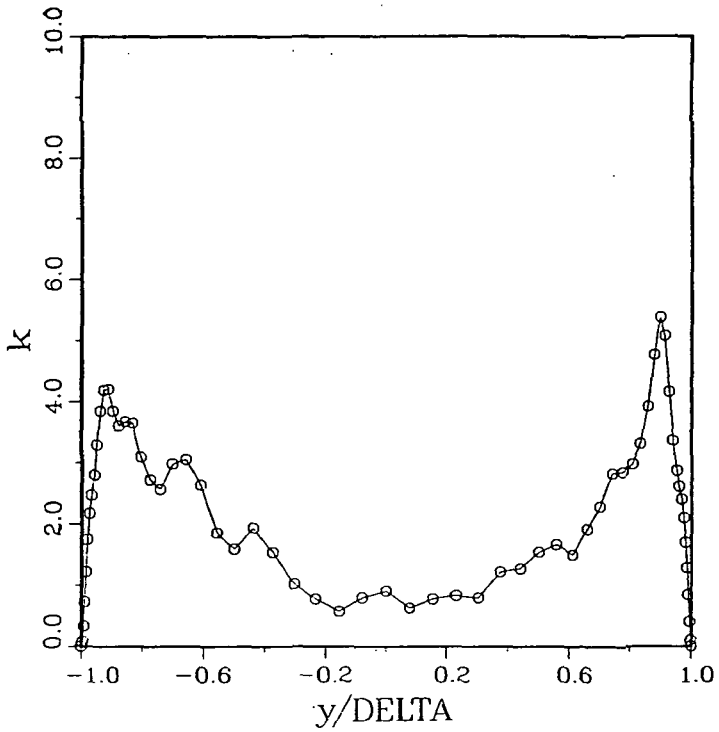

(d) Unperturbed solution at LWS station

Figure 25.- Concluded.

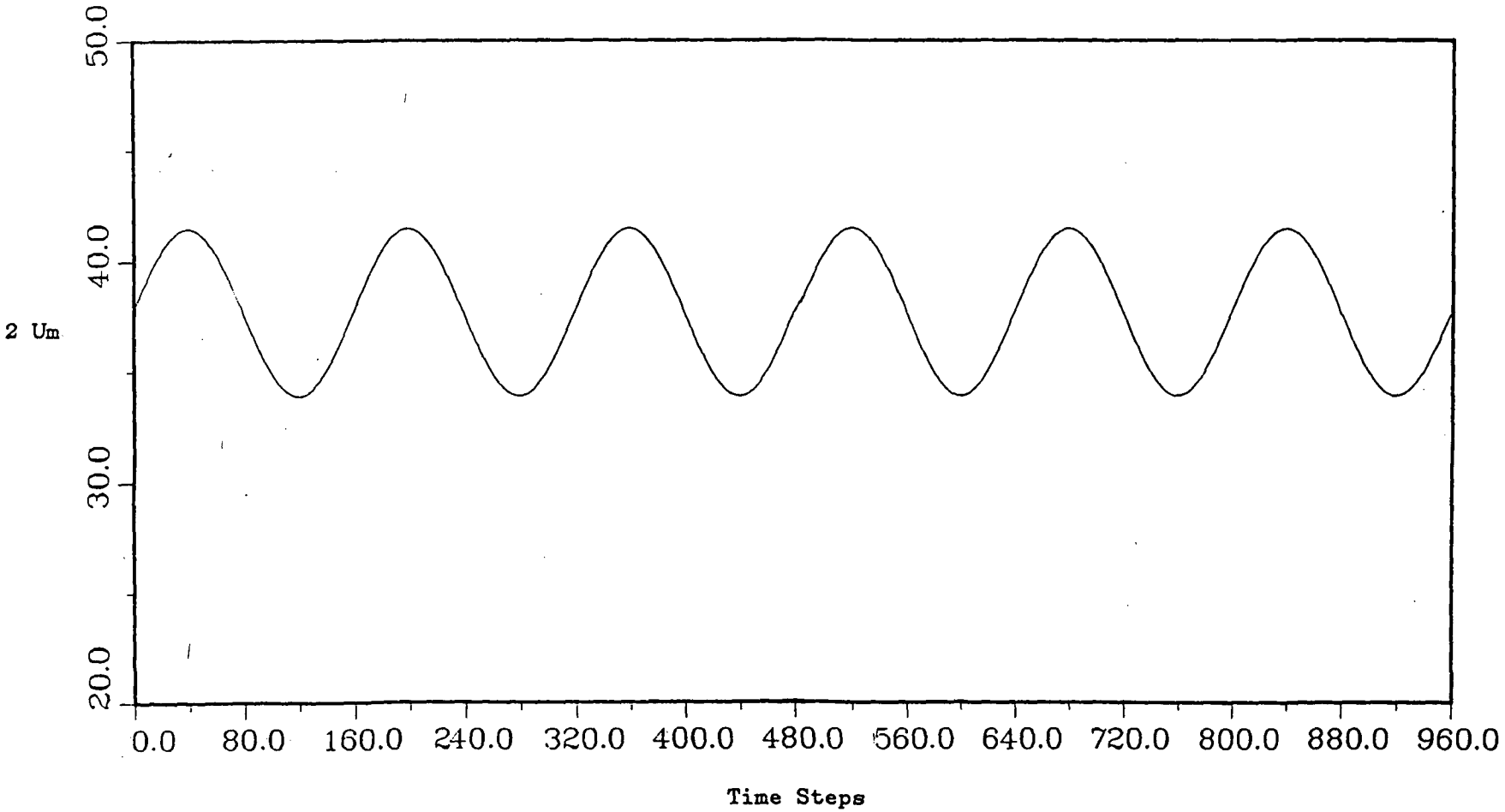

Figure 26.- Variation of the mass flow rate in the channel.

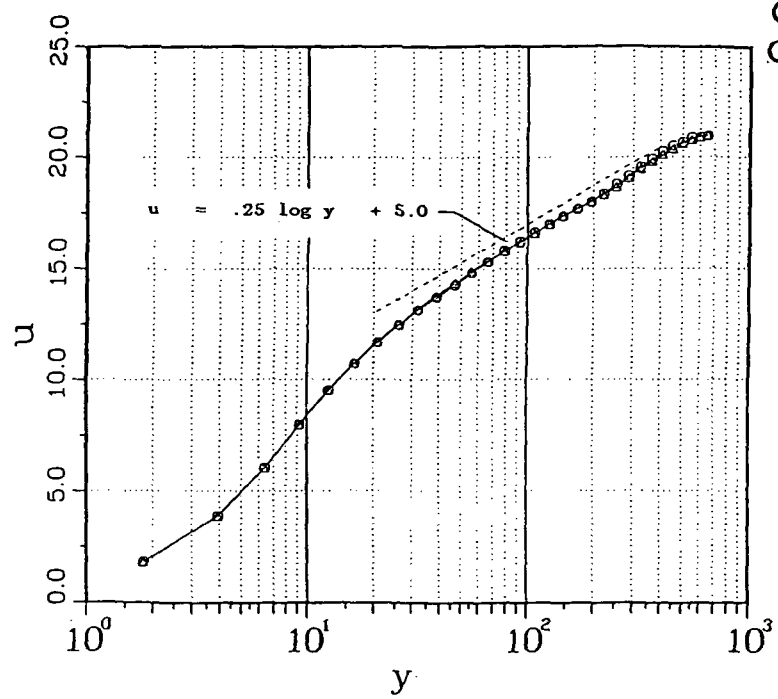

(a) Steady mean flow.

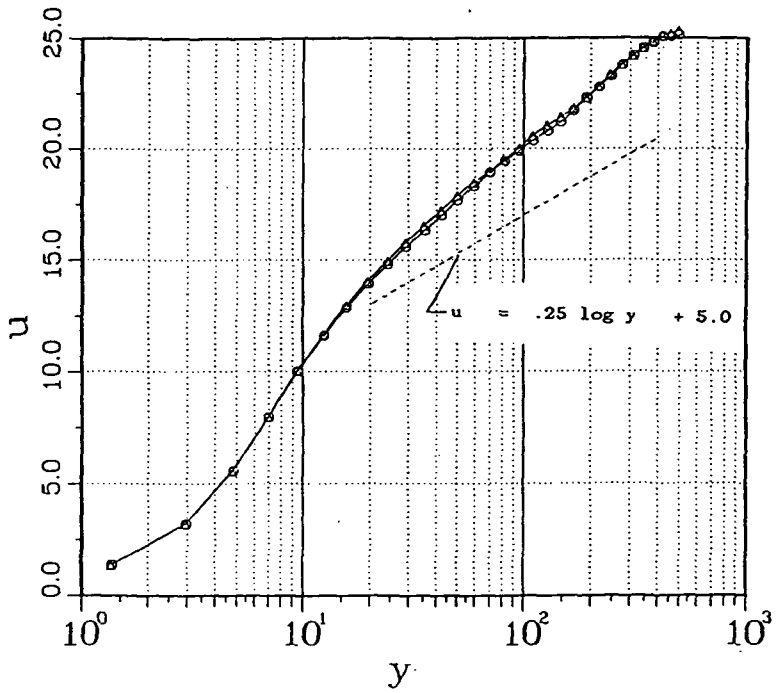

(b) Unsteady mean flow.

Figure 27.- Mean velocity distributions in the channel at time step 920 for the steady and unsteady mean flow.

○ lower half of channel,

△ upper half of channel.

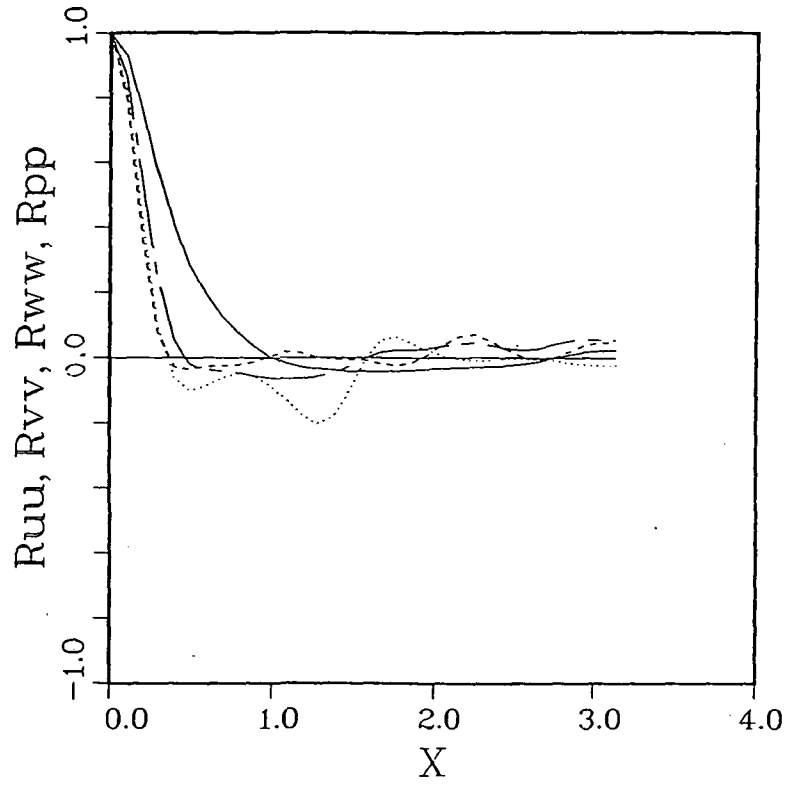

(a) Steady channel flow, y = 3.85

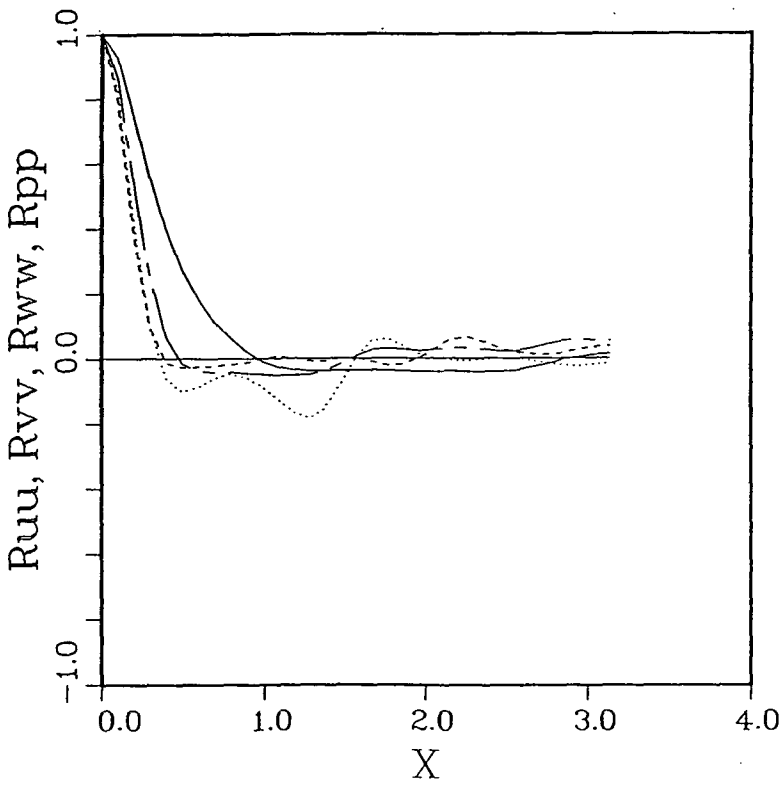

(b) Oscillating channel flow, y = 3.85, $\omega\delta/u_\tau$ = 78.54

Figure 28.- Two-point correlation for steady and oscillating channel flow.

C-2

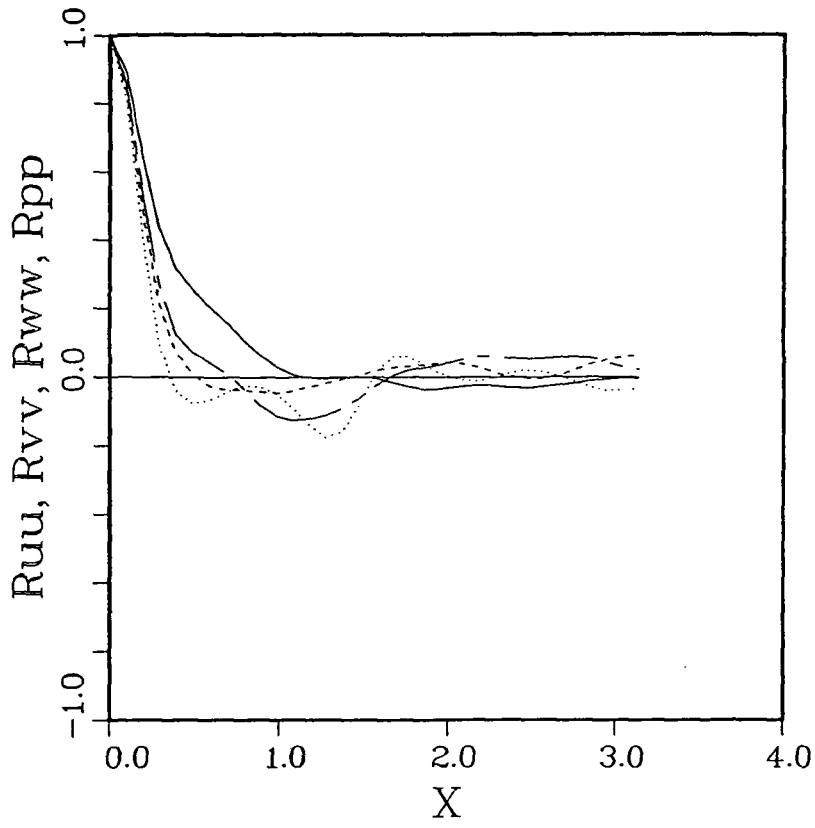

(c) Steady channel flow, y = 20.5

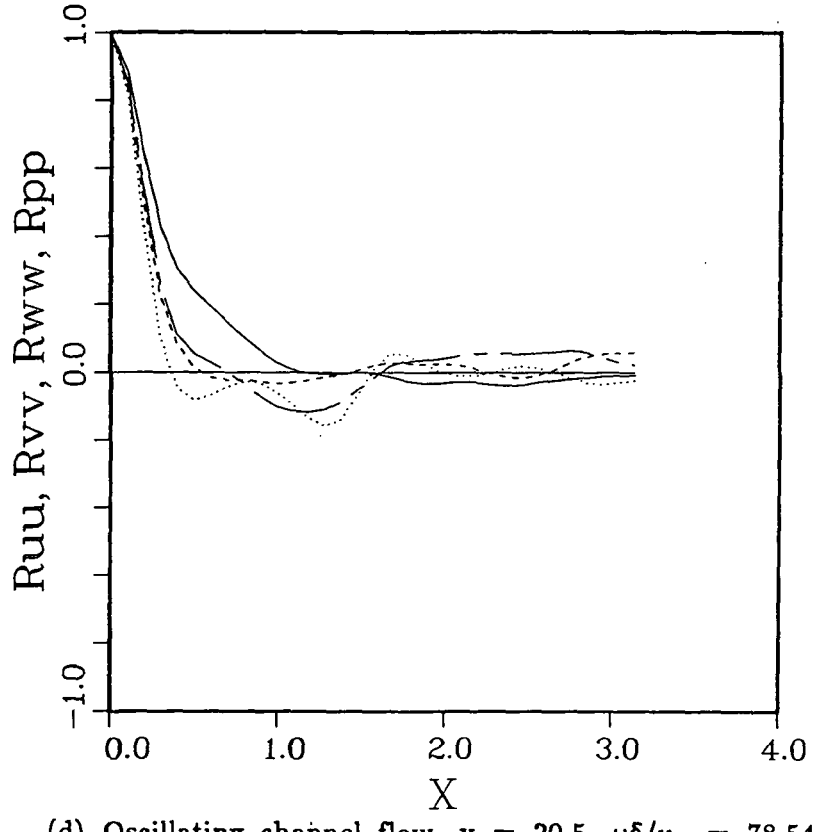

(d) Oscillating channel flow, y = 20.5, $\omega\delta/u_\tau$ = 78.54

Figure 28.- Concluded.

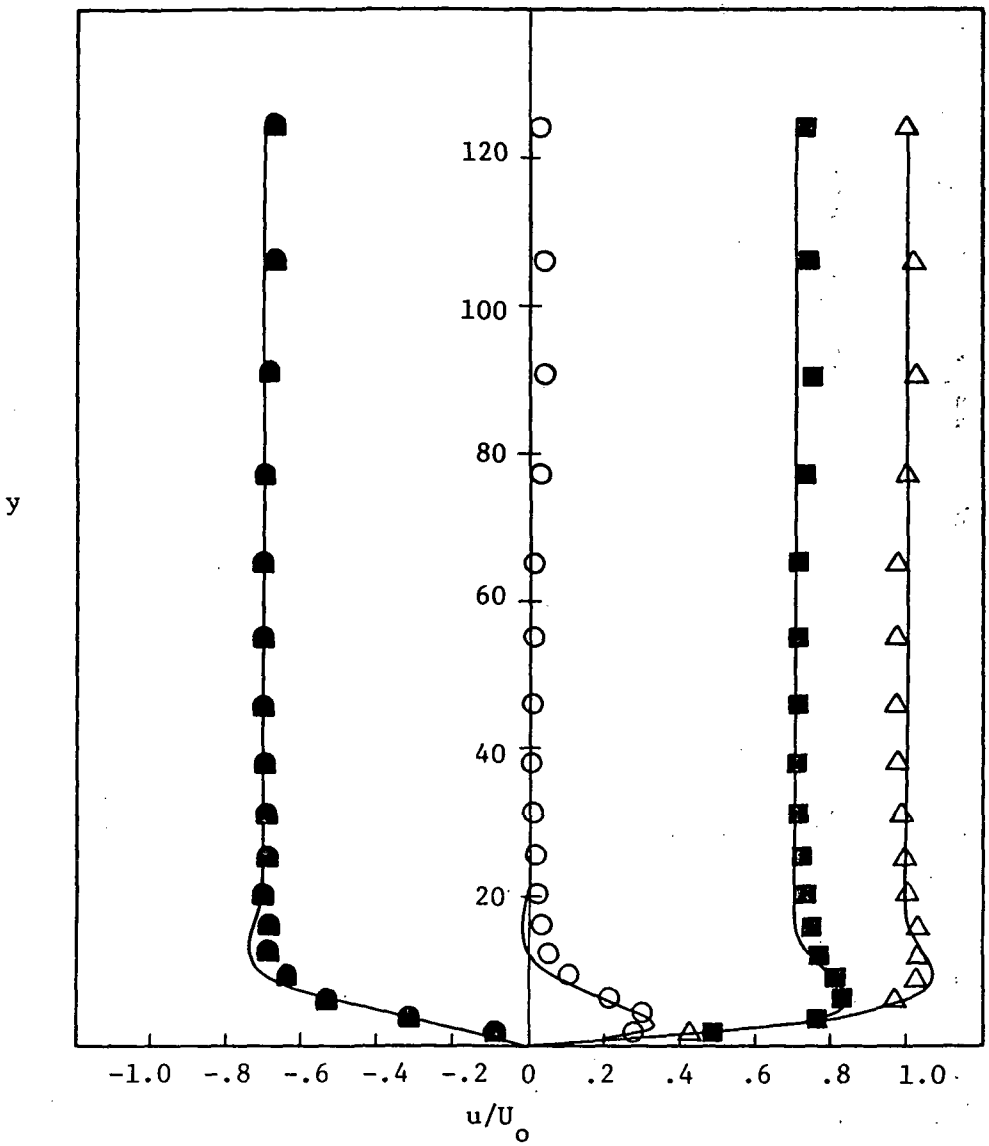

(a) Acceleration period. ○ -0°, ■ -45°, △ -90°, ● -315°, _____ Stokes Solution

Figure 29.- Periodic Component of planar average velocity near the wall for case 1.

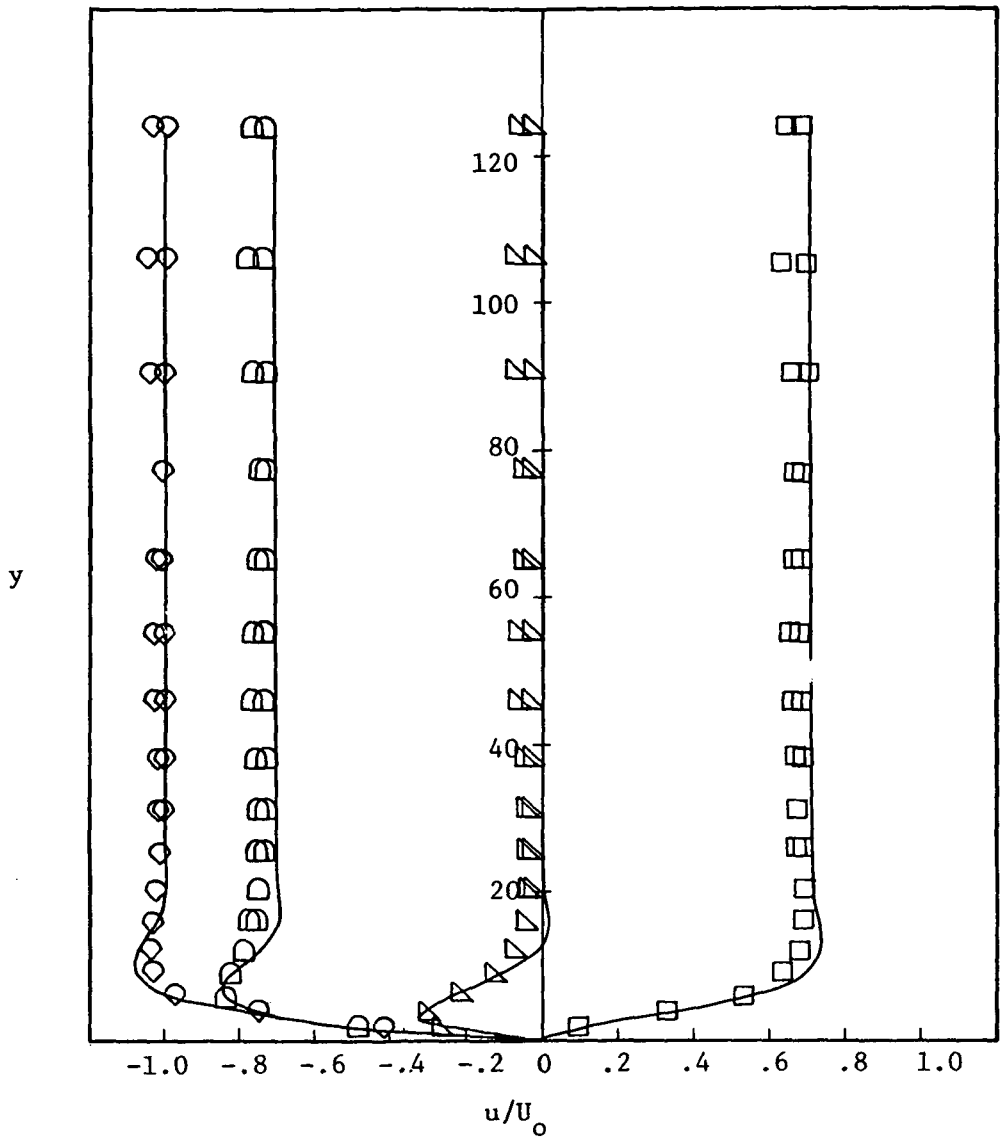

(b) Deceleration period. □ -135°, △ -180°, ⬭ -225°, ◇ -270°, _____ Stokes Solution

Figure 29.- Concluded.

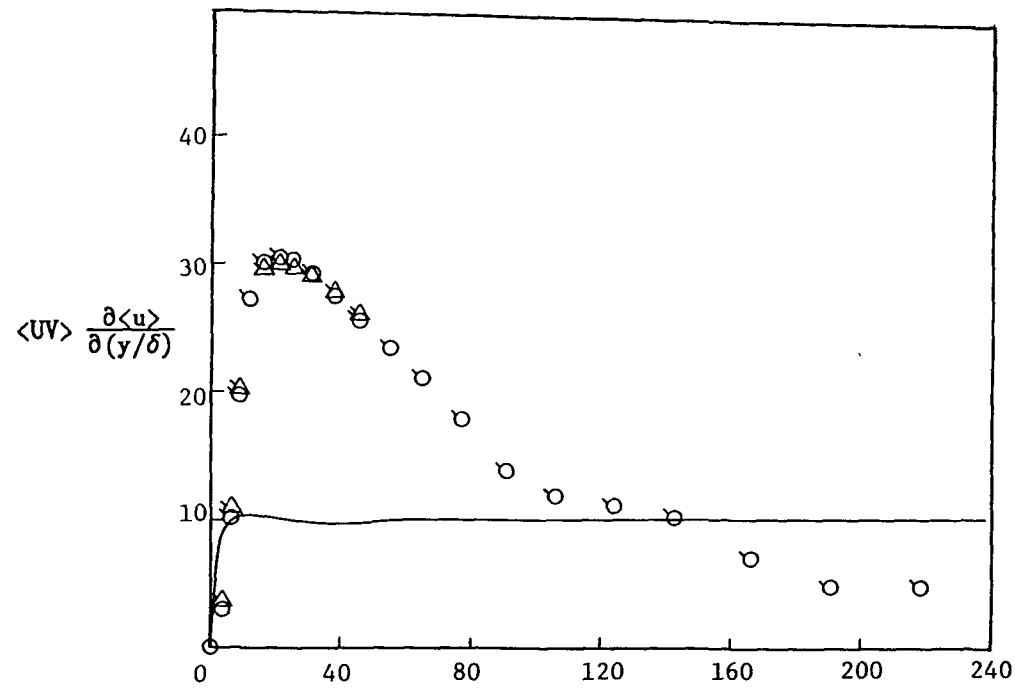

(a) Upper wall

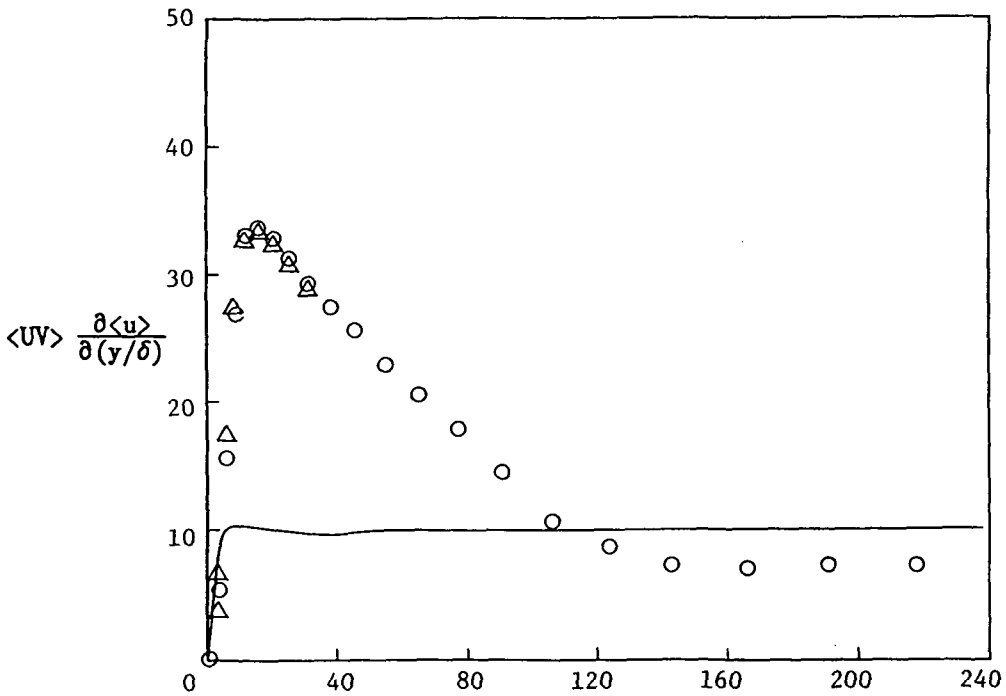

(b) Lower wall

Figure 30.- Comparison of Production of turbulence energy for steady channel flow and for oscillating channel flow for case 1. Phase angle = 90° (T = 840).

O, O steady mean flow

Δ, Δ oscilllating mean flow

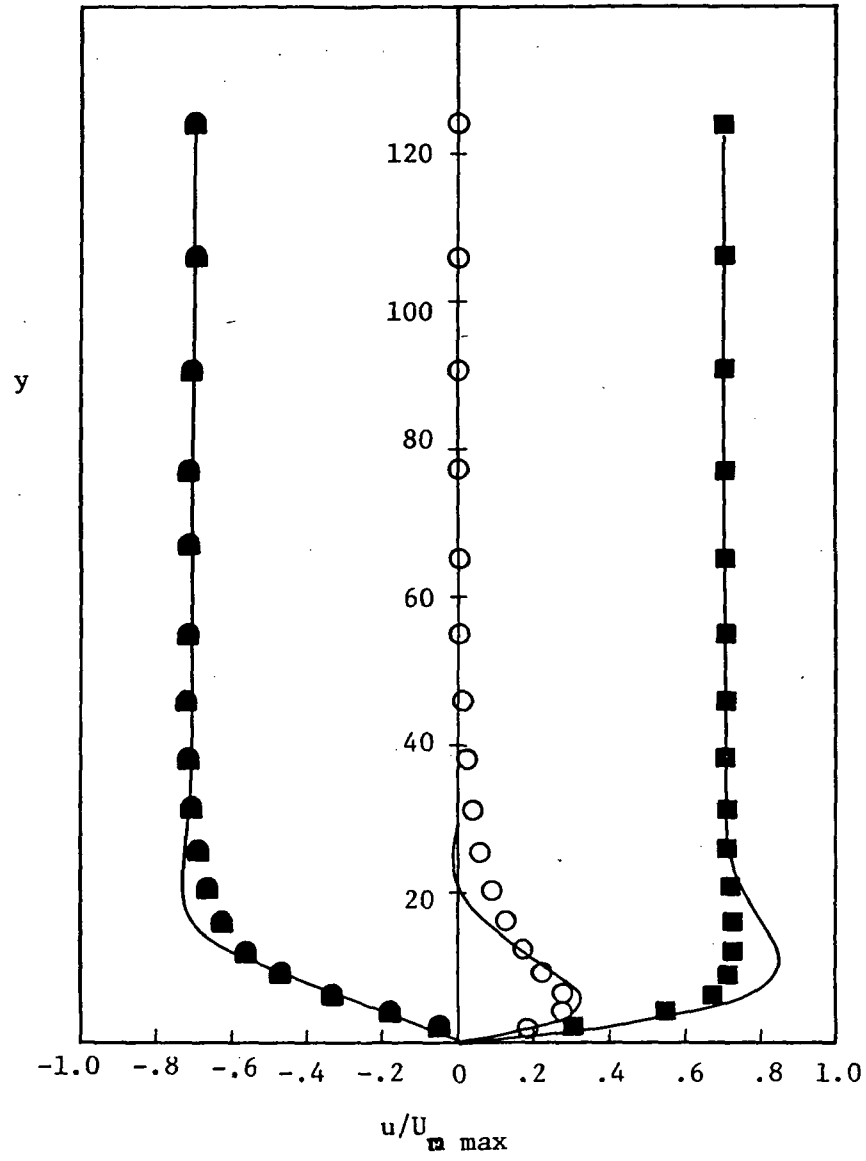

(a) Acceleration period ○ -0°, ■ -45°, ● -315°, _____ Stokes Solution

Figure 31.- Periodic component of planar average velocity near the wall for Case 2.

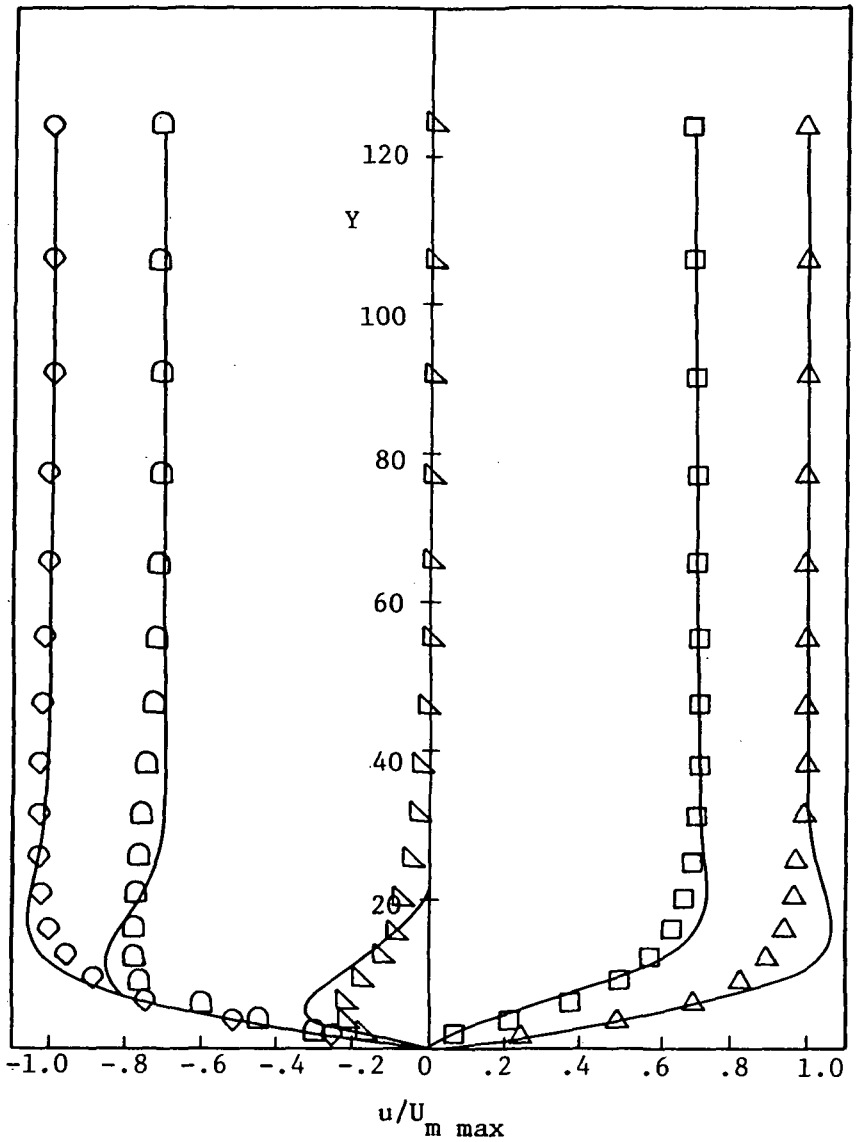

(b) Deceleration period ○ -270°, ◠ -225°, ◺ -180°, □ -135°, △ -90°, _____ Stokes Solution.

Figure 31.- Concluded.

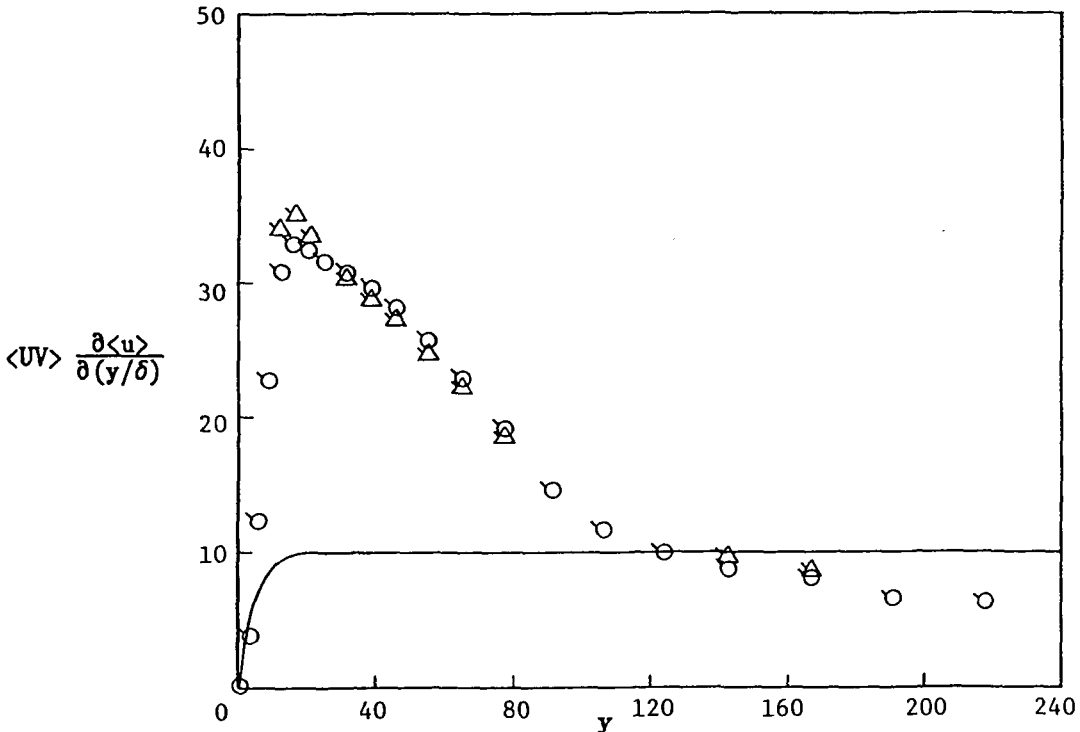

(a) Upper wall

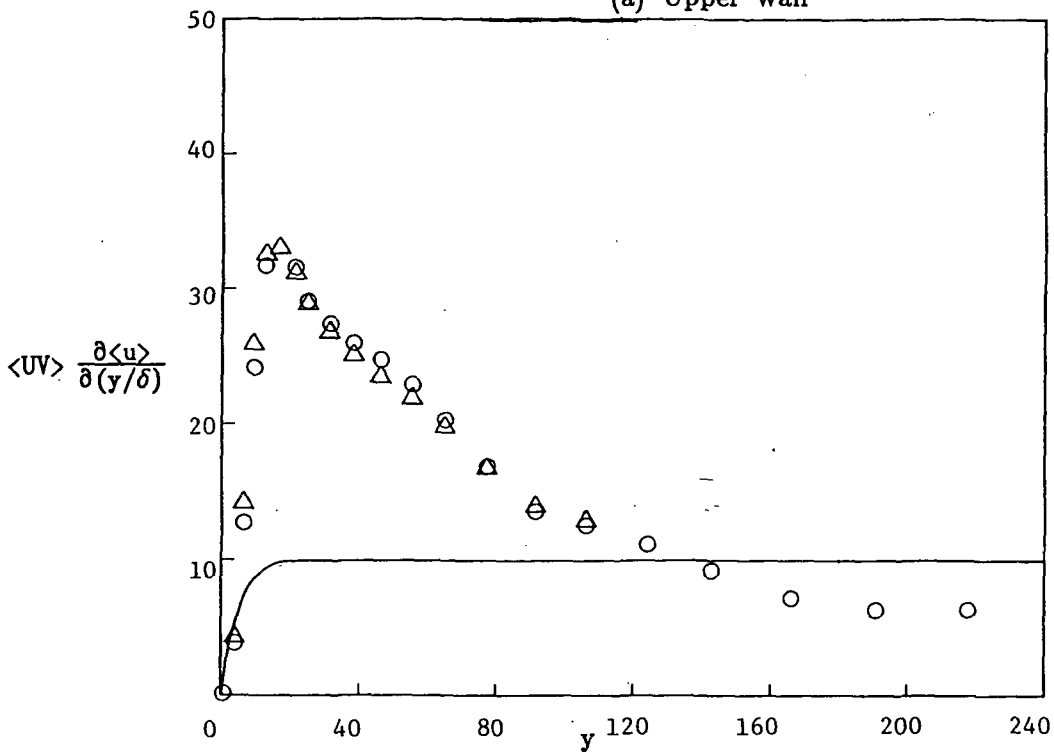

(b) Lower wall

Figure 32.- Comparison of Production of turbulence energy for steady channel flow and oscillating channel flow for case 2. Phase angle = 90° (T = 600)

O, O steady mean flow

Δ, Δ oscillating mean flow

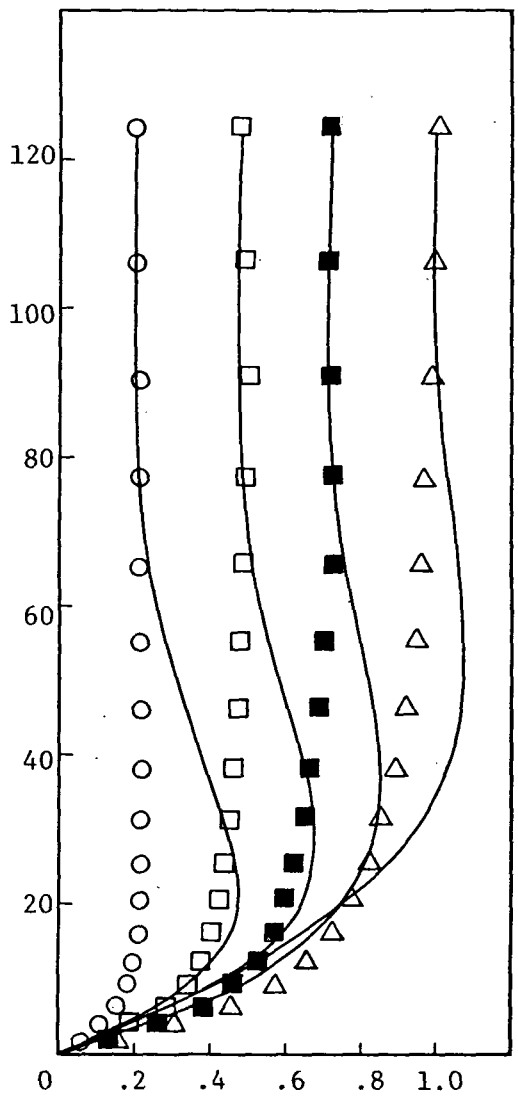

Figure 33.- Periodic component of planar average velocity near the wall for case 3. ○ -160 steps, □ - 380 steps, ■ -600 steps, △ -1200 steps, _____Stokes solution.

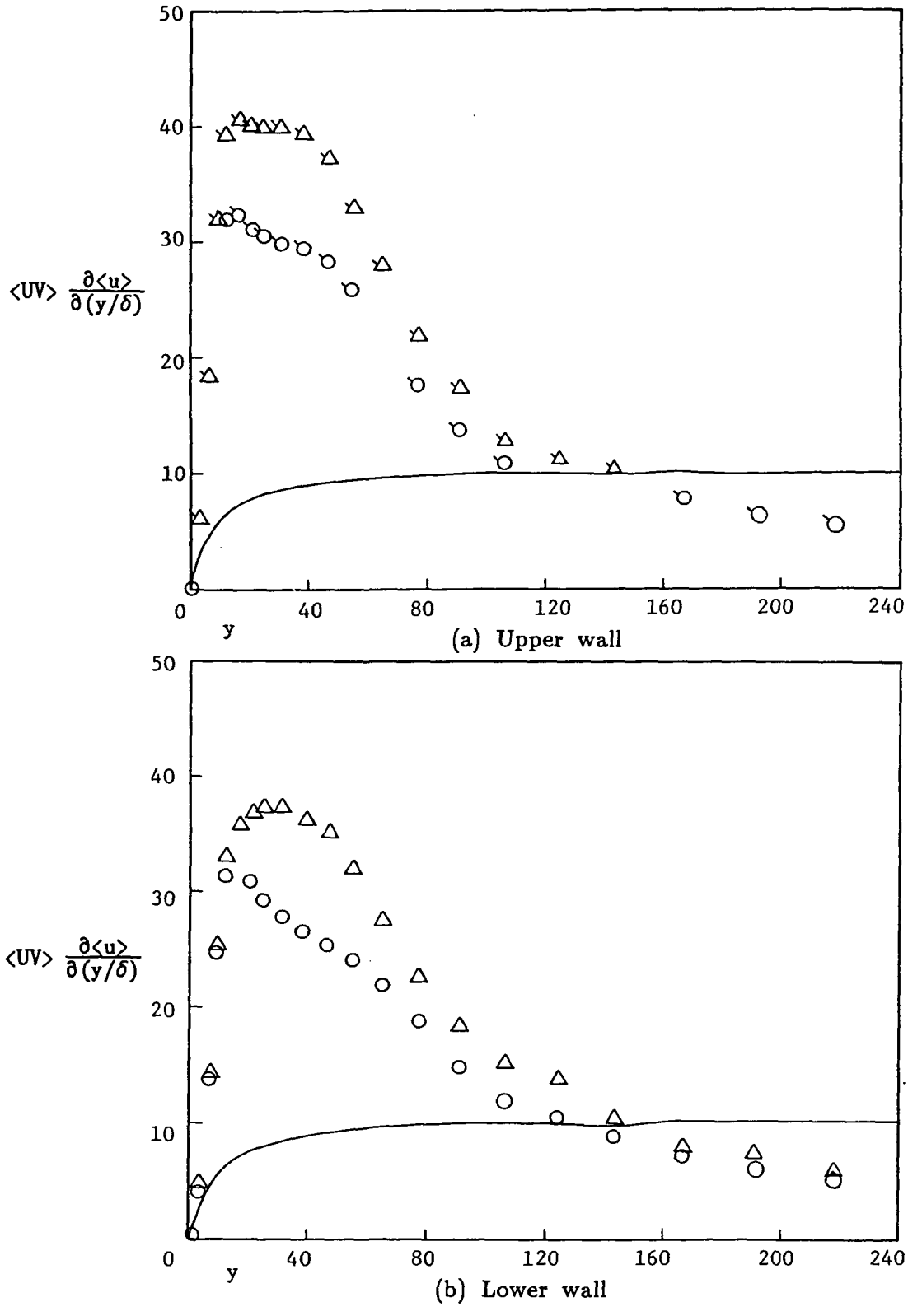

Figure 34.- Conparison of production of turbulence energy for steady channel flow and for oscillating channel flow for case 3. Phase angle = 90° (T = 1200)

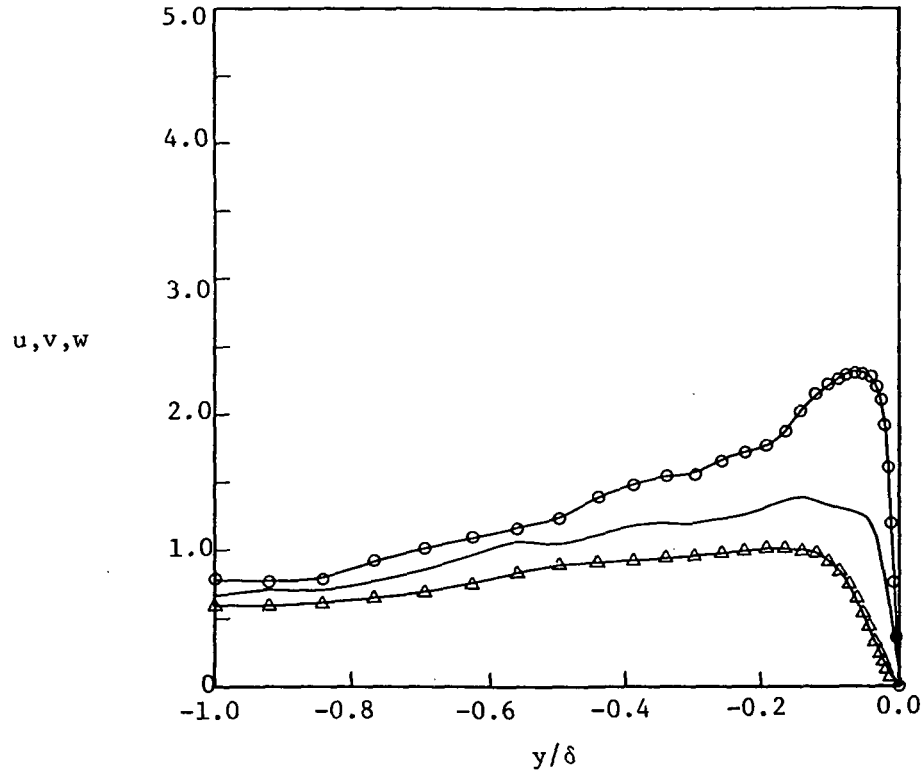

(a) Steady flow, upper wall

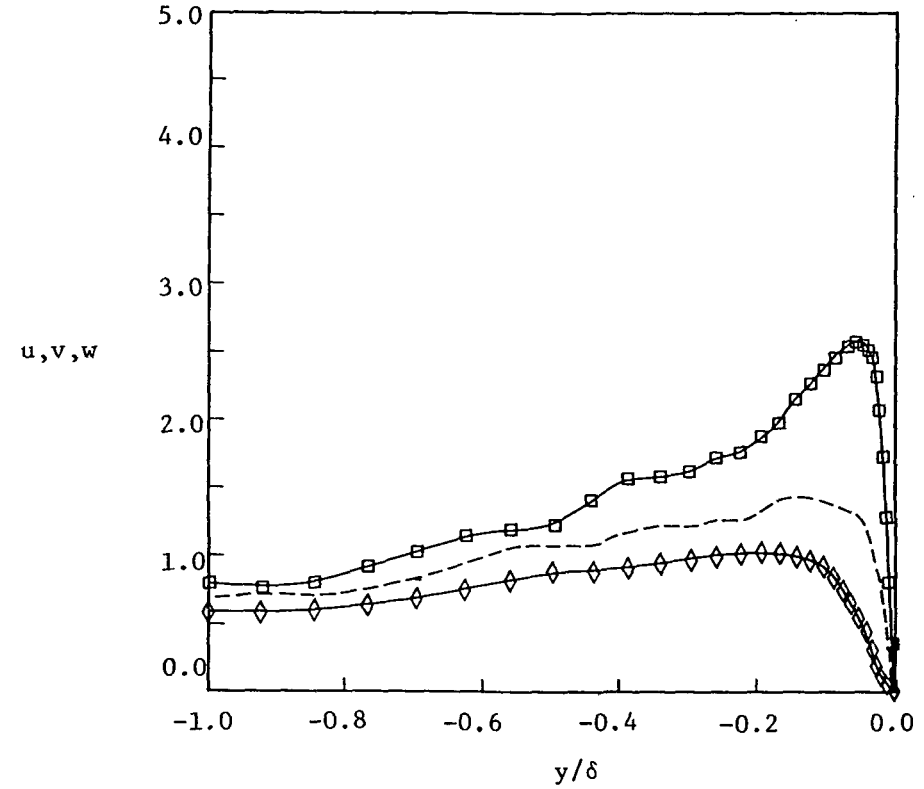

(b) Oscillating flow, $w\delta/u_\tau$ = 2.618, T = 1200, upper wall.

Figure 35.- Comparison of turbulence intensities for steady and oscillating channel flow for case 3.
○ , □ u; △ , ◇ ,v; ____, _ _ _, w.

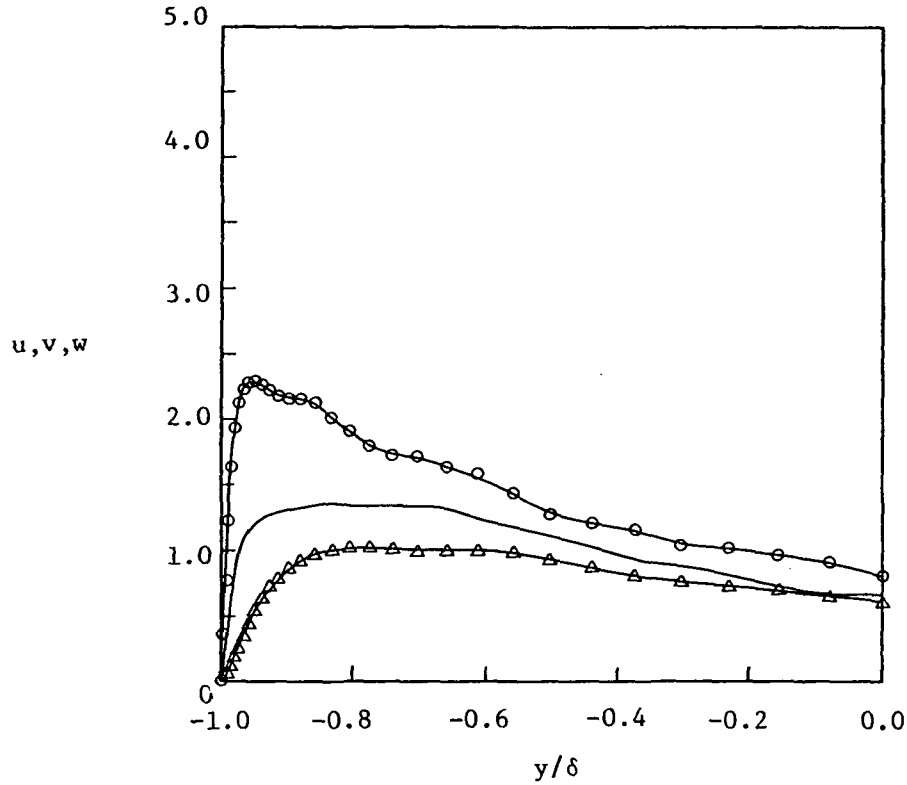

(c) Steady flow, lower wall

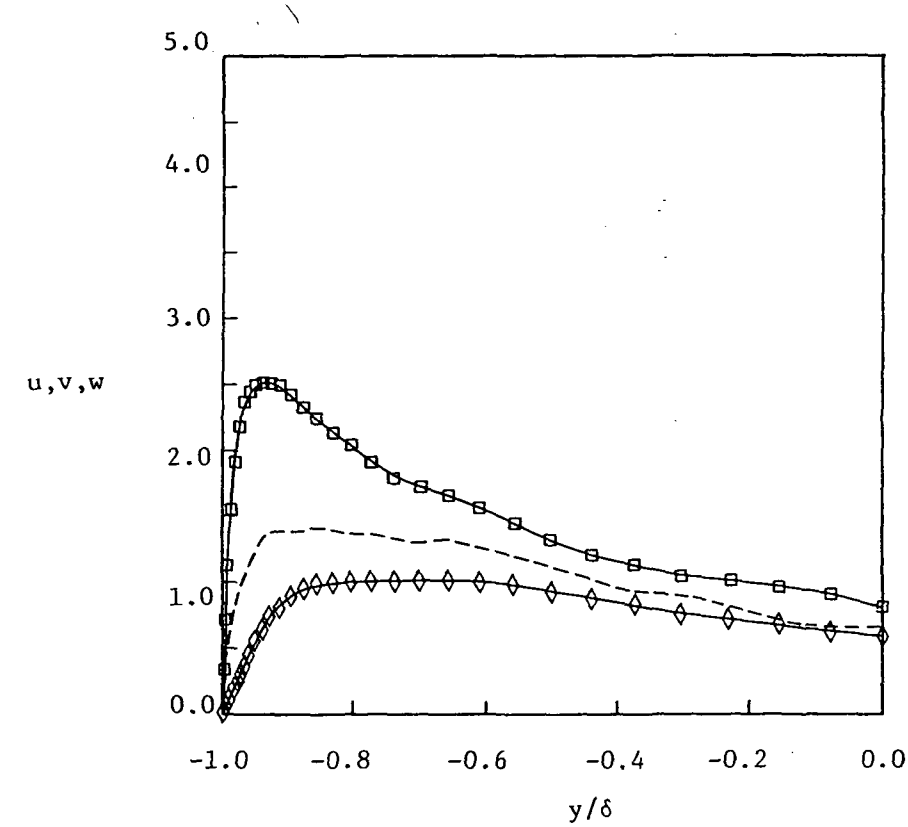

(d) Oscillating flow, $\omega\delta/u_\tau$ = 2.618, T = 1200, lower wall

Figure 35.- Concluded.

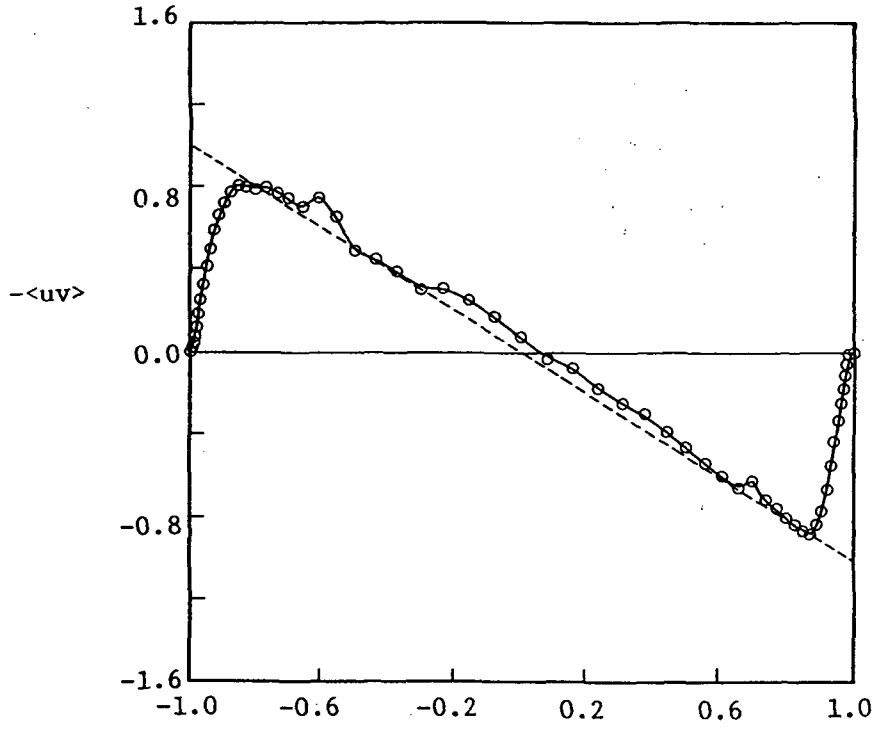

(a) Steady flow

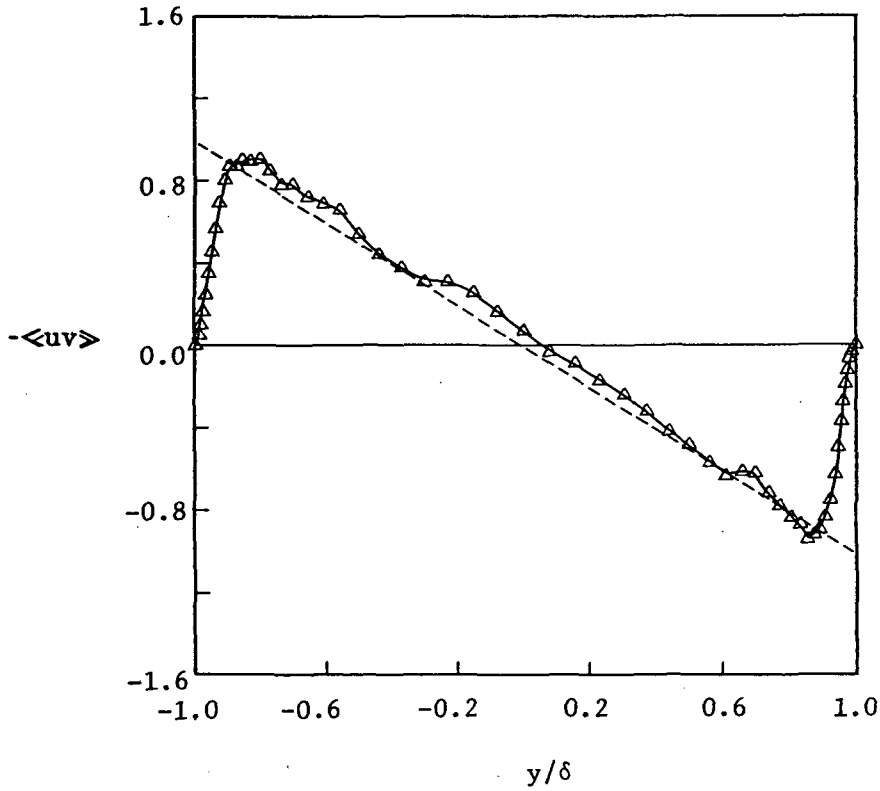

(b) Oscillating flow, $\omega\delta/u_\tau$ = 2.618, T = 1200

Figure 36.- Comparison of Reynolds shear stress for steady and oscillating channel flow for case 3.

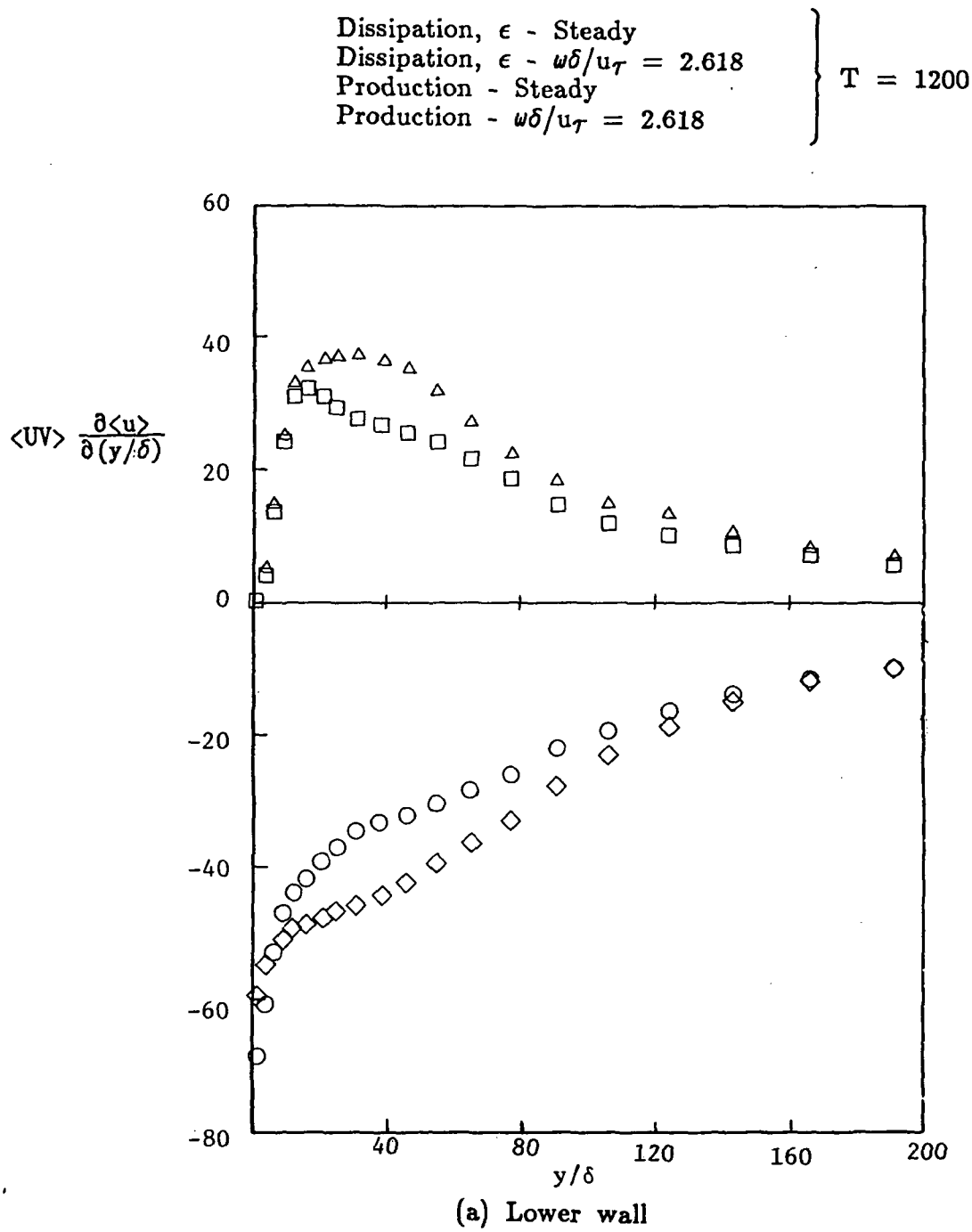

(a) Lower wall

Figure 37.- Comparison of turbulence production and dissipation between steady flow and oscillating flow case 3.

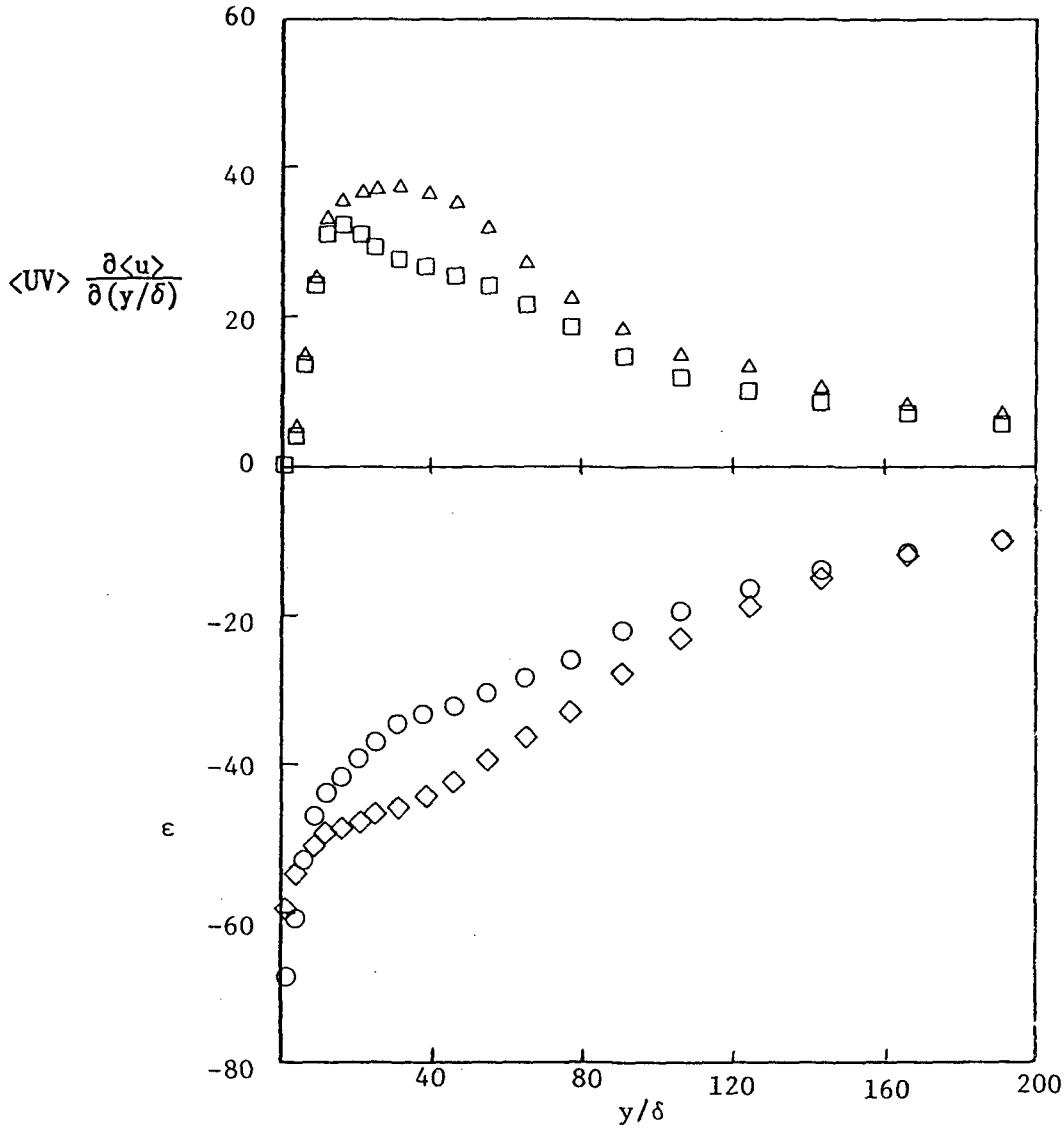

(a) Lower wall

Figure 37.- Comparison of turbulence production and dissipation between steady flow and oscillating flow case 3.

○ Dissipation, ϵ - Steady
◇ Dissipation, ϵ - $\omega\delta/u_\tau = 2.618$
□ Production - Steady
△ Production - $\omega\delta/u_\tau = 2.618$

} T = 1200

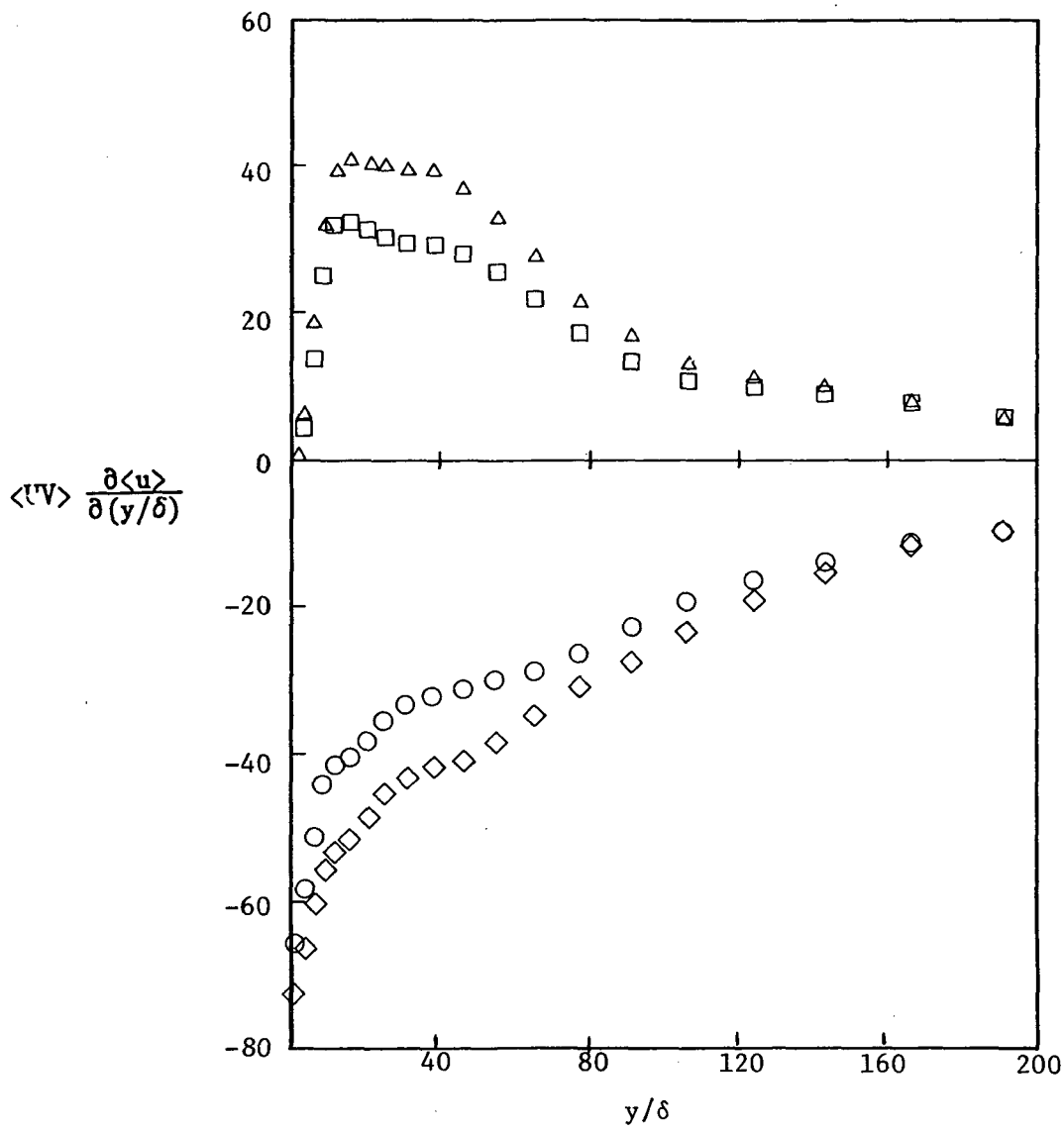

(b) Lower wall

Figure 37.- Concluded.

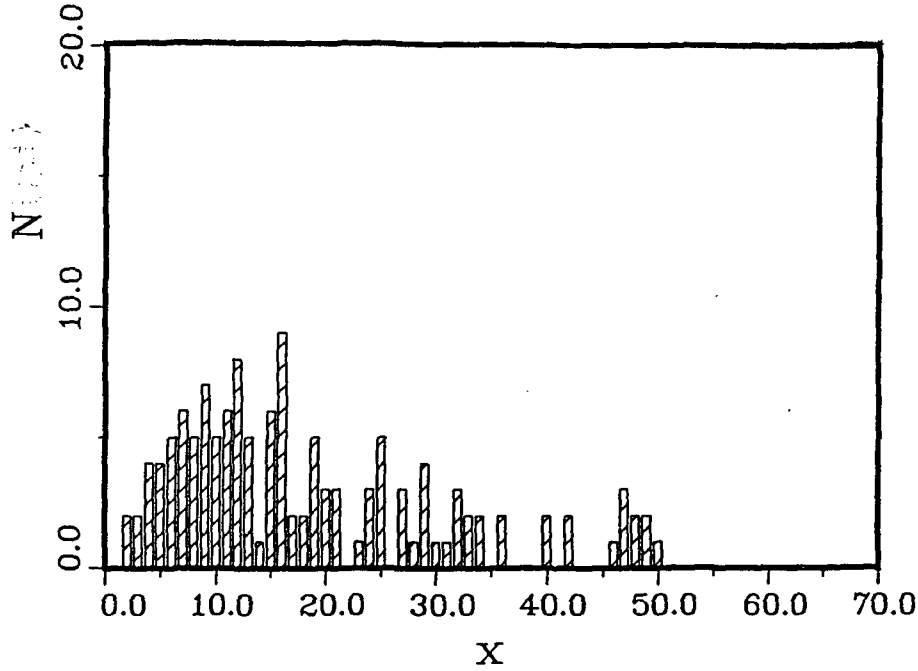

(a) Steady flow, plane 8, y = 20.5, lower wall, T = 1200

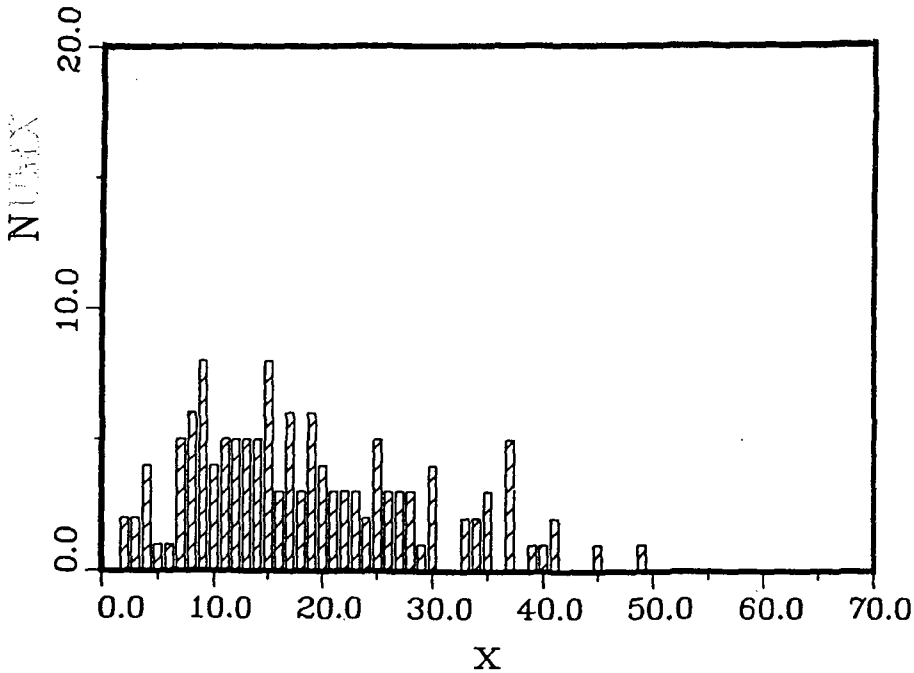

(b) Oscillating flow, plane 8, y = 20.5, w = 2.618, T = 1200

Figure 38.- Comparison of turbulence burst intervals for steady flow and oscillating flow case 3.

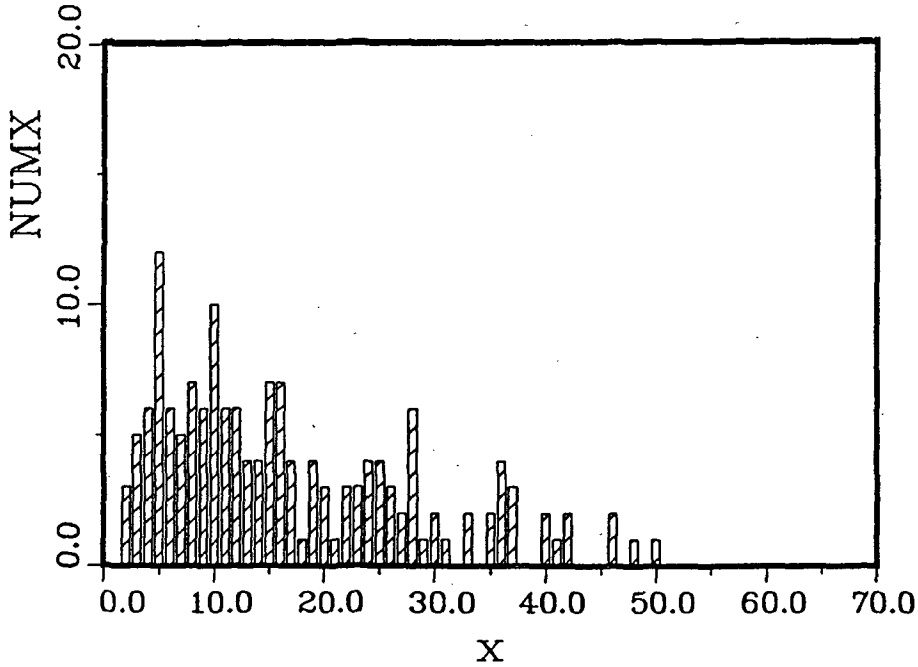

(c) Steady flow, plane 56, y = 20.5, upper wall T = 1200

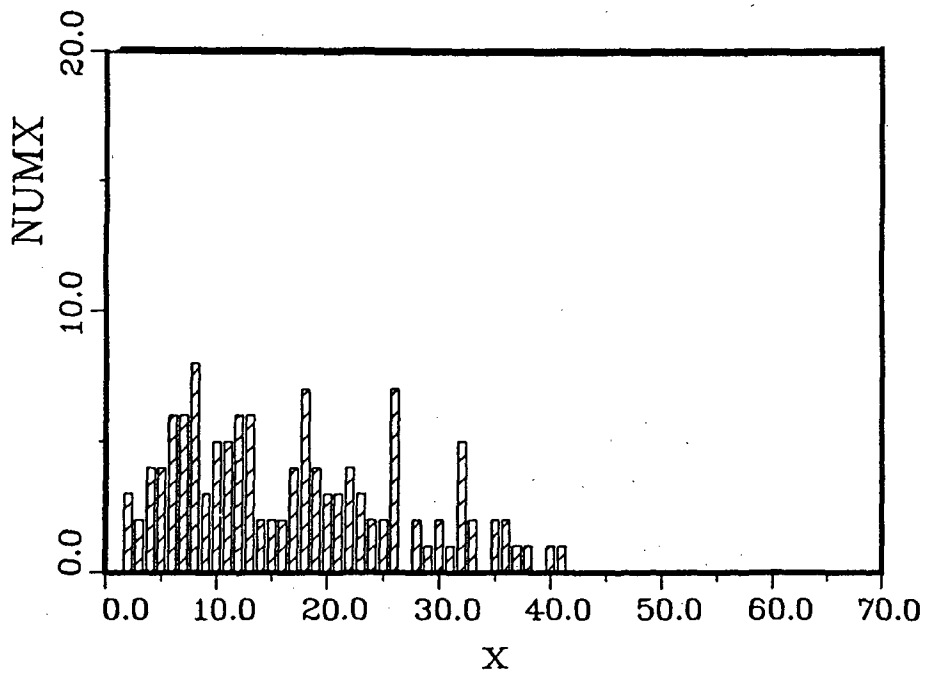

(d) oscillating flow, plane 56, w = 2.618 T = 1200

Figure 38.- Concluded.

NASA
National Aeronautics and Space Administration

Report Documentation Page

1. Report No.	2. Government Accession No.	3. Recipient's Catalog No.
NASA CR-182162		

4. Title and Subtitle

Investigation of the Validity of Reynolds Averaged Turbulence Models at the Frequencies That Occur in Turbomachinery

5. Report Date

July 1988

6. Performing Organization Code

7. Author(s)

Gary D. Kuhn

8. Performing Organization Report No.

NEAR TR-381

10. Work Unit No.

506-42-11

9. Performing Organization Name and Address

Nielsen Engineering and Research, Inc.
510 Clyde Avenue
Mountain View, California 94043-2287

11. Contract or Grant No.

NAS3-24618

12. Sponsoring Agency Name and Address

National Aeronautics and Space Administration
Lewis Research Center
Cleveland, Ohio 44135-3191
and
AFOSR
Bolling AFB, DC 20332-6448

13. Type of Report and Period Covered

Contractor Report
Final

14. Sponsoring Agency Code

15. Supplementary Notes

Project Managers: Kestutis C. Civinskas, Propulsion Directorate, U.S. Army Aviation Research and Technology Activity—AVSCOM, Lewis Research Center, Cleveland, Ohio 44135 and Dr. J.D. Wilson, AFOSR/NA. Work funded under Interagency Agreement Number AFOSR-ISSA-86-0030.

16. Abstract

Turbulent flows subjected to various kinds of unsteady disturbances were simulated using a large-eddy-simulation computer code for flow in a channel. The disturbances were: a normal velocity expressed as a traveling wave on one wall of the channel; staggered blowing and suction distributions on the opposite walls of the channel; and oscillations of the mean flow through the channel. The wall boundary conditions were designed to simulate the effects of wakes of a stator stage passing through a rotor channel in a turbine. The oscillating flow simulated the effects of a pressure pulse moving over the rotor blade boundary layer. The objective of the simulations was to provide better understanding of the effects of time-dependent disturbances on the turbulence of a boundary layer and of the underlying physical phenomena regarding the basic interaction between the turbulence and external disturbances of the type found in turbomachinery. The results of the simulations showed that turbulence is sensitive to certain ranges of frequencies of disturbances. However, no direct connection was found between the frequency of imposed disturbances and the characteristic "burst" frequency of turbulence. New insight into the nature of turbulence at high frequencies was found. The viscous phenomena near solid walls was found to be the dominant influence for high frequency perturbations. At high frequencies, the turbulence was found to be undisturbed, remaining the same as for the steady mean flow. A transition range exists between the high frequency range and the low, or quasi-steady frequency range in which the turbulence is not predictable by either quasi-steady models or the steady flow model. The limiting lowest frequency for the use of the steady flow turbulence model is that for which the viscous Stokes layer based on the blade passing frequency is thicker than the laminar sublayer.

17. Key Words (Suggested by Author(s))	18. Distribution Statement
Turbomachinery Turbulence Mathematical models Computerized simulation	Unclassified – Unlimited Subject Category 20

19. Security Classif. (of this report)	20. Security Classif. (of this page)	21. No of pages	22. Price*
Unclassified	Unclassified	116	A06

NASA FORM 1626 OCT 86

*For sale by the National Technical Information Service, Springfield, Virginia 22161

*U.S. Government Printing Office 1988: 548-157/81004